THREE-PHASE NETWORK SIMULATOR FOR HORIZONTAL WELLS WITH COMPLEX ADVANCED WELL COMPLETIONS

JIYI LIU

Three-phase network simulator for horizontal wells with complex advanced well completions

Jiyi Liu, M.Eng.

A thesis submitted to School of Graduate Studies in partial fulfillment of the requirements for the degree of (Master of Engineering)

Faculty of Engineering and Applied Science

Memorial University of Newfoundland

April, 2009

St John's Newfoundland Canada

Abstract

This study presents an integrated steady-state flow network model to predict the flow parameters in horizontal wells and the near wellbore region. The flow parameters are solved for pressure, flow rates and phase fractions. The fundamental network model is flexible and modular in order to simulate the fluid phase behaviors in various production conditions and different advanced well completions.

Compared to an existing three phase flow model that is based on a liquid-gas formulation, the model for three individual phases proposed in this research is more proper and systematic to portray the fluid behavior during production and enhanced oil recovery processes.

The network model is based on black oil three phase model in an isothermal environment, and the Newton-Raphson iterative technique is used to solve for the unknowns. The well completions and the near wellbore region are represented by the distribution of nodes that are interconnected by flow channels.

By using this proposed model, the fluid phase behavior could be predicted for horizontal wells with complex completions, including the open hole, stinger completion, slotted liner, and multiple inflow control devices.

Generally, water is the third phase flow in addition to oil and gas in the reservoir and wellbore. Therefore, in this research the three-phase flow was considered as oil-water-gas.

Acknowledgments

My sincere appreciation to my supervisor Dr. Thormod E. Johansen for his guidance, trust, encouragement and financial support during my study at Memorial University of Newfoundland; I also thank him very much for his time and effort in polishing this thesis. Without his help, I could not accomplish this research. I would like to thank my co-supervisor Dr. Faisal I. Khan as well for his help on my course study and thesis correction.

Besides my supervisors, I would like to thank some more people who were very important to this research. First, Worakanok Thanyamanta, thank you for helping me to get the research started. Without your previous work, my research would be very difficult to finish. I would also like to thank Vitaly Khoriakov and Christian Johansen for your work on developing the network model and helping me when I encountered difficulties.

In addition, I would like to thank the Department of Engineering and Applied Science of Memorial University of Newfoundland, for financial support from both the graduate scholarship and the teaching assistantship.

I am deeply grateful to my parents; your lifelong love has been supporting me happily to live and study in Canada. Thank you for always believing in me and constantly encouraging me; your love is precious.

My thanks are also sent to Jamal Siavoshi, Heather O'Brien and Moya Crocker. Your help is much appreciated.

Nomenclature

Abbreviations

EOS equation of state

GOR Solution gas oil ratio

R_s Gas solubility

ICD Inflow control device

STC Stock tank condition

RC Reservoir condition

PI Productivity Index

VLE Vapor-liquid equilibrium

Greek Symbols

α Oil volume fraction

β Water volume fraction

μ Viscosity

μ_{od} Dead-oil viscosity

μ_{os} Saturated-oil viscosity

ϖ Acentric factor

ρ Density

π Stress tensor

$\bar{\rho}$ Average three-phase density

τ_w Wall shear stress

ε_D Pipe roughness

Symbols

A Cross-section area

B_g Gas formation volume factor

B_w Water formation volume factor

B_o Oil formation volume factor

D Diameter

D_h Hydraulic diameter

f Friction factor

g Gravitational acceleration

K Absolute permeability

K_{ro} Oil relative permeability

K_{rg} Gas relative permeability

K_{rw} Water relative permeability

L Length

m Mass flux

N Number of network segments

n Number of moles

P Wetting perimeter or pressure

p Pressure

P_b Bubble-point pressure

PI Productivity index

q Flow rate

R Universal gas constant

r Radius

r_e Drainage radius

r_i Well inner radius

r_o Well outer radius

R_e Reynolds number

s Skin factor

T Temperature

V Volume

v Velocity

Z Compressibility factor

Subscripts

dg Dissolved gas

I Inflow

o Oil phase

ref Reference condition

res Reservoir

S Slot

Superscripts

STC Stock tank condition

RC Reservoir condition

Table of Contents

Chapter 1 Introduction and Overview

1.1 Background

Horizontal drilling technology achieved commercial viability during the late 1980's. The purpose of a horizontal well is to enable greater contact with the reservoir, and thereby to enhance well productivity or injectivity. Presently horizontal wells with different kinds of completions and production techniques have been extensively and effectively applied in many cases including (Joshi, 1992):

- To intersect fractures and drain the reservoir effectively in the naturally fractured reservoir.
- To equalize the pressure drop along the horizontal wellbore, achieving the longer producing life due to delay of water/gas coning, and improving the production per unit length.
- To decrease flow rate of high mobility fluids and reach better sweep efficiency.
- To improve drainage area per well and reduce the number of the wells required to drain the reservoir in low permeability reservoirs.
- To reduce near wellbore velocities or turbulence and improve well deliverability in high-permeability reservoirs.
- To enhance the injectivity in thermal Enhance Oil Recovery Processes.
- Commingle production from different reservoirs.

The typical difference between a horizontal well project and a vertical well project is that the well productivity depends on the well length; horizontal wells could achieve higher production than vertical wells with lower drawdown.

There are also some limitations for horizontal wells. Horizontal wells are usually much

more expensive than vertical wells because of the drilling method and the completion technique used. However, the cost of horizontal wells can be reduced by the increasing drilling experience and knowledge of the reservoir and production system. Therefore, accurate reservoir and wellbore simulation may be very helpful to reduce the drilling and completion expenses.

In order to optimize productivity or injectivity performance during the well's complete lifetime and ensure the field is produced reliably and safely, advanced completions are precisely positioned to achieve good control of fluid flow in horizontal wells. As a result, the fluid flow geometry becomes more and more complicated and the traditional reservoir simulators might not provide precise and effective simulation of the completion details.

In order to precisely portray and simulate flow parameters along the wellbore and the flow geometries through the complex well completion paths, several new simulation methods have been developed and applied in the industry. The iterative network solver is one of the most recent techniques for simulating completed horizontal wells. So far, the iterative method has already been used to accurately predict well performance while encountering complex completions and drilling problems, and has been extensively applied in industry.

The multi-phase problem is one of the most important problems in oil production. Presently the injection method is the main method used in the Enhanced Oil Recovery (EOR) process to improve the oil recovery by maintaining the reservoir pressure and displacing the oil. Various materials are injected into the reservoir, such as water, steam, CO_2, polymers, and even hydrocarbons, and all of these injection fluids have completely different physical and chemical properties. Consequently, multi-phase problems become more complicated.

The iterative network solver in the open literature is based on two-phase network solver.

As a result, when it encounters the three-phase (oil-water-gas) problem, it solves the liquid-gas two phase problem first, and then separates the oil and water phase using mass balance between these two phases. This simplification may not meet the simulation demands when the injected materials have complicated physical and chemical properties.

1.2 Objective of the thesis

The objective of this work is to:

- Develop an integrated three-phase network model which simulates three phases individually.
- Investigate flow behaviors with different reservoir and well conditions, such as under the bubble point in production, two phase problems (either oil-gas or water-gas).
- Construct complex completion paths in the proposed three-phase network model and predict the flow parameters along the completed horizontal well.
- Provide recommendations on further development of the model.

To accomplish these objectives, the major target is to extend an existing two-phase network model to three-phase model by adding in the third phase, since generally water is the third flowing phase in the reservoir and well. To simplify the problem, the three-phase problem in this work is considered to be oil-water-gas flow.

In addition, the network solver in this work applies Newton-Raphson method to solve non-linear equations, so the success of the simulation is therefore greatly related to the initial guess, which should follow the physical principle of the flow geometries through the different completion components.

1.3 Scope of the study

This research is to extend an existing two-phase iterative network solver to three phases and to predict the flow parameters and phase behaviors along the wellbore and the near wellbore region. This model was first implemented as a single phase model by A. C. Johansen, and extended to oil-gas flow model by Worakanok Thanyamanta. Fluid physical properties including density, viscosity, flow rates, and phase fractions are simulated in the three individual phases of oil, water and gas. Pressure drop along the wellbore will be determined for the horizontal well, as well as advanced completions such as the open hole, stinger, slotted liner, and inflow control devices.

Only non-volatile and isothermal reservoirs are considered here, reservoir temperatures are well away from critical temperatures of fluids, and the evolved gas phase contains few heavy compounds. In the other words, a black oil three phase (oil/water/gas) model is chosen.

1.4 Layout of the Thesis

This thesis includes six chapters. The first chapter, Introduction and Overview, gives the introduction to the thesis: background information, objective of the research, scope of the study, and layout of the thesis. Chapter two, Literature Review, reviews the simulation method for horizontal wells in recent decades. Chapter three, Network Model, introduces the formulation of the network solver. The chapter presents the flow geometries and transport mechanisms in the horizontal well using the structure of the network model. The governing equation system for the network model and the approach used to solve unknown parameters are laid out. Chapter four, Stability Test for the Network Solver. The three-phase model deals with the fluids in the oil/water/gas phases, and the oil phase contains the dissolved gas which

will break out once the pressure is below the bubble point. The stability of the network model is tested in this chapter by implementing several special cases as follows: test two-phase flow by three-phase flow solver, either as oil-gas or water-gas system; pressure decreasing to bubble point during the production and the entire production under bubble point. The descretization error of the network model is also presented in this chapter. Chapter five, Completions and Initial Guess Generate, specific completion paths are demonstrated and simulated, and the well completion components are individually mapped in the network model. The initial guesses for the specific physical problems with different completions are discussed in this chapter. Simulation results and discussions, the plots for the pressure distribution, flow rate and phase fractions in each phase through the well completions are presented, together with discussion of the flow conditions and phase behavior. Conclusions and Recommendations are given in Chapter six.

Chapter 2 Literature review

As the numerical simulation of the horizontal wells with complex completion configurations is a relatively new domain in reservoir simulations, there is not much research done in this field. However the scientists did introduce several innovative approaches to provide the accurate predictions of the flow parameters inside the well and near the wellbore.

Dikken (1990) did research on the pressure drop in long horizontal wells. Pressure drop is caused by friction when fluids move from the toe to the heel in the well. This is usually neglected in vertical wells. A second-order differential equation for a simple analytical approach was solved numerically with boundary conditions; this differential equation describes mass and momentum conservation in single-phase turbulent well flow. Flow rates and pressure drop along the horizontal well during the production were plotted in dimensionless manner.

Economides, et al. (1991) developed a comprehensive simulator for horizontal wells using a locally refined grid system to precisely describe horizontal wells which are partially penetrating the reservoir. The effects of well positioning between the vertical boundaries, distance from the parallel horizontal boundaries, and the permeability anisotropy were accurately represented.

Bendlksen, et al. (1991) actually represented a dynamic two-fluid model, OLGA which applied the basic equations and two-fluid models, and this method compared the steady-state pressure drop prediction, liquid hold-up, and flow-regime transitions with the data from the SINTEF Two-Phase Flow Laboratory, previous research records and evaluated field data.

With the development of drilling and completion techniques in horizontal wells, flow

geometries in such wells are increasingly complex and analytical methods could hardly provide accurate prediction of well performance. Brekke and Johansen (1993) introduced a comprehansive simulation approach called the Network model for the horizontal wells with complex flow paths. This network model described the wellbore. The network model was coupled to a reservoir simulator as a series of nodes that were interconnected by the flow paths. The network simulator was used to plan well location, well trajectory and completion design.

Ouyang, et al. (1996) presented a general wellbore flow model incorporating frictional, accelerational, gravitational pressure drops and the pressure drop caused by inflow. This model was applied to horizontal, vertical, and slanted well completions. It was concluded that comparing to frictional pressure drop, pressure drop caused by acceleration could be important depending on the pipe geometry, fluid properties and other conditions.

Based on the basic network model, Brekke (1996) incorporated uncertainties related to the completion, near wellbore geology and formation damage into the network solver. The research demonstrated the influence of geological uncertainties and completion efficiency to the well productivities along the horizontal wells.

Brekke and Thompson (1996) developed an efficient method which applied semi-analytical network approach and upscaled reservoir properties for the radial flow to simulate the well and reservoir. This method could demonstrate the influence of geology uncertainties and completion efficiency to the distribution of total well productivity for finite and infinite conductivity horizontal wells of different lengths. Model verification was done for the permeability upscaling procedure, fully penetrating horizontal well, partially penetrating horizontal well, pseudo steady-state reservoir response using superposition in space.

Permadi, et al. (1997) conducted a laboratory experiment to treat the water coning

problems using a stinger completion. It was showed that horizontal well with stinger might not achieve good early recovery performance, but in long term Stinger completion could ease the cone of water, decrease the rate of water cut and enhance the recovery significantly.

Holmes, et al. (1998) developed a model to simulate horizontal and multilateral wells and well with flow control devices. The proposed well model which could simulate the fluid flow rate, the wellbore contents and pressure drop along the well, also indicated an accurate treatment of cross flow and multiphase flow. Two different well completions with flow control devices were discussed in the paper, and the drift flux multiphase flow model could provide stable results at low flow rates while the phases tending to counter flow.

Schulkes et al. (1999) presented experiments on the pressure loss for pipe flow with radial inflow for which they derived the formulation of an effective friction factor relating to the rate at which the radial momentum is transferred in the axial direction. An accurate and simple model was established to predict the pressure loss in pipe flow with radial inflow, and it could be applied in long, flat oil reservoir with high permeability.

Penmatcha, et al. (1999) presented research on the effects of pressure drop in horizontal wells and optimum well length. Well length is a critical parameter. While it is increasing, the contact with reservoir is increasing. However, the well costs are also increasing. Wisely planning the well length would optimize the overall economy of a horizontal well. A semi-analytical well model was presented for homogenous reservoirs.

Holmes (2001) did research on modeling advanced wells which include horizontal, multilateral and smart wells such as sensors, flow control, and other devices in reservoir simulation. The model was able to accurately predict the pressure and fluid flow rate at all locations in the well over the lifetime of the reservoir and the pressure drop across control

devices.

Jansen (2003) presented a semianalytical model for calculating pressure drop along horizontal wells with stinger completions. The purpose for this work was to treat the unequal drawdown due to the pressure drop along the horizontal well. The model was able to simulate fluid flow in a looped configuration using an iterative method combining numerical integration or analytical integration in terms of Jacobian elliptic functions.

Johansen and Khoriakov (2006) applied an iterative two-phase network solver to predict the flow performance and investigated complex wellbore situations, such as three phase flow, more general boundary conditions, phase slippage, flow regimes, multi-lateral wells and coupled well flow and reservoir flow.

Thanyamanta (2007) adopted the iterative network model to predict asphaltene precipitation by incorporating compositional and non-isothermal effects into the base two-phase network solver, and investigated the precipitation problems in the different well completions.

Chapter 3 Network Model

A horizontal well has longer wellbore, which means it has more contact with reservoir, but the resistance to the flow in the well also increases. Compared to vertical wells, horizontal wells have more uncertainty in achieving good productivity. Therefore, in order to produce hydrocarbons at a commercial rate, horizontal wells are equipped with various complex completions which make the flow geometries more complicated; recently the well completions techniques became more and more complex and the traditional simulator using grids may no longer reach the precision needed to accurately predict the well performance along the complex well completion paths.

Because of its efficiency and accuracy, mathematical simulation models are extensively used to predict flow conditions and phase behaviors in complex well completions. One of these models, 'Network solver' has been widely applied to accurately predicted the flow conditions inside the wellbore and near the wellbore region for complex horizontal wells (Brekke and Johansen, 1993).

3.1 Structure of the network model

In the network model, the horizontal well geometry is discretized to a network system consisting of nodes with flow connections. As show in figure 3.1.1, three kinds of nodes exist. The upper row represents the reservoir, the bottom row represents wellbore, and the middle row represents the annulus. The bridges connecting each pair of nodes represent flow channels. All these nodes and bridges constitute a network tracking the flow paths that represent the whole well from toe to heel as show in figure 3.1.1. This is a basic network solver commonly used in simulation. The entire horizontal well is divided into a finite number of segments (N)

with specified length as shown in Figure 3.1.1. The number of segments or the density of the node distribution depends on the degree of accuracy required.

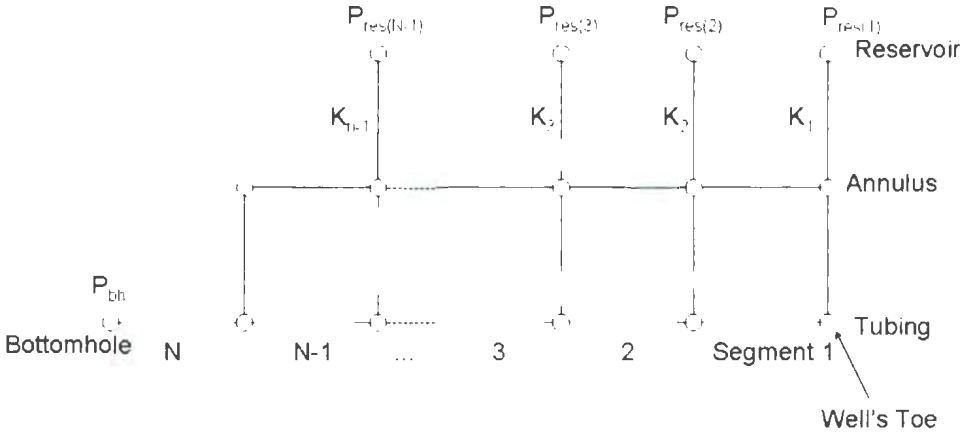

Figure 3.1.1. Network structure and flow parameters at segments

One segment consists of 3 nodes and 4 flow connections, these nodes are reservoir node, annulus node, and tubing node and flow connections include flows between reservoir and annulus (inlet flow), annulus and tubing, two adjacent annulus nodes, and two adjacent tubing nodes. All the nodes represent specific locations in the reservoir, annulus or wellbore. Therefore they may have different reservoir properties, such as pressure (P_{res}), temperature (T_{res}) and permeability (K). Because of the pressure difference between reservoir and wellbore bottom hole, reservoir fluids enter the perforations into the well annulus and then flow into the wellbore through the slot liners on the wellbore casing. Finally, fluid in the wellbore travels from the toe, through the horizontal well and arrives at heel. Fluid in tubing flows from well toe to well heel, however, the flow direction in reservoir and annulus may be reversed depending on the configurations of the well completion, the pressure distribution and fluid properties.

The nodes of the Network solver could be sorted as one of the following three kinds

a) Nodes with unknown flow rate and pressure nodes

(Typically used for internal nodes: 1, 2, 4, 5, 7, 8)

b) Nodes with specified pressure, but unknown mass flow rate

(Typically used for boundary nodes: 3, 6, 9 and outlet nodes which stand for reservoir)

c) Specified mass flow rate, but unknown pressure

(Typically used for boundary nodes: 3, 6, 9, and outlet nodes)

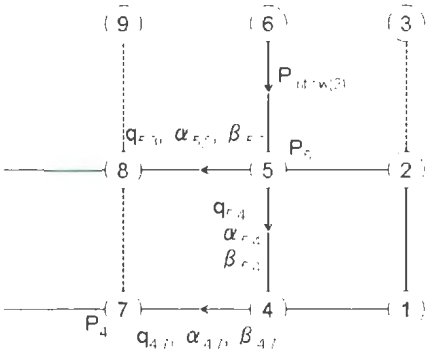

Figure 3.1.2. Unknowns in segment 2 of the Network

In order to solve the unknown flow parameters, unknown pressures are assigned at the nodes, flow rates and phase fractions are assigned at the bridges (Figure 3.1.2). Since the network solver for the flow problem is constructed from mass and momentum balances, each segment will have 12 unknowns (tubing pressure, annulus pressure, flow rate at tubing, flow rate at slot, flow rate at annulus, inlet flow rate, water phase fraction at tubing, water phase fraction at slot, water phase fraction at annulus, oil phase fraction at tubing, oil phase fraction at slot, and oil phase fraction at annulus). However the last segment is an exception (Segment N in fig 3.1.3), which does not have inlet flow rate and annulus flow rate and annulus phase fraction. Therefore, the total number of unknowns is 8. If the entire length of well is divided into N segments, the total number of unknowns is $12 \times N - 4$ for the whole network system. In this research, we adopt Newton-Raphson iterative method to solve the unknown flow

parameters from the non-linear equations corresponding to mass and momentum balances.

3.2 Multi-phase flow Models

As three phase fluid behavior is the target subject for this research, the proposed network model considers multi-phase flow and mass transfer between phases in the governing equations. Brill and Mukherjee (1999) proposed black-oil model and compositional model for multi-phase flow. Black-oil model, Pressure-Volume-Temperature (PVT) model, uses the correlations to determine the fluid properties in terms of stock-tank oil, gas gravities, and phase ratios at different temperatures and pressures. The compositional model analyses the fluid in terms of components, their individual properties and the fluid composition.

Petroleum reservoir fluids are mainly composed of hydrocarbon, but in enhanced oil recovery procedures, other fluids including non-hydrocarbon gas, chemicals, steam, etc. are injected into the reservoir to achieve improved recovery, which makes reservoir phase behavior more and more complicated. Therefore, an appropriate multiphase model which correctly describes the interactions between phases for specific reservoir is very important to simulate fluid properties for multi-phase flows. First of all, we identify which type of reservoir we deal with, and then choose a suitable multi-phase flow model to start the simulation. Reservoir temperature, pressure and fluid phase envelope are commonly used for the classifications of reservoirs.

3.2.1 Black oil model

The typical phase diagram of a reservoir hydrocarbon system is shown in Figure 3.2.1, which is used to describe various types of reservoir fluids conveniently. The most common

type of oil reservoirs is black oil reservoirs, in which the oil is generally composed of more than 20 mole% heptanes and heavier compounds. This character makes black oil reservoir phase-envelop the widest of all types of reservoir fluid, and have broadly spaced quality (iso-volume) lines and relatively lower saturation pressure; the hydrocarbon mixture's critical temperature is well above the reservoir temperature. These characteristics lead to a low shrinkage of produced oil and less gas produced from reservoir.

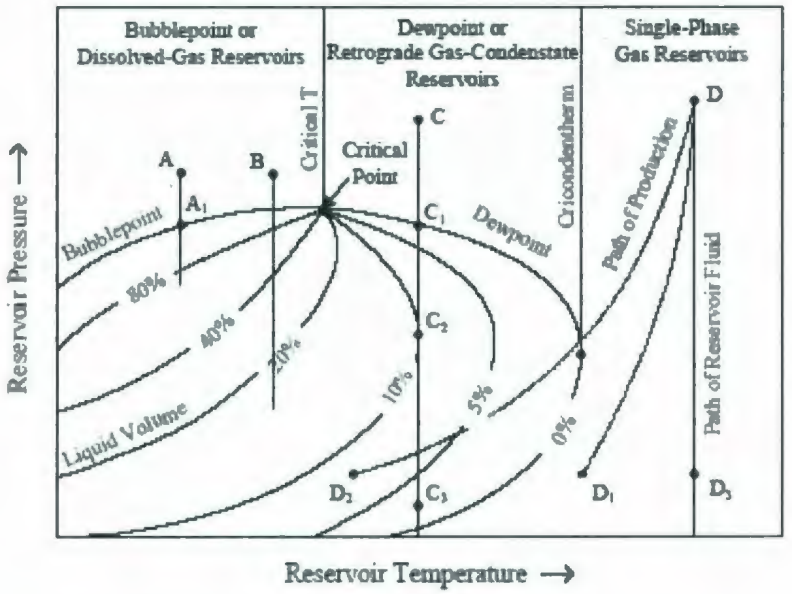

Figure 3.2.1 Reservoir Classification

As shown in Figure 3.2.1, at the reservoir condition of point A, the black oil reservoir fluid stays in single liquid phase initially. During the oil production, reservoir pressure continuously decreases and eventually drops below the bubble-point pressure (A_1) where gas phase starts to occur. There are oil and gas (two phases) inside the phase envelope.

When the reservoir temperature is near the critical point (Point B in Figure 3.2.1), the reservoir fluids are classified as 'Volatile oils' which are also called 'near-critical oils'. As shown in Figure 3.2.1, the iso-volume lines of volatile oils are closer to the bubble point curve,

so that any reduction of pressure below the bubble point could cause significant decrease of oil fractions in reservoir and increase of gas production.

While temperature lies between the critical temperature and the cricondentherm (Point C in Figure 3.2.1), the reservoirs are so called condensate reservoirs, or retrograde reservoir. In the reservoir, when the pressure falls below the dew point as demonstrated in Figure 3.2.1 from C_1 to C_2, liquid drops out because of the condensation effect resulting in liquid volume increases. However, after Point C_2 the liquid volume resumes decreasing.

The reservoir temperature is above the cricondentherm (Point D in Figure 3.2.1) in the gas reservoir where only gas phase appears. Dry gases are mainly composed of methane and non-hydrocarbons like nitrogen and carbon dioxide, the produced fluids from these dry gas reservoirs remain single phase at separator conditions (Point D_1). To the contrary, if the produced fluids at separator conditions (Point D_1) contain oil and gas, these gas reservoirs are called wet gases.

As the water is the common third phase in the reservoir during the depletion, we consider water as the third phase in this work. Only non-volatile and isothermal reservoirs are considered here, reservoir temperatures are well away from critical temperatures of fluids, and the evolved gas phase contains few heavy compounds. In the other words, a black oil three phase (oil/water/gas) model is chosen.

Black oil models in this research consider a fluid as a system consisting of three components: water, oil, and gas at stock-tank conditions. As usually the water in reservoir contains salt, the water phase in the model is described as brine with certain salt concentration, since the solubility of hydrocarbon compounds in water decreases with increase of water salinity. To simplify the model we would ignore mass transfer between water phase and the

other two phases. The oil phase is composed of black oil with dissolved gas. Therefore, the mass transfer between oil and gas phases is defined by the solubility of gas which is represented as Solution gas oil ratio (R_s)in the oil phase due to the different reservoir conditions.

Before defining the black oil model parameters, related terms in oil and gas production are introduced as following. Oil volume and water volume under reservoir condition are assigned as V_o^{RC} and V_w^{RC} , respectively. Oil and water volume under stock tank condition are V_o^{STC} and V_w^{STC} , respectively. The volume of gas at reservoir condition is V_g^{RC} , and the volume at stock tank condition is V_g^{STC} . The volume of dissolved gas in oil phase (dg) at stock tank condition is V_{dg}^{STC} . The volume of free gas (fg) at reservoir condition is V_{fg}^{RC} , and the volume of fg at stock tank condition is V_{fg}^{STC} .

3.2.2 Basic Black oil-water-gas model parameters

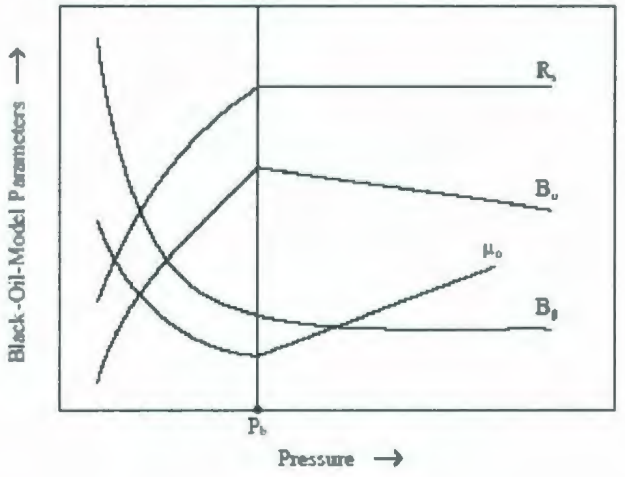

Figure 3.2.2 Black oil parameters

3.2.2.1 Gas Oil Solubility Ratio

Gas oil solubility Ratio (GOR), also called gas solubility (R_s) factor, is defined as the ratio of produced gas to produced oil: $R_s = \frac{V_{dg}^{STC}}{V_o^{STC}}$ (3.2.1)

$$\text{Or } R_s = \gamma_g \left(\frac{P}{18.10^{.000091^{T_{res}}-0.0125\,API}}\right) \quad (3.2.2)$$

Where γ_g is gas gravity, API is a specific gravity scale developed by the American Petroleum Institute (API) for measuring the relative density of various petroleum liquids, expressed in degrees, P is the reservoir pressure above bubble point pressure (Danesh, 1998).

This parameter describes the mass transfer between oil and gas phases according to the reservoir pressure and temperature change during the productions. Figure 3.2.2 shows that above bubble point pressure, R_s retains constant while the pressure increasing, and the oil phase is treated as 'under saturated'. Once the reservoir pressure decreases and reaches the

bubble point pressure, the oil fluid is considered as saturated; moreover if the pressure continues falling below the bubble point pressure, R_s decreases sharply along the pressure decreasing and the gas which could not be dissolved in the oil would break out from the oil phase.

3.2.2.2 Oil Formation Volume Factor

When the reservoir fluids including water and oil are brought to the surface, the volume of the fluids would change due to the pressure and temperature difference between the reservoir condition and stock tank condition. As most measurements of oil and gas production are undertaken at surface, but the fluid flow happens in the reservoir formation and production well, so that volume factor need to be converted from volume measured from surface at stock tank condition to that at reservoir condition.

Then the formation volume factor of oil (B_o) is defined as oil and dissolved gas volume at reservoir conditions divided by oil volume at standard conditions, in formulation:

$$B_o = \frac{V_o^{RC}}{V_o^{STC}} \tag{3.2.3}$$

$$\text{Or } B_o = 0.972 + 0.000147 F^{1.175} \tag{3.2.4}$$

$$\text{Where } F = R_s \sqrt{\gamma_g / API} + 1.25T$$

γ_g is gas gravity, T is reservoir temperature (Danesh, 1998).

The oil formation volume factor value could be affected by the combined effect of liberated gas, thermal compaction, and pressure expansion.

As shown in Figure 3.2.2, while the reservoir pressure is above bubble point pressure, the oil formation volume factor (B_o) increases with the decreased pressure, which means that oil

volume in the reservoir swells while the reservoir pressure is falling down, and the solubility of gas in oil fluid remains almost constant; on the other hand when reservoir pressure falls below the bubble point pressure, gas solubility decreases while the reservoir pressure decreases, and the dissolved gas in oil fluid breaks out, this is why the oil volume decreases while the pressure decreases at this condition.

3.2.2.3 Gas formation volume factor

The gas formation volume factor is defined as gas volume at reservoir conditions divided by gas volume at stock tank conditions:

$$B_g = \frac{V_g^{RC}}{V_g^{STC}} \tag{3.2.5}$$

Figure 3.2.2 shows that gas formation volume factor is monotonically decreasing with pressure, and applying the real gas equation-of-state, i.e., $PV = ZnRT$, where P, V, T represents reservoir pressure, gas volume, and reservoir temperature respectively; n is mole number of gas and Z is a correction factor called the gas compressibility factor or simply Z-factor. Substituting for the volume V in the $B_g = \frac{V_g^{RC}}{V_g^{STC}}$ gives the real gas law:

$$B_g = Z \frac{P_{STC}}{P_{RC}} \frac{T_{RC}}{T_{STC}} \tag{3.2.6}.$$

Where P_{STC} and T_{STC} are pressure and temperature at stock tank conditions, then P_{RC} and T_{RC} are those at reservoir conditions.

3.2.2.4 Water Formation Volume Factor

Water formation volume factor is defined as water and dissolved gas volume at reservoir conditions divided by water volume at standard conditions, in formulation

$$B_{w} = \frac{V_{w}^{RC}}{V_{w}^{STC}} \tag{3.2.7}$$

This value can often be neglected, since it is always close to 1.0.

In case we need to consider the dissolved gas in the formation water, due to the combined effect of liberated gas, thermal compaction, and pressure expansion which is the same as the oil phase, the volume of water would generally increase while it is taken to the surface. According to Peneloux and Rauzy (1982), we have the following correlation,

$$B_{w} = (1 + \Delta V_{wP})(1 + \Delta V_{wT}) \tag{3.2.8}$$

where ΔV_{wP} and ΔV_{wT} are the volume changes caused by pressure and temperature, and

$$\Delta V_{wP} = -(3.598922 \times 10^{-2} + 1.95301 \times 10^{-9} T)P - (2.25341 \times 10^{-10} + 1.72834 \times 10^{-13} T)P^2$$

..... (3.2.9)

$$\Delta V_{wT} = -1.0001 \times 10^{-2} + 1.33391 \times 10^{-4} T + 5.50654 \times 10^{-7} T^2 \tag{3.3.10}$$

This correlation is valid at $T < 260^{\circ}F$ and $P < 5000 psia$, over a wide range of salt concentration.

3.2.3 Phase Viscosity Calculations

Viscosity is an important property of fluids, which indicates their resistance to flow, so the fluid is a key factor to estimate the wellbore pressure drop and it is defined as shear stress divided by shear rate, in formulation:

$$\mu = \tau / \gamma \tag{3.2.11}$$

Where μ is viscosity [$Pa \cdot s$], τ is shear stress in [Pa], and γ is shear rate in [$1/s$]. This is a general equation for all fluids, but for different type of Newtonian fluid, the calculations are

different, the outline of viscosity calculations for oil and water is listed below.

3.2.3.1 Oil Viscosity

As shown in the Figure 3.2.2, oil viscosity is a strong function of pressure because of the combined effects of liberated gas, and pressure expansion related to pressure condition, at the same time bubble point pressure is also a critical factor for the value of oil viscosity. Below the bubble point oil viscosity decreases while the pressure increasing as the dissolved gas volume increasing. Above the bubble point pressure, the oil viscosity increases with pressure because of the oil shrinkage or compressibility.

Numerous black oil viscosity correlation methods have been proposed and all of them are based on fitting available field-measured variables to an empirical equation, these variables include a combination of gas solubility (R_s), bubble point pressure, oil API gravity, temperature, specific gas gravity, and dead oil viscosity (oil at sufficiently low pressure that it contains no dissolved gas).

Among all viscosity prediction correlation, Beggs and Robinson (1975) is one of the best correlations which could reasonably fit empirical equations.

Dead oil viscosity correlation is defined as:

$$\mu_{od} = 10^{X} - 1 \tag{3.2.12}$$

Where $X = 10^{(3.0324 - 0.02023 \cdot API)} T^{-1.163}$, μ_{od} is dead oil viscosity, T is system temperature, and API is oil gravity.

Bubble point oil correlations are as follow:

$$\mu_{ob} = a(\mu_{od})^{b} \tag{3.2.13}$$

Where $a = 10.715(R_s + 100)^{-0.515}$ and $b = 5.44(R_s + 150)^{-0.338}$, μ_{ob} is oil viscosity at the bubble

point which is considered saturated oil viscosity.

Finally the under saturated oil viscosity which is at the pressure above the bubble point pressure can be calculated from the correlations as below:

$$\mu_o = \mu_{ob} + 0.001(P - P_b)(0.024\mu_{ob}^{1.6} + 0.038\mu_{ob}^{0.56}) \quad (3.2.14)$$

Where P_b is bubble point pressure, and P is the pressure of the system.

3.2.3.2 Water Viscosity

McCain (1990) proposed correlations to predict saline water viscosity. First the viscosity of brine at atmospheric pressure could be estimated from:

$$\mu_{w1} = (109.574 - 8.40564W_s + 0.313314W_s^2 + 8.72213\times10^{-3}W_s^3)T^{-D} \quad (3.2.15)$$

Where $100\ F < T < 400\ F$, $W_s < 26\%$ and W_s is the weight percent of salt in brine, and

$$D = 1.12166 - 2.63951\times10^{-2}W_s + 6.79461\times10^{-4}W_s^2 + 5.47119\times10^{-5}W_s^3 - 1.55586\times10^{-6}W_s^4$$

And the viscosity of brine at reservoir conditions can be estimated from the effect of pressure on the brine viscosity,

$$\mu_w / \mu_{w1} = 0.9994 + 4.0295\times10^{-5}P + 3.1062\times10^{-9}P^2 \quad (3.2.16)$$

where $86\ F < T < 167\ F$ and $14,000 psia < P$.

3.2.3.3 Gas viscosity

Lee, et al. (1966) measured the viscosity of four natural gases over a temperature range of 311-444 K, up to 5.5168×10⁴KPa, and proposed the following correlation,

$$\mu_g = 10^{-4} a \exp[b(\rho_g / 62.43)^c] \quad (3.2.17)$$

where $a = (9.379 + 0.0160M)T^{1.5}/(209.2 + 19.26M + T)$,

$b = 3.448 + 0.01009M + (986.4/T)$, $c = 2.4 - 0.2b$

μ_g is the gas viscosity (CP) at absolute temperature of T (R), M is the gas molecular weight, and ρ_g is the gas density at prevailing pressure and temperature in [lbm/ft^3].

3.2.4 Phase Density Calculations

The density of the reservoir fluid at reservoir conditions should be estimated; so that we could estimate the shrinkage effect in volume while the reservoir fluids are taken to the stock tank conditions.

3.2.4.1 Oil Density

The correlations for oil density calculation applied in this research were introduced by Danesh (1998). First of all, by using the calculated oil formation volume factor, the density of saturated oil could be estimated from

$$\rho_o = (62.4\gamma_o + 0.0136R_s\gamma_g)/B_o \qquad (3.2.18)$$

where ρ_o is saturated oil density, R_s is gas solubility, B_o is the calculated oil formation volume factor, γ_o and γ_g are specific gravity, relative density at 288 K for oil and gas respectively.

Vasquez and Beggs (1980) proposed correlation to estimate the isothermal compressibility coefficient (C_o) over the pressure range of bubble point pressure to system pressure as follow:

$$C_o = (-1433.0 + 5.0R_s + 17.2T - 1180.0\gamma_g + 12.61API)/(10^5 P) \qquad (3.2.19)$$

Applying C_o above, we could adjust the calculated saturated oil density due to

compression for an under saturated oil.

$$\rho_{op} = \rho_o \exp[C_o(P - P_b)] \tag{3.2.20}$$

where ρ_{op} is the oil density at pressure P.

3.2.4.2 Water Density

McCain, et al. (1986) proposed correlations to estimate the density of saline water. The density of formation water at standard condition could be estimated from:

$$\rho_{w(sc)} = 62.368 + 0.438603W_s + 1.60074 \times 10^{-3} W_s^2 \tag{3.2.21}$$

where W_s is the weight percent of salt in brine.

Therefore neglecting the dissolved gas in water at reservoir conditions, the water density could be estimated as,

$$\rho_w = \rho_{w(sc)} / B_w \tag{3.2.22}$$

where B_w is the formation volume factor at the prevailing conditions.

3.2.4.3 Gas Density

From Gay-Lussac law and Avogadro's law, we have the equation of state for real gases:

$$PV = ZnR_u T \tag{3.2.23}$$

Where n is the number of moles of the gas, N_a is Avogadro's number ($N_a = 6.023 \cdot 10^{23}$), R_u is the universal gas constant, $R_u = N_a k = 8.31 J/K$, k is the universal Boltzman's constant, $k = 1.38 \cdot 10^{-23} J/K$.

From (3.3.23), we could derive equation of state for specific gas as follow.

$$\rho = \frac{P}{ZRT} \tag{3.2.24}$$

ρ is gas density, R is gas constant for the specific gas, $R = \frac{R_u}{W}$, W is the molecular weight of the gas, T is the prevailing temperature.

3.3 Conservation Models

As we discussed before, the network model is based on mass balance and momentum balance. There is no accumulation of mass allowed anywhere in the system, i.e. the flow is steady-state. The mass balance is shown in following equation:

$$\sum_{i=1}^{n} \dot{m}_i = 0 \tag{3.3.1}$$

This formula is suitable for each node in network accounting for all fluid mass flowing in and out through the flow bridges, and n stands for the number of the bridges connected to the specific node.

And mass balance law is implemented in three individual phases, which could be formulated in:

$$\dot{m}_{in\ oil} = \dot{m}_{out\ oil} \tag{3.3.2}$$

$$\dot{m}_{in\ water} = \dot{m}_{out\ water} \tag{3.3.3}$$

$$\dot{m}_{in\ gas} = \dot{m}_{out\ gas} \tag{3.3.4}$$

For one-dimensional steady-state momentum balance, the following equations model the pressure drop caused by acceleration, friction, and gravity.

$$\dot{m}v = -\left[pA - \tau_w P\right]_z - \rho g A\left[z\sin\theta\right] \tag{3.3.5}$$

Or in differential form:

$$\frac{dp}{dz} = -\frac{\dot{m}}{A}\frac{\partial v}{\partial z} - \frac{\tau_w P}{A} - \rho g \sin\theta \qquad (3.3.6)$$

where τ_w is the wall stress, A is the cross section area of the duct and P is the wetting perimeter. Applying Poiseuille theory to the friction term $\frac{\tau_w P}{A}$, and $\tau_w = \frac{A}{P}\frac{dp}{dx}$, as the number $\frac{A}{P}$ has a physical significance, the hydraulic diameter (D_h) is defined as $D_h = \frac{4A}{P}$, therefore the pressure loss due to friction is given by

$$\frac{dp}{dx} = \frac{f\bar{\rho}u^2}{2D_h} \qquad (3.3.7)$$

where f is the friction factor, the value of this parameter is

$f = 4\frac{Wall\_Shear\_Stress}{Dynamic\_Pressure} = \frac{64}{\mathrm{Re}}$, and Re is the Reynolds number of $\frac{\bar{\rho}uD_h}{\mu}$.

When flow is laminar, $\mathrm{Re} < 2000$; when flow is turbulent, $\mathrm{Re} > 3000$; when $2000 < \mathrm{Re} < 3000$, there is a transition between laminar and turbulent flow.

The momentum balance equation is formed in another way with the friction factor:

$$\frac{dp}{dz} = -\frac{\dot{m}}{A}\frac{dv}{dz} - \frac{f\bar{\rho}v^2}{2D_h} - \bar{\rho}g\sin\theta \qquad (3.3.8)$$

This is applied to the mixed three phase fluid, and $\bar{\rho}$ and μ are the average density and viscosity of the mixed three phase fluid respectively.

3.4 Governing Equations for Network Solver

The three phase network model is formulated to solve flow with mass transfer between phases and momentum balance problems in three individual phases under isothermal

conditions. The fundamental three phase network model is developed by modifying the two-phase solver network developed for one phase flow by Johansen (2005) which were later modified by Thanyamanta (2007) to apply to two phases, oil and gas. In this research conservation of the water phase is built into the two phase model to achieve the three individual phase black oil network model. The model solves pressure distribution, flow rates and phase fractions in the completion and in the wellbore region.

We use Segment 2 in Figure 3-1-1 and 3-1-2 to formulate the governing equations. Given reservoir pressure (P_{res}), temperature (T_{res}), phase fractions (oil: α , water: β), fluid and reservoir properties, there are 12 unknowns associated with segment 2: Pressure at tubing node (P_4), pressure at annulus node (P_5); flow rate in tubing bridge (q_{4-}), the rate in slot bridge ($q_{5,4}$), flow rate in annulus bridge ($q_{5,8}$), inlet flow bridge ($q_{inlet\ flow(2)}$); phase fractions at tubing bridge (oil: α_{4-} , water: β_{4-}), phase fractions in slot bridge (oil: $\alpha_{5,4}$, water: $\beta_{5,4}$), and phase fractions in annulus bridge (oil: $\alpha_{5,8}$, water: $\beta_{5,8}$). All subscripts represent the specific nodes in segment 2, and gas phase fraction could be easily derived from:

$$Gas\_Phase\_Fraction = 1 - Oil\_Phase\_Fraction - Water\_Phase\_Fraction$$

12 equations are required to solve these 12 unknowns and 4 types of models or equations are involved to obtain the governing equations for the network solver. These are:

- Mass balance (Material balance) equations for three individual phases at tubing and annulus nodes.
- Inlet flow equation or productivity equation
- Momentum balance equations for flow bridges: tubing bridge, annulus to tubing bridge, annulus bridge and reservoir to annulus bridge.

●Split equations

3.4.1. Material Balance for three individual phases at nodes

As discussed early in this chapter, the mass balance could be formulated for three phases based on the equation (3.4.1) as follow:

$$\sum_{i=1}^{n} \dot{m}_i = \dot{m}_{in} - \dot{m}_{out} = 0$$

It could also be written as

$$\sum_{i=1}^{n} \dot{m}_i = \sum_{i=1}^{n} \rho_i q_i = 0 \qquad (3.4.1)$$

where q is the mixed three phase flow rate (oil, water and gas) connected to a specific node and ρ is the phase density at specific bridge. For the flow direction, we assign flow towards the nodes (inflow) a positive sign, and flow away from nodes (outflow) a negative sign.

For Node 4, there are 3 associated flow bridges: Bridge 1 – 4, 5 – 4, 4 – 7 as shown in Figure 3-1-2. The material balance for oil component at Node 4 is:

$$\rho_{o1,4}^{RC} q_{1,4} \alpha_{1,4} + \rho_{o5,4}^{RC} q_{5,4} \alpha_{5,4} + \rho_{o4,7}^{RC} q_{4,7} \alpha_{4,7} = 0 \qquad (3.4.2)$$

Where ρ_o^{RC} 's are oil density at reservoir conditions.

We convert the oil parameters measured at reservoir conditions (ρ_o^{RC}) to stock tank conditions (ρ_o^{SC}) by the oil formation volume factor ($\rho_o^{SC} = \rho_o^{RC} B_o$). So equation (3.4.10) could be written as:

$$\frac{q_{1,4} \alpha_{1,4}}{B_{o1,4}} + \frac{q_{5,4} \alpha_{5,4}}{B_{o5,4}} - \frac{q_{4,7} \alpha_{4,7}}{B_{o4,7}} = 0 \qquad (3.4.3)$$

Similarly, the material balance for the water component could be written as:

$$\frac{q_{1,4}\beta_{1,4}}{B_{o1,4}}+\frac{q_{5,4}\beta_{5,4}}{B_{o5,4}}+\frac{q_{4,7}\beta_{4,7}}{B_{o4,7}}=0 \qquad (3.4.4)$$

The material balance for gas component must include two phases: Free gas ($\rho_g^{RC} q(1-\alpha-\beta)=\rho_g^{STC} q(1-\alpha-\beta)/B_g$) and the dissolved gas in oil phase in the term of $\rho_g^{RC} q_{dg}$ where q_{dg} is the dissolved gas volumetric flow rate, and using gas solubility (R_s),

$$\begin{aligned}\rho_g^{RC} q_g^{RC} &= \rho_g^{RC} B_g q_{dg}^{STC} \\ &= \rho_g^{RC} B_g q_o^{STC} R_s \\ &= \rho_g^{RC} B_g \frac{q_o^{RC}}{B_o} R_s \\ &= \frac{\rho_g^{STC} q_o^{RC} R_s}{B_o} \end{aligned} \qquad (3.4.5)$$

Gas material balance is formulated as:

$$\left(\frac{q_{1,4}(1-\alpha_{1,4}-\beta_{1,4})}{B_{g1,4}}+\frac{q_{1,4}\alpha_{1,4}R_{s1,4}}{B_{o1,4}}\right)+\left(\frac{q_{5,4}(1-\alpha_{5,4}-\beta_{5,4})}{B_{g5,4}}+\frac{q_{5,4}\alpha_{5,4}R_{s5,4}}{B_{o5,4}}\right)$$
$$+\left(\frac{q_{4,7}(1-\alpha_{4,7}-\beta_{4,7})}{B_{g4,7}}+\frac{q_{4,7}\alpha_{4,7}R_{s4,7}}{B_{o4,7}}\right)=0$$

..... (3.4.6)

3.4.2 Inlet flow equation or productivity equation

As near wellbore region has great pressure gradient perpendicular to the well trajectory, so we assume that the inflow is in radial directions. Therefore the inflow into the wellbore could be easily simulated by the inlet bridges connecting reservoir nodes and annulus nodes as shown in Figure 3-1-2. The inflow rate could be calculated by the Productivity Index (PI)

which is a mathematical means of expressing the ability of a reservoir to deliver fluids to the wellbore:

$$q_{\text{inflow}(2)} = PI\left(\frac{k_{ro}}{\mu_o} + \frac{k_{rw}}{\mu_w} + \frac{k_{rg}}{\mu_g}\right)(p_{res(2)} - p_5) \tag{3.4.7}$$

where $p_{res(2)}$ and p_5 is the reservoir pressure and annulus pressure at segment 2, k_{ro} , k_{rw} and k_{rg} are the relative permeabilities at near wellbore region in reservoir, and μ_o , μ_w and μ_g are the viscosities of oil, water and gas phase respectively.

The productivity index for a homogeneous and isotropic reservoir is $PI = \frac{2\pi KL}{\ln(\frac{r_e}{r_o}) + s}$,

where r_e is the drainage radius, r_o is the outer radius of horizontal well, s is the skin factor, K is the absolute permeability of reservoir for the specific segment which may vary from segment to segment.

3.4.3 Momentum Balance for flow bridges in the network system

Reservoir fluids flow through inlet bridges into wellbore, pass annulus bridges, annulus to tubing bridges and tubing bridges, and finally reach the well heel. Therefore, for each of these three types of bridges, a momentum balance equation is formulated as equation (3.3.6). According to Darcy's law, the total pressure drop is accounting for the effect of acceleration, friction, and gravity in equation 3.3.6. We consider only horizontal wells in this work. Hence, the gravity term is not present. Total pressure drop over the segment includes pressure drop due to wall friction and that due to acceleration of fluids. Usually pressure drop due to acceleration is less than 10% of total pressure drop, therefore after prior investigation pressure

drop due to acceleration could be neglected. Moreover, the friction effect is especially important in the case of long horizontal wells and high permeability reservoirs. The pressure drop through internal bridges of the network model is assumed to result mainly from wall friction in equation 3.3.7. Therefore, only friction term would be considered in momentum balance.

As additional roughness caused by perforations and pressure drop caused by reservoir inflows, it is more complicated to simulate the frictional pressure drop than a smooth pipe. Furthermore, reservoir inflows through perforations cause pressure drop due to the acceleration effect. The inflow fluid radially enters the wellbore through perforations, crosses the completions and combines with the main flow in the well. This fluid flow changes the wellbore's boundary layer, and increases the pressure loss due to the fluid moving from upstream to downstream.

In order to account frictional pressure drop and additional pressure drop for the active inflows , Asheim, et al. (1992) proposed a model to calculate an 'equivalent' friction factors for smooth pipes. This correlation is applied to calculate pressure loss due to reservoir inflows in completed horizontal wells. And the total friction factor is the sum of the wall friction factor and the inflow equivalent friction factor.

Flows in the annulus and tubing space are calculated by the term of turbulent friction factor. Blasius (1913) proposed a simple friction factor for turbulence flows in smooth pipes; this friction factor correlation applies for the Reynolds number more than 3000.

$$f = \frac{0.3164}{\sqrt[4]{R_{eD}}} \tag{3.4.8}$$

Where R_{eD} is the Reynolds number calculated with hydraulic diameter D_h.

Su and Gudmundsson (1993) modified this correlation for completed-well friction, and called it 'Blasius-type':

$$f = \frac{a}{\mathrm{R}_e^{\,m}} \tag{3.4.9}$$

Parameters a and m were achieved by experimental method and represented the friction effect due to inflow perforations; the Reynolds number $\mathrm{R}_e = \frac{\rho v D_h}{\mu}$.

To simplify the model, the original Blasius' friction factor (Equation 3.4.8) is applied in the pressure drop equations for the annulus and tubing bridge.

And annulus to tubing flows pressure drop is calculated using a nozzle equation with a discharge coefficient, which is introduced in the following Annulus to Tubing Flow Equation part in equation 3.4.13 and 3.4.14.

Annular Flow Equation

The simplified momentum balance for the annulus bridges is:

$$\frac{dp}{dz} = \frac{f\rho v^2}{2D_h} \tag{3.4.10}$$

For segment 2, the above equation is:

$$\frac{p_5 - p_8}{L} = \frac{f\bar{\rho}}{2D_h}\left(\frac{q_{5,8}}{A}\right)^2$$

$$p_5 - p_8 = \frac{q_{5,8}^2 L f \bar{\rho}}{2D_h A^2} \tag{3.4.11}$$

where L is the length of segment 2, A is the cross-section area of annulus, $D_h = D_{out} - D_{in}$ (D_{out} is the wellbore diameter, and D_{in} is the tubing diameter) and $\bar{\rho}$ is the density for the three-

phase fluid.

Tubing Flow Equation

Similarly, the momentum balance for tubing in segment 2 is formulated as follow:

$$p_4 - p_5 = \frac{q_{4,5}^2 L f \overline{\rho}}{2 D_t A^2} \tag{3.4.12}$$

Where D_t is the tubing diameter.

Annulus to Tubing Flow Equation

Pressure drop in annulus to tubing bridge is caused not only by wall friction, but convergence of flow through slotted liner or valve openings which have small cross section area. In this research a discharge coefficient (c) is introduced to formulate the pressure drop along this bridge, which is similar to the flows through nozzles:

$$p_{annulus} - p_{tubing} = c \rho v^2 \tag{3.4.13}$$

Applying the above equation in segment 2, we obtain:

$$p_5 - p_4 = c \rho v^2 = c \overline{\rho} \left(\frac{q_{5,4}}{A} \right)^2 = \frac{q_{5,4}^2 c \overline{\rho}}{A^2} \tag{3.4.14}$$

where A is the total slot cross-section area, $A = \varpi LHW$; ϖ is the slot density, H is the slot height, and W is the slot width.

3.4.4 Split Equations

The above types of models give 10 equations (6 mass balance equations, 1 inflow equation, and 3 momentum balance equations). In order to solve 12 unknowns, the governing

equation system needs another 2 equations to make the network solver work, which is provided through 'split equations'. For internal nodes where fluids exit, splitting in two different directions occurs. We assume individual phase fractions in the directions are equal. These are the 'split equations'. For instance, if the flow direction in main wellbore is from well toe to well heel, then two streams ($q_{5,4}$ and $q_{5,8}$) exiting from Node 5 in segment 2. Therefore, we have two split equations:

$$\alpha_{5,8} = \alpha_{5,4} \tag{3.4.15}$$

$$\beta_{5,8} = \beta_{5,4} \tag{3.4.16}$$

Similarly, if the flow directions in the network system are assumed in the initial guess, then the split equations could be specifically assigned.

Applying the models and equations discussed before to the entire network system, totally $12 \times N - 4$ equations are achieved for $12 \times N - 4$ unknowns (the last segment at heel only has 8 unknowns) in the network solver. Since the governing equation system has been constructed, the Newton-Raphson iterative method could be implemented to solve the whole network with proper boundary condition and initial guess.

3.4.5 Boundary Conditions

Proper boundary conditions are required to solve the network system. First of all, the values of pressure at terminal nodes including reservoir nodes and the bottom-hole node are given as p_{res} and p_{bh} respectively.

Secondly, the temperatures, absolute permeabilities, saturations of oil water and gas phases at reservoir nodes are also provided.

To simplify the model: Before the simulation starts, the flow directions in the wellbore are assumed and assessed according to pressure distribution, the flow directions in tubing

bridges are assumed from well toe to bottom-hole (well heel) as positive direction; the flows through the inlet flow bridges are considered from reservoir towards wellbore as positive; the flow in annulus to tubing bridges are considered from annulus towards tubing as positive, all the flows in above bridges are always positive, and the flow directions in annulus bridges could be either from toe to heel (positive) or from heel to toe (negative) depending on the different flow paths due to different complex completions.

To effectively simulate the flow direction in the network model, the bridge indices are introduced to assign the flow direction in the well network model as positive (+1) or negative (-1) following the rules mentioned above (Thanyamanta, 2007). For the cases with complex completions, the bridges at specific nodes could be assigned to zero or negative (-1) in order to remove the flow bridges or change the flow directions, which enable the network system to simulate the complicated flow paths through the well completions.

3.4.6 Network Solver Flowchart

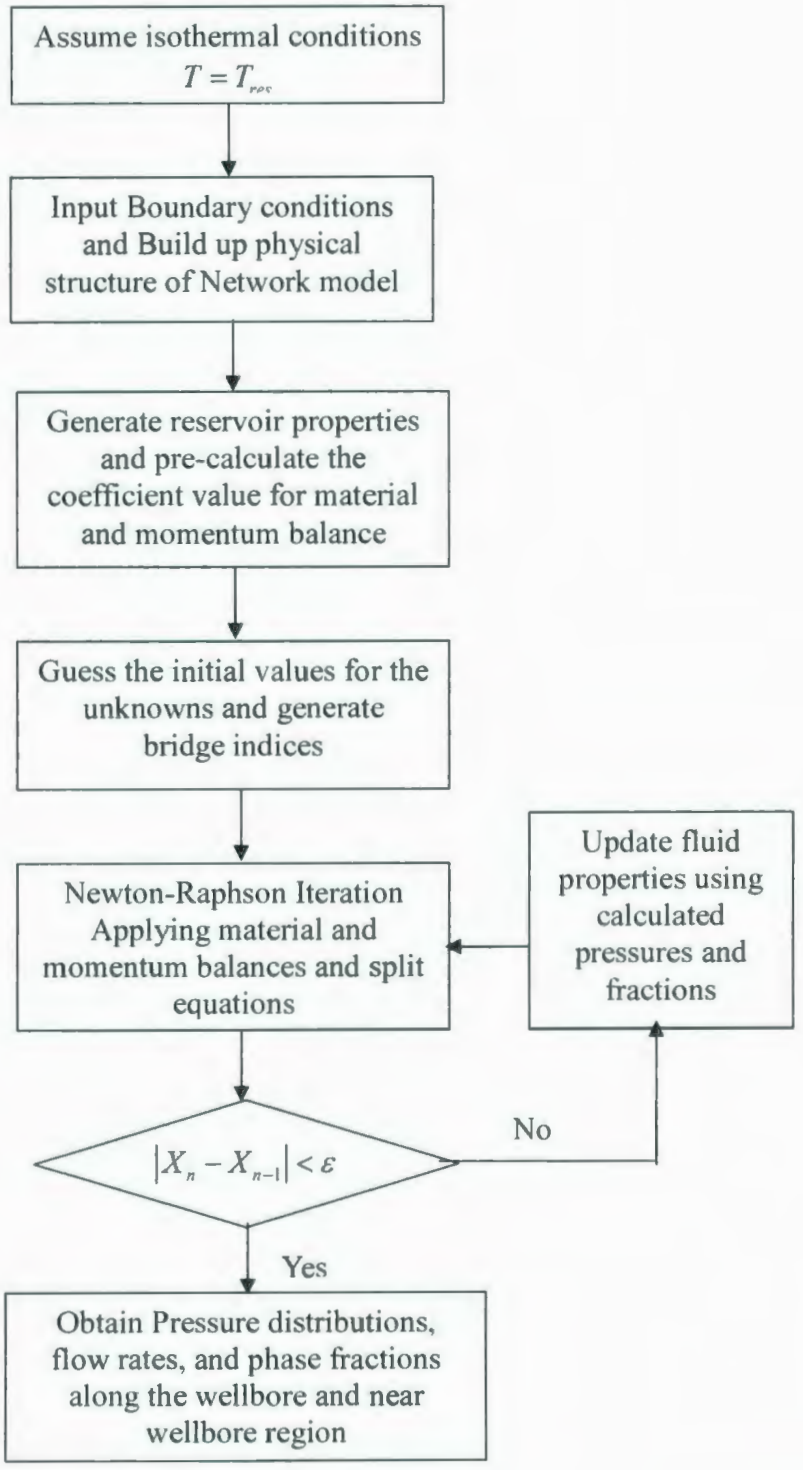

Figure 3.4.1 Network Solver Flowchart

Working steps of network solver for isothermal condition is shown in Figure 3.4.1,

Network solver would start from building up the frame and data structure of the network model to describe the physical configuration of the wellbore and near well region, and inputting boundary conditions. Secondly, generate reservoir fluid properties from boundary conditions and pre-calculate the values of the coefficients for material and momentum balances to improve the efficiency of calculations. Thirdly, guess the initial values for the unknowns for the entire network model and generate the bridge indices to indicate the flow directions. Newton-Raphson iterative method is implemented in next step to calculate the unknowns, and convergence threshold is used to decide the accuracy of the solutions of network solver. If the accuracy is not reached, iteration starts over using the pressure and fluid properties calculated by the previous iteration. The iteration would stop until the threshold is reached and finally network solver obtains pressure distribution, flow rate and phase fractions along the whole wellbore and near wellbore region.

Chapter 4 Stability test for the Network Solver

4.1 Network model stability test

After establishing the network solver for the three phase model, several special cases would be tested in order to ensure of consistency and robustness for the fundamental network solver. These cases are:

·Case 1: Two phase case as Oil/gas system above the bubble point pressure

·Case 2: Two phase case as Water/gas system

·Case 3: Three phase case with open hole without annulus flow and completion

·Case 4: Three phase case with pressure under bubble point for the entire well

·Case 5: Three phase case with encountering pressure under bubble point during the production

As the three-phase model was developed based on two-phase fluid model, first of all we should test and simulate two- phase system using three phase model by setting either oil or water saturations to be zero to obtain water-gas system or oil-gas system. In these cases (1,2) the well is completed with slotted liner (with slot length of .01 meter, width of .001 meter and density of 30000 slots per meter) which means reservoir fluids cross well annulus, through the slots, and finally into the well tubing. In the following plots, the three phase model deliveries the reasonable results for flow parameters including pressure loss, flow rate and phase fractions. Case 1 with oil-gas system is simulated as follow

Case 1: Two phase case as Oil/gas system above the bubble point pressure

Properties	Value
Well Length (m)	1000
Segment length (m)	10
Reservoir pressure (bara)	370
Pressure at heel (bara)	357.5
Reservoir temperature	100
Permeability (Darcy)	1
Near-wellbore skin factor	1
Oil saturation	1
Water saturation	0
Tubing diameter (m)	0.127
Well outside diameter (m)	0.167
Discharge coefficient for slot flow ($Pa \cdot (kg/m^3)^{-1} \cdot (m/s)^{-2}$)	10

Table 4.1 Properties and initial values for Oil/gas system above the bubble point pressure

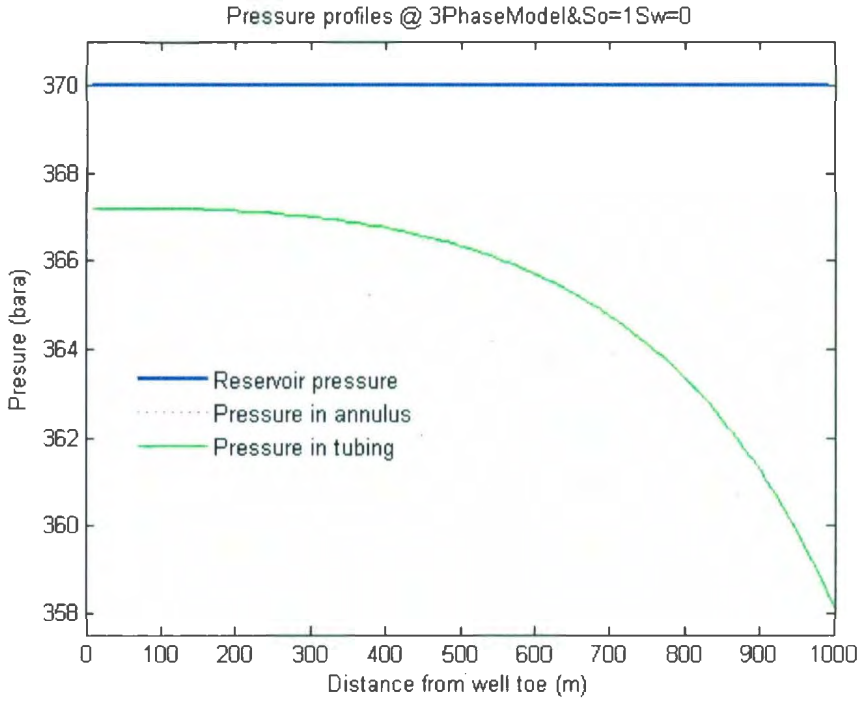

Figure 4.1 Pressure profile for Case 1

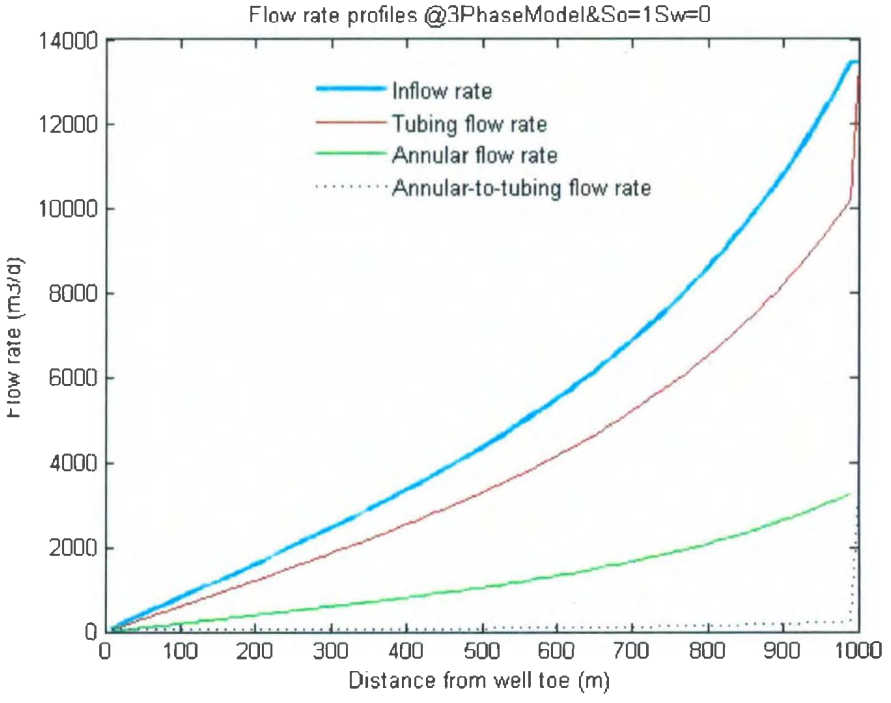

Figure 4.2 Flow Rate profile for Case 1

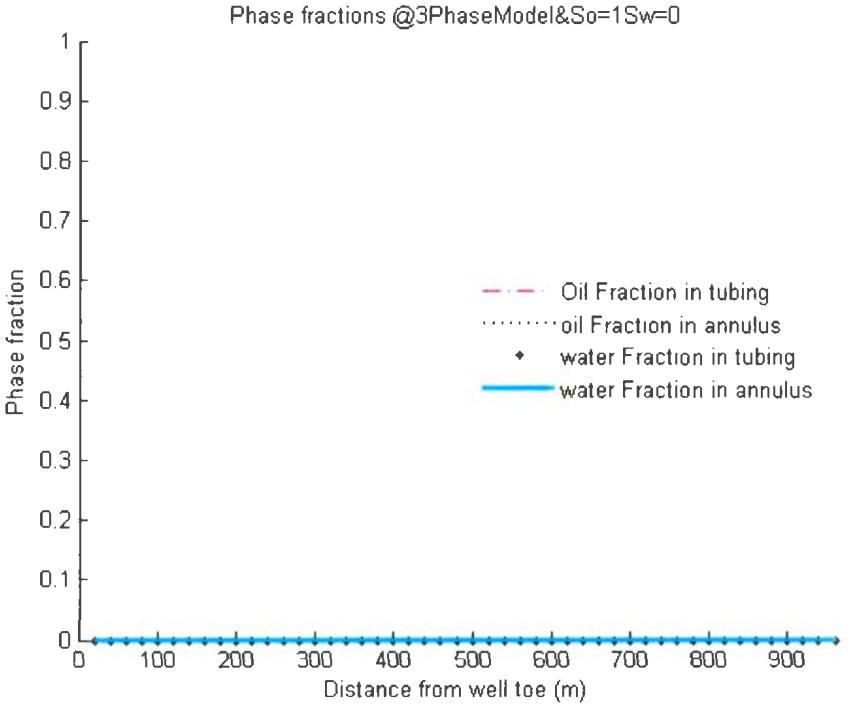

Figure 4.3 Phase fraction profile for Case 1

As shown in above three figures, the entire 1000 meter horizontal well is divided into 100 segments; the length of each segment is 10 meters. During the production, reservoir pressure maintains constant, and annulus and tubing pressures are decreasing from well toe to well heel, finally reach the bottom-hole pressure. With the pressure loss along the horizontal well, the producing flow rates in annulus and tubing are increasing from well toe to well heel. As the pressure in the model is always above the bubble point, and there is no free gas in the reservoir, the oil fraction stays as 1, and gas fraction is zero.

Case 2: Two phase case as water/gas system

Case 2 remains all the initial values in Case 1 except changing the saturation values of oil and water, then oil saturation is zero and water saturation is equal to one. Flow parameters for Case 2 with water-gas system are as follow:

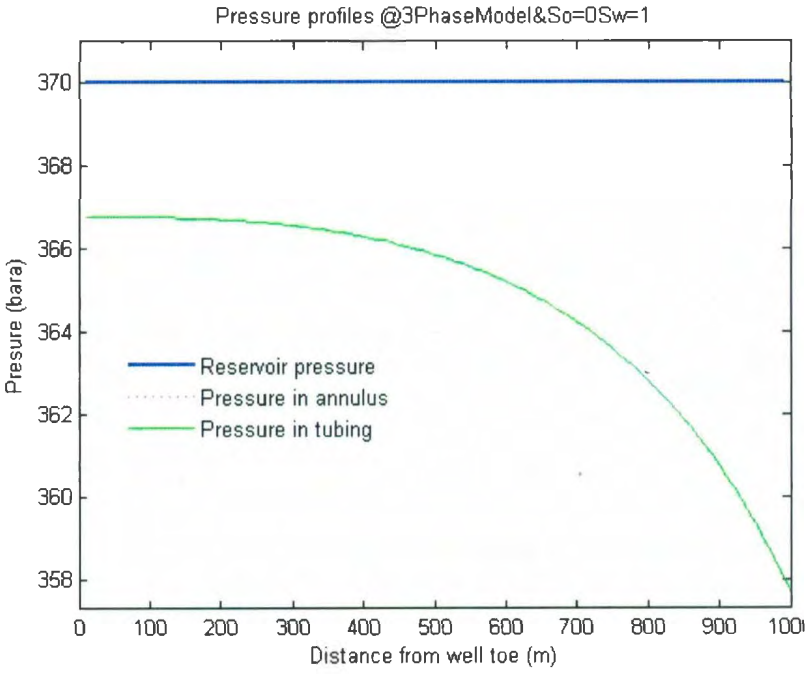

Figure 4.4 Pressure profile for Case 2

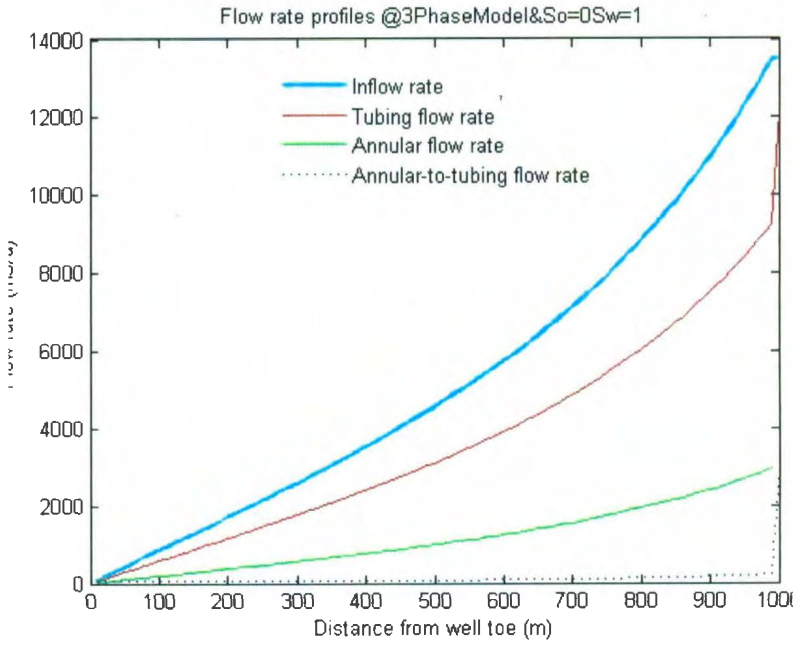

Figure 4.5 Flow Rate profile for Case 2

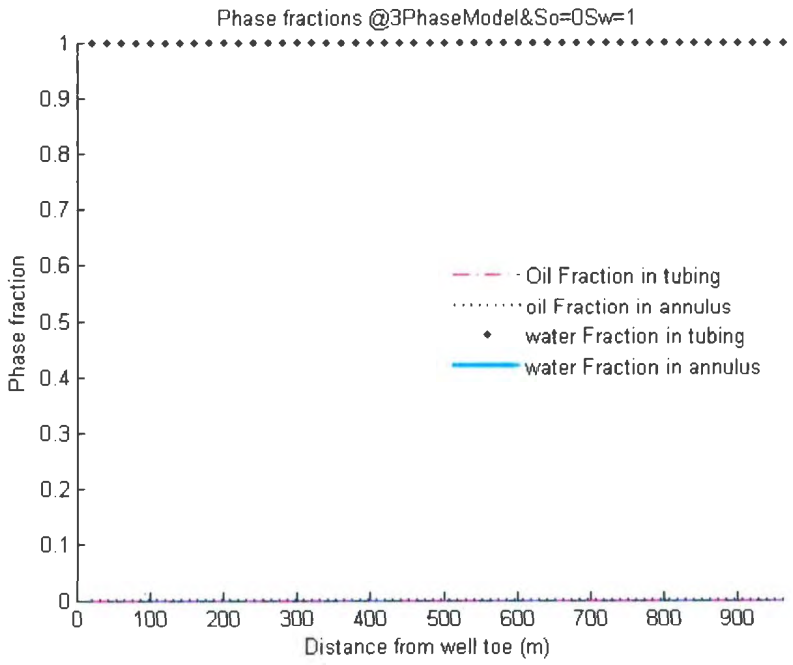

Figure 4.6 Phase fraction profile for Case 2

The results of Case 2 are similarly to those of Case 1, except the water fraction stays 1 instead of oil fraction.

Case 3: Open hole without annulus flow and completion

We would test the three phase model with Open Hole Case which is the most original and common scenario, and this case is modeled by setting annulus radius to an infinitesimal number (Not to set its value to zero is to avoid the singularity of network model). The boundary condition and initial values are listed below:

Properties	Value
Well Length (m)	1000
Segment length (m)	10
Reservoir pressure (bara)	370
Pressure at heel (bara)	357.5
Reservoir temperature	100
Permeability (Darcy)	1
Near-wellbore skin factor	1
Oil saturation	.8
Water saturation	.2
Tubing diameter (m)	0.167
Well outside diameter (m)	0.167
Discharge coefficient for slot flow ($Pa \cdot (kg/m^3)^{-1} \cdot (m/s)^{-2}$)	10

Table 4.2 Properties and initial values for Open hole without annulus flow and completion

In Case 3, annulus and annulus-to-tubing flow rates no longer exist since the annulus channels are removed, therefore the tubing channel is the only path for fluid producing, as the pressure is above the bubble point pressure, the phase fractions remain constant during the production. As there is no completion in this case, the production flow rate of this case is much lower than the previous two cases.

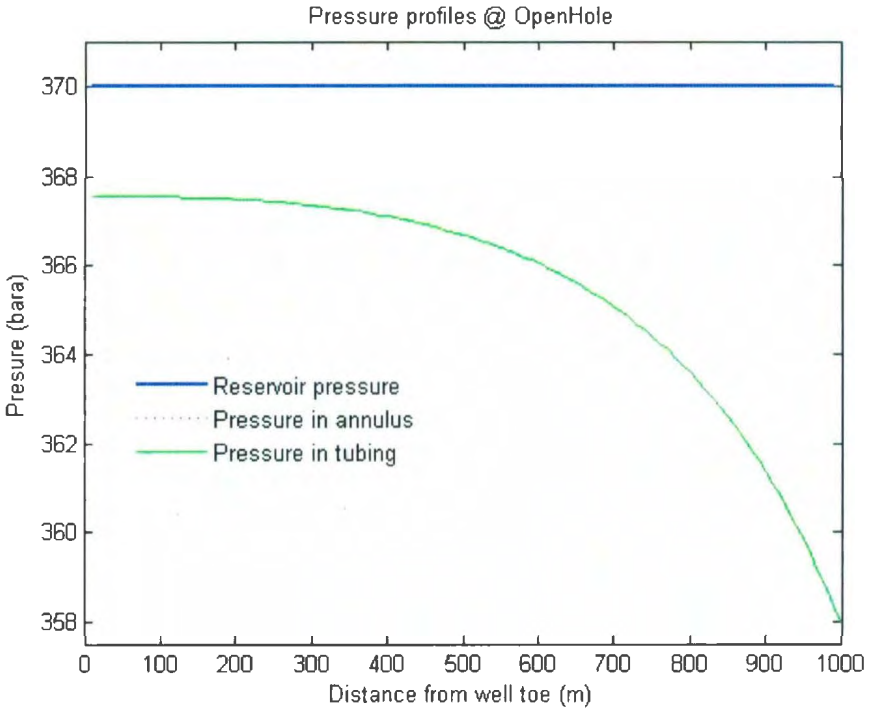

Figure 4.7 Pressure profile for Case 3

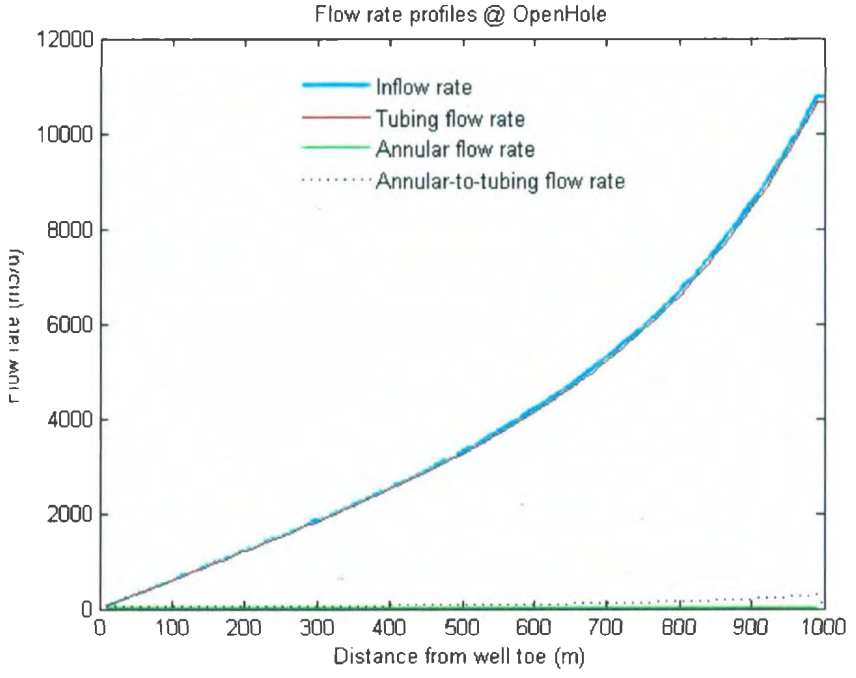

Figure 4.8 Flow Rate profile for Case 3

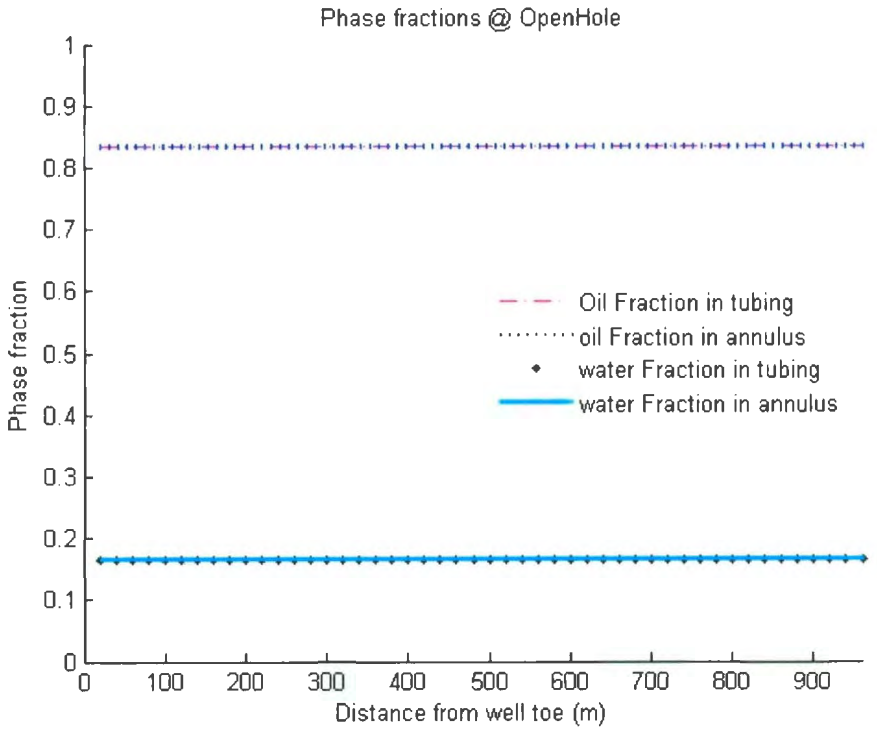

Figure 4.9 Phase fraction profile for Case 3

As the pressure drop due to the friction is a great concern for horizontal well, we should test the three phase model with the bubble point pressure. In this research, two different scenarios would be tested, one is the entire horizontal well under Bubble point in Case 4, and the other is pressure reducing to meet the Bubble point during the production in Case 5. The outputs are shown as below.

Case 4: Pressure under bubble point for the entire well

Properties	Value
Well Length (m)	1000
Segment length (m)	10
Reservoir pressure (bara)	204.4
Pressure at heel (bara)	180
Reservoir temperature	100
Permeability (Darcy)	1
Near-wellbore skin factor	1
Oil saturation	.8
Water saturation	.2
Tubing diameter (m)	0.167
Well outside diameter (m)	0.167
Discharge coefficient for slot flow ($Pa \cdot (kg/m^3)^{-1} \cdot (m/s)^{-2}$)	10

Table 4.3 Properties and initial values for Pressure under bubble point for the entire well

The bubble point pressure is calculated at 204.4 bara, so the reservoir pressure of this case is set to be 204.4 bara and the bottom-hole pressure is 180 bara, the pressure difference between reservoir and bottom-hole is 20 bara. From the output figures, in the figure 4.11 the flow rates in the well system surge heavily due to the gas breaking out from the oil phase, and the gas fraction grows up gradually with the oil and water fractions going down.

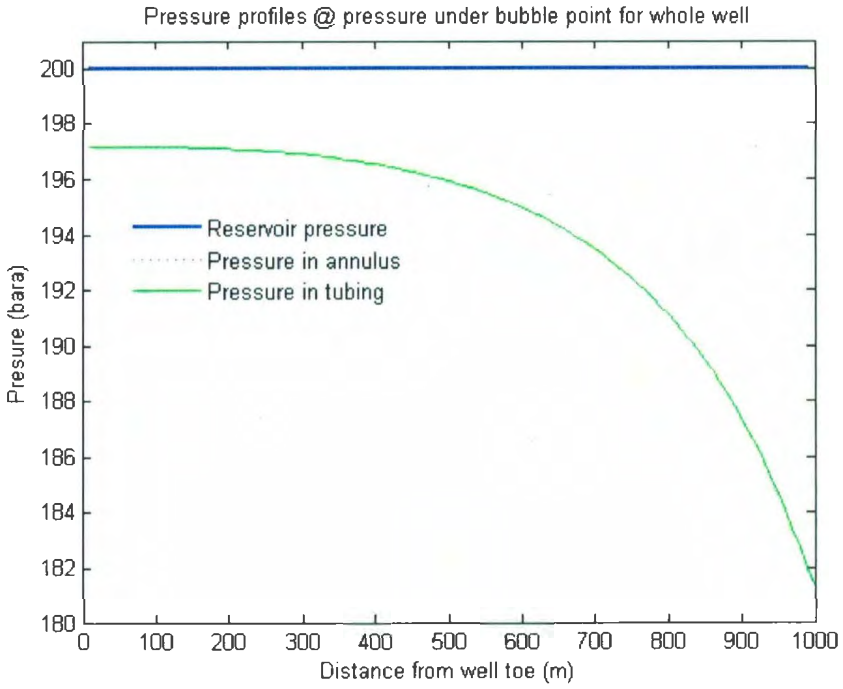

Figure 4.10 Pressure profile for Case 4

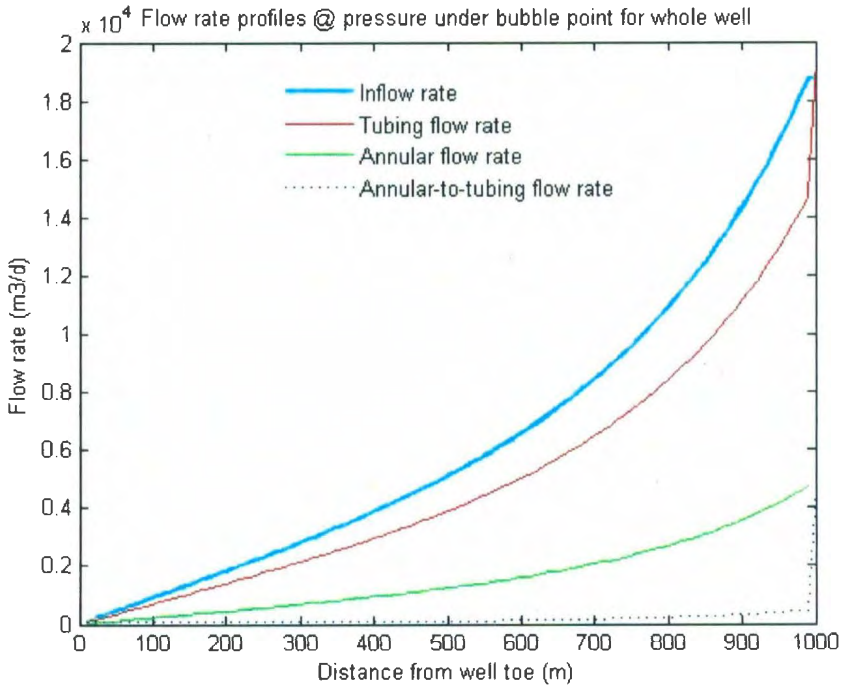

Figure 4.11 Flow Rate profile for Case

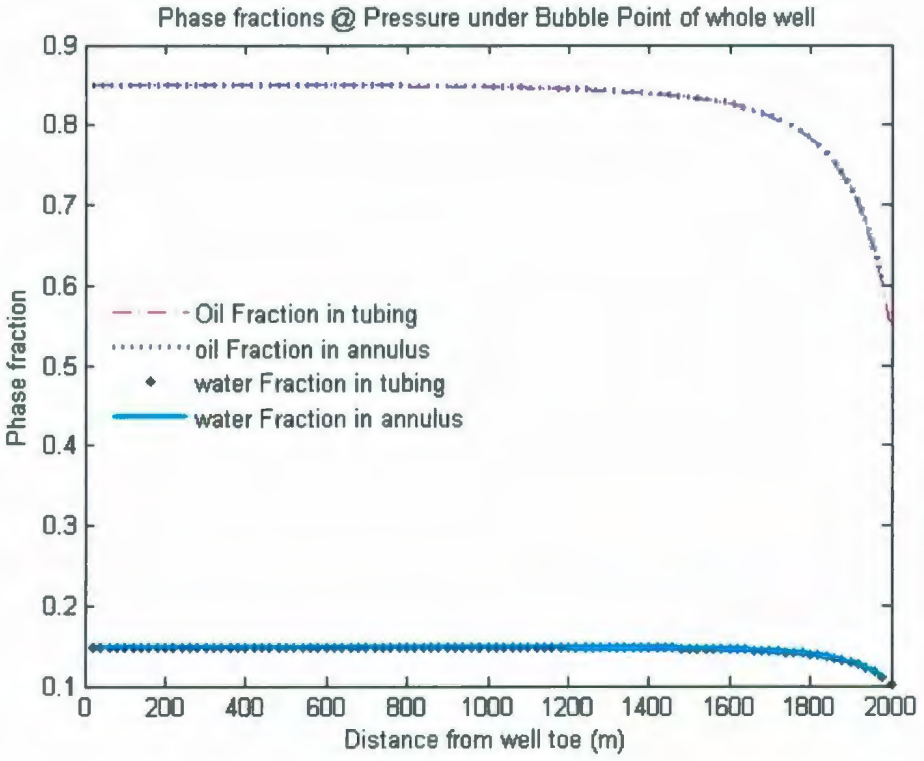

Figure 4.12 Phase fraction profile for Case 4

Case 5: Encountering pressure under bubble point during the production

In this case, the reservoir pressure is set to be 368 bara, and bottom-hole pressure is 120 bara, the pressure difference between reservoir and bottom-hole is 148 bara which is more 7 times to that of Case 4. Besides these changes, the other initial inputs are the same as Case 4. As shown in the output figures, the pressures in wellbore system decrease from well toe and hit the bubble point pressure at 200 bara roughly at segment 95, finally reach the bottom-hole pressure at heel. Due to the significant pressure drop and gas breaking out in this case, the production flow rates are especially high. Around the segment 95 where the wellbore pressures reach the bubble point and encounter the gas breaking out, the oil and water fractions decrease sharply with the gas fraction rising up from this point till the bottom-hole.

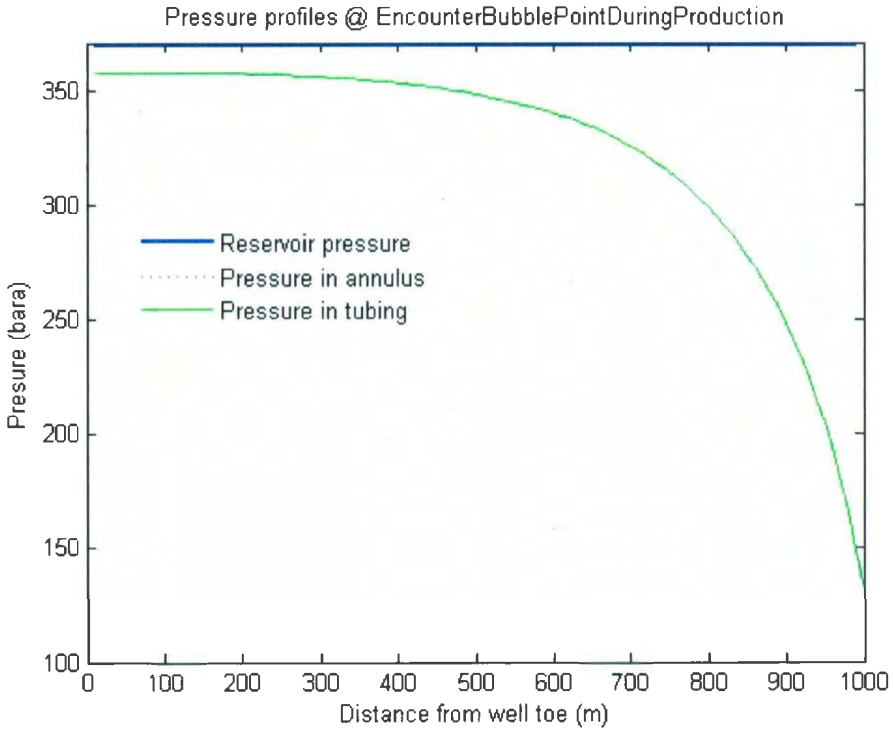

Figure 4.13 Pressure profile for Case 5

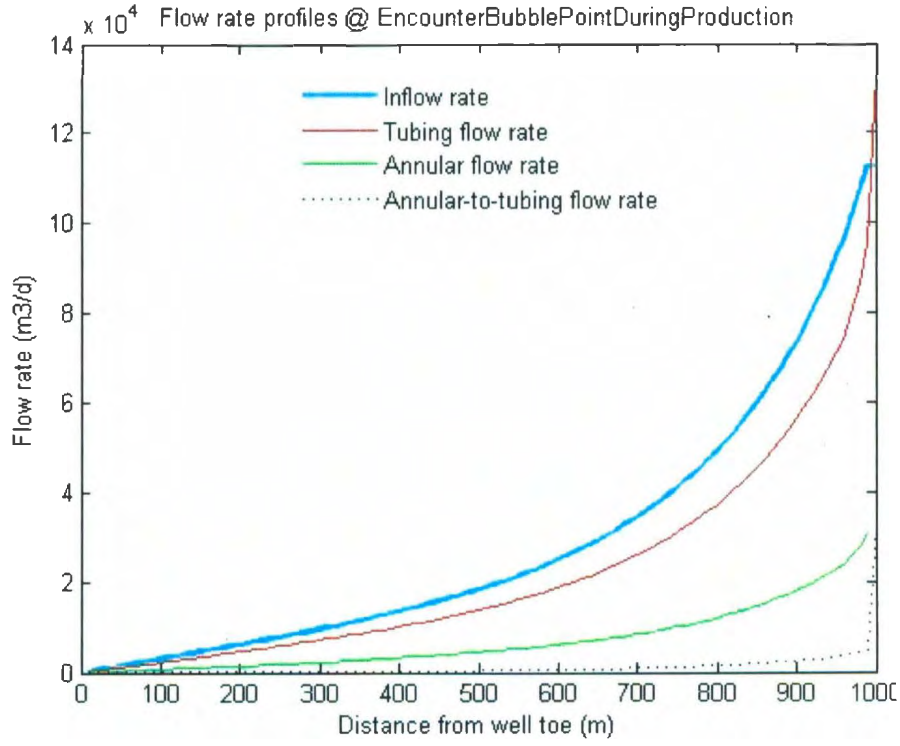

Figure 4.14 Flow Rate profile for Case 5

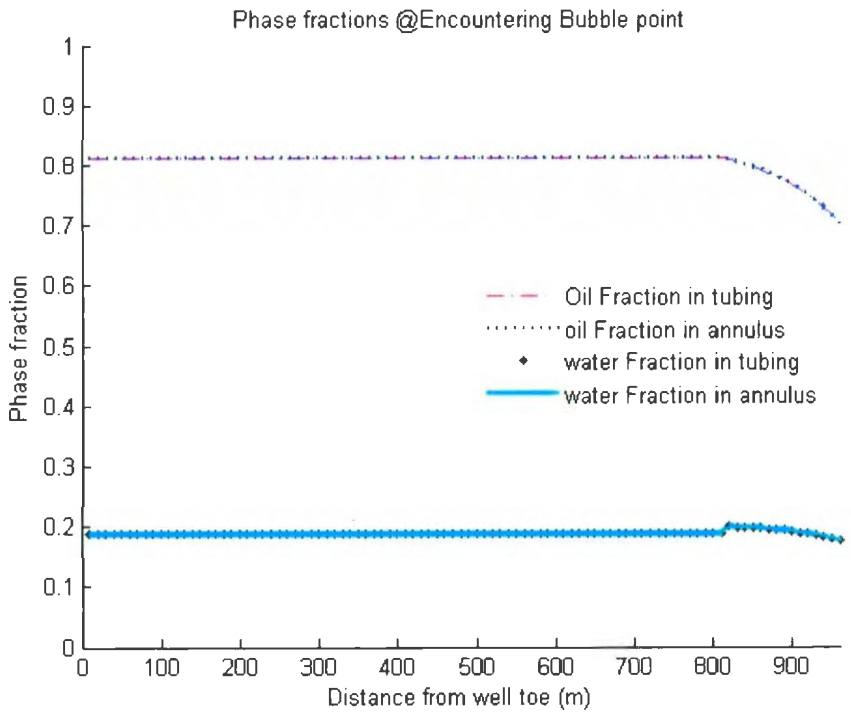

Figure 4.15 Phase fraction profile for Case 5

Properties	Value
Well Length (m)	1000
Segment length (m)	10
Reservoir pressure (bara)	357.5
Pressure at heel (bara)	140
Reservoir temperature	100
Permeability (Darcy)	1
Near-wellbore skin factor	1
Oil saturation	.8
Water saturation	.2
Tubing diameter (m)	0.167
Well outside diameter (m)	0.167
Discharge coefficient for slot flow ($Pa \cdot (kg/m^3)^{-1} \cdot (m/s)^{-2}$)	10

Table 4.4 Properties and initial values for Case 5

After the case studies done before, the proposed fundamental three phase model has been proved as a comprehensive model to simulate the well performance physically and stably.

4.2 Error caused by Discretization for the Network Model

The entire length of horizontal well is divided into a finite number of segments, and the network solver is based on the discretization approaches which transfer the continuous differential equations of flow parameters for whole horizontal well to the discrete difference equations at each well segment by the numerical schemes. The accuracy of the discretization method is depending on the numerical schemes and scheme steps; suitable parameter

correlations and equations are selected to ensure the accurate numerical schemes. For the scheme steps concern, the more steps (segments) are calculated, the more accurate results are achieved. In this chapter, the discretization error is examined by simulating a 1000 meter horizontal well using four different scheme steps which are 200, 100, 50 and 10 steps. The simulations are done respectively by dividing the whole length of well into 200, 100, 50, 10 segments with the length of 5, 10, 20, 100 meters respectively.

Properties	Value
Well Length (m)	1000
Reservoir pressure (bara)	368.5
Pressure at heel (bara)	357.5
Reservoir temperature	100
Permeability (Darcy)	1
Near-wellbore skin factor	1
Oil saturation	.6
Water saturation	.4
Tubing diameter (m)	0.127
Well outside diameter (m)	0.167
Discharge coefficient for slot flow (Pa·(kg/m3)-1·(m/s)-2)	10

Table 4.4: Basic well parameters for discretization error analysis

Flow Parameters	10 Segments	50 Segments	100 Segments	200 Segments
Total pressure loss in well (bara)	5.36	6.95	8.42	8.63
Production flow rate (m^3/d)	8279.1	10401	11862	12099
Oil fraction	0.60512	0.60511	0.60456	0.60456
Water fraction	0.39488	0.39489	0.39544	0.39544

Table 3.4.5: Simulation Results of two segment densities

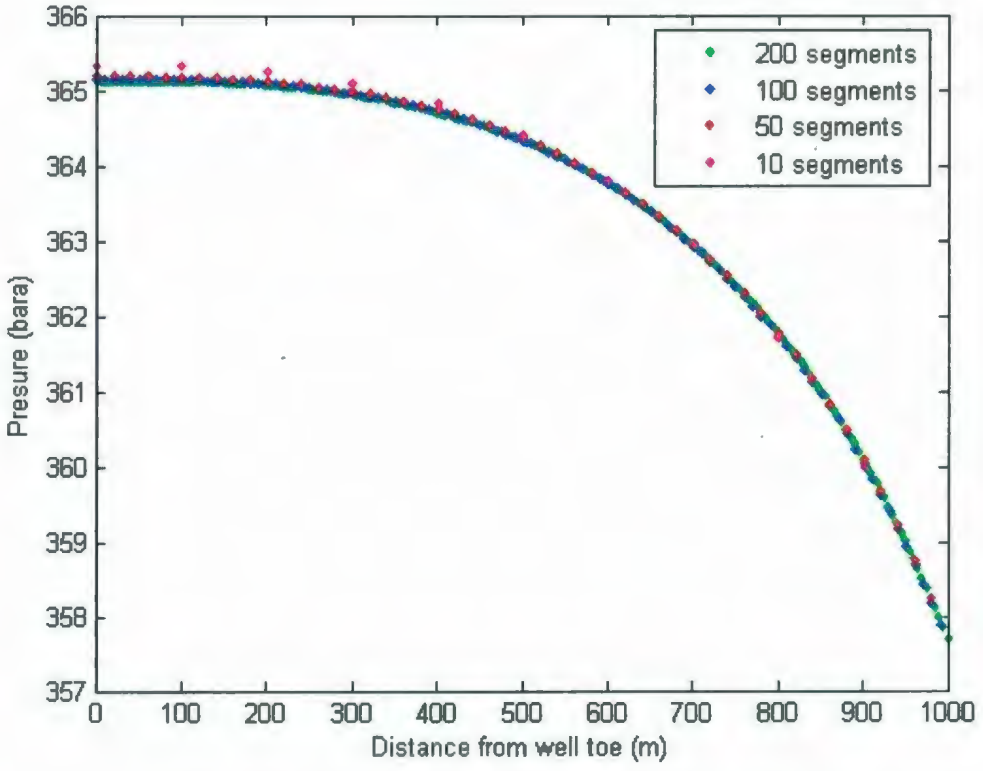

Figure 4.2.1 Pressure profile for different segment densities

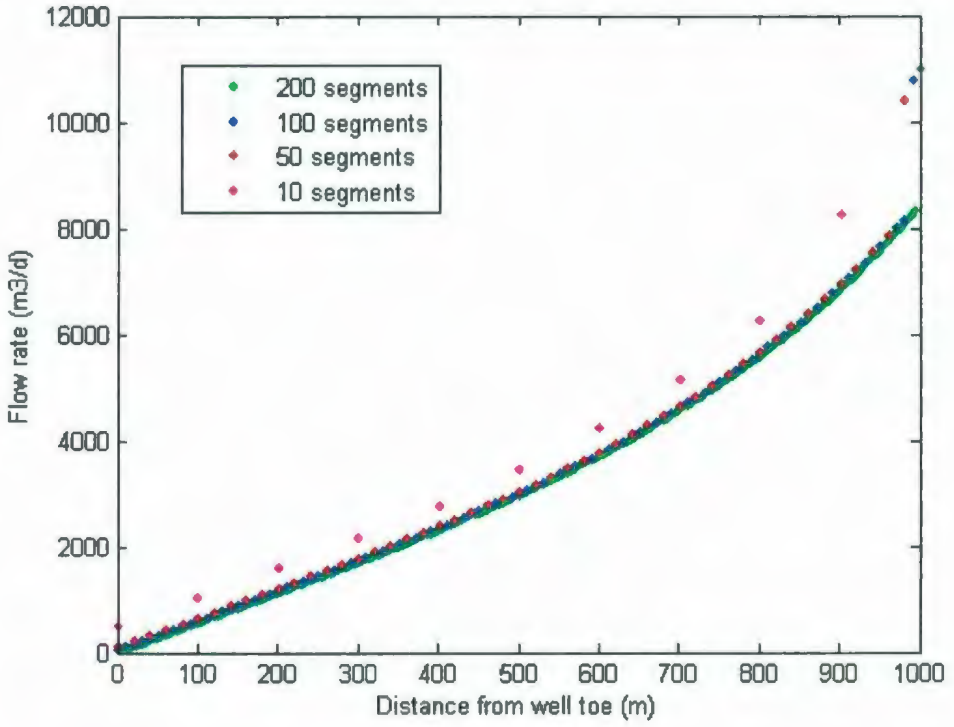

Figure 4.2.2 Tubing flow rate profile for different segment densities

Figure 4.2.1 and Figure 4.2.2 show the comparison of the simulation results given by the proposed three phase network model using 200-segment, 100-segment, 50-segment, and 10-segment scheme. As shown in above figures, the pressure distribution and production flow rate calculated by 200-segment and 100-segment schemes are identical to each other. The detail comparison is shown in Table 3.4.5. The total pressure drop of whole well at 100-segment case is 8.42 bara, while that at 200-segment case is 8.63 bara (-2.49% error); the total inflow rate for the 100-segment case is 11862 m^3/d, while that for 200-segment case is 12099 m^3/d (2.00% error); but the phase fractions for both cases are the same. For 50-segment and 10 segment schemes, the discretization errors are large. The total pressure drop at 50-segment case is 6.95 bara (-17.4% error), and the total pressure drop at 10-segment case is 5.36 bara (-36.3% error); the total inflow rate for 50-segment case is 10401 m^3/d (-12.3% error), and the total inflow rate is 8279.1 m^3/d (-30.2% error).

Chapter 5 Completions and Initial Guess Generation

5.1 Completion introduction

Completion is the procedure to have a well ready for production. In order to optimize production or injection performance, and optimize equipment life time; ensure that the field is produced reliably and safely, different types of well completions are extensively used in the horizontal wells. And a suitable completion design for a specific reservoir and horizontal well could be decided based on following constraints and parameters (Perrin, 1999):

- the type of producing fluids and their characteristics
- the reservoir and its petro-physical characteristics
- whether it is necessary to proceed to additional operations (well stimulation, sand control, etc.)
- whether it is necessary to implement techniques to maintain reservoir pressure (water, gas, solvent or miscible product injection) immediately or at a later date
- the eventuality of having to do any work on the pressurized well during the production phase with a concentric tubular (annulus and tubing in this research)

The completion involves the bottom-hole preparation, running in the production tubing and related perforation and stimulation. There are basically three types of completions for horizontal wells in different reservoirs and perforations; they are barefoot completion, open-hole completion, and cased-hole completion.

Barefoot completion is the most basic one without any tubular and it is suitable for hard rock, multilaterals and underbalance drilling; open-hole completion has the tubular across the production zone but not cemented in place, slotted liner with multiple longitudinal slots is one

of most popular open-hole completions. Cased-hole completion involves a casing or liner down through the production zone which is cemented in place. In this type of completion, perforations connecting between the wellbore and the reservoir could be precisely positioned; the main purpose of completions is wellbore integrity and sand control. Also the completions could give good control of fluid flow, as a result the cased-hole completion is the most common form of completions.

5.2 Case 1: Slotted liner

Slotted liner completions are mainly used in compact sandstones reservoirs with slots of various width, length and liner density milled along the liner length. This type of completions is considered as the most basic and cost effective completions for the horizontal wells in heavy oil reservoirs. By inserting a slotted liner, it can prevent horizontal well from hole collapse. Moreover, a liner forms a convenient path to insert production tools such as coiled tubing, blank pipe or measurement equipment, etc., also slotted liners could act as sand control screens by selecting hole and slot sizes (Joshi, 1991). A simple slotted liner is depicted as below.

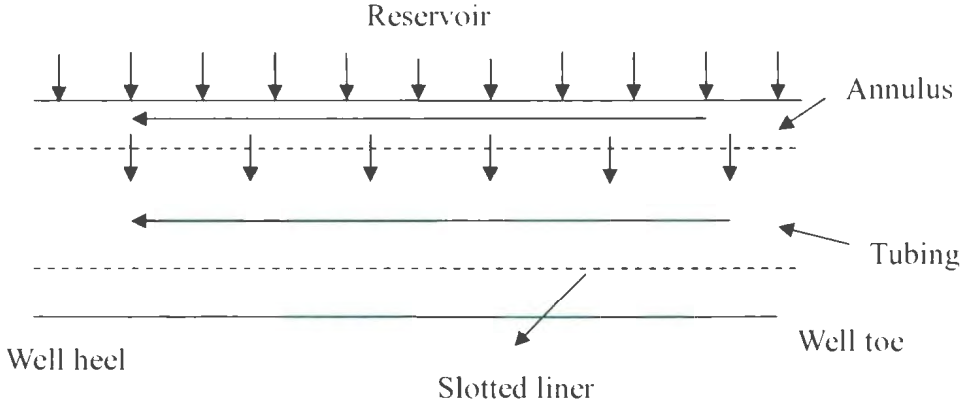

Figure 5.2.1 Sketch of basic Slotted Liner completion

The reservoir fluids flow into the annulus and split to two directions, one flow along the annulus channel and the other cross the slots in to the tubing channel. Tubing flow and annulus flow parallelly move from well toe to the bottom-hole. Physically the pressure in annulus and tubing would decrease from well toe to well heel during the productions, and due to the split equations used in network model, the oil and water fractions would remain constant.

The slotted liners in this research are set with density of 30000slots/meter, width of 0.001 meter and length of 0.01 meter. As discussed in Chapter 3, the fluid flow through the slots is evaluated by 'equivalent' friction factors with a discharge coefficient.

Properties	Value
Well Length (m)	1000
Segment length (m)	10
Reservoir pressure (bara)	385
Pressure at heel (bara)	345
Reservoir temperature	100
Permeability (Darcy)	1
Near-wellbore skin factor	1
Oil saturation	.7
Water saturation	.3
Tubing diameter (m)	0.127
Well outside diameter (m)	0.167
Discharge coefficient for slot flow ($Pa \cdot (kg/m^3)^{-1} \cdot (m/s)^{-2}$)	10

Table 5.2.1 Properties and initial values for Slotted Liner

The simulation results are shown as below:

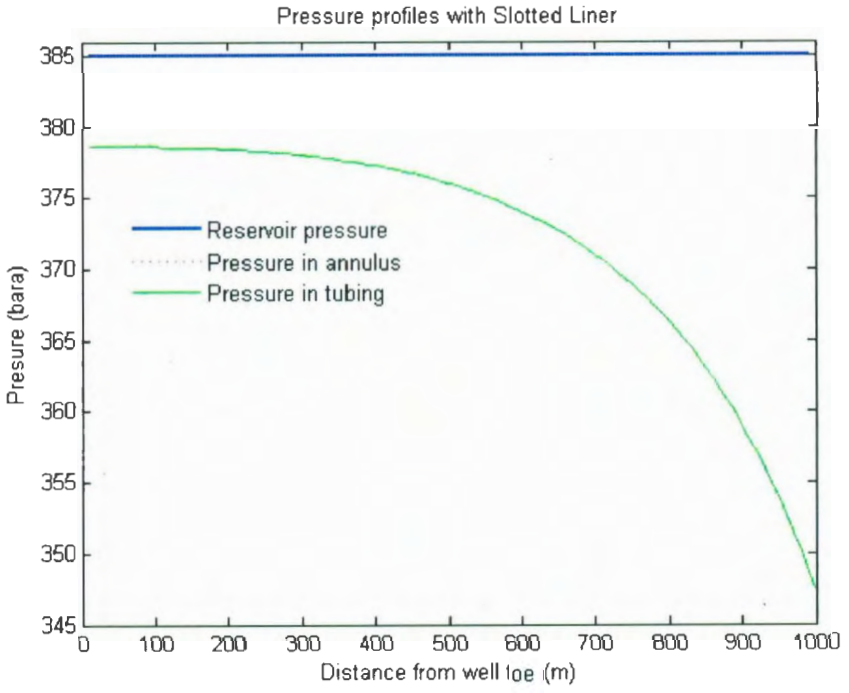

Figure 5.2.2 Pressure profile with Slotted Liner

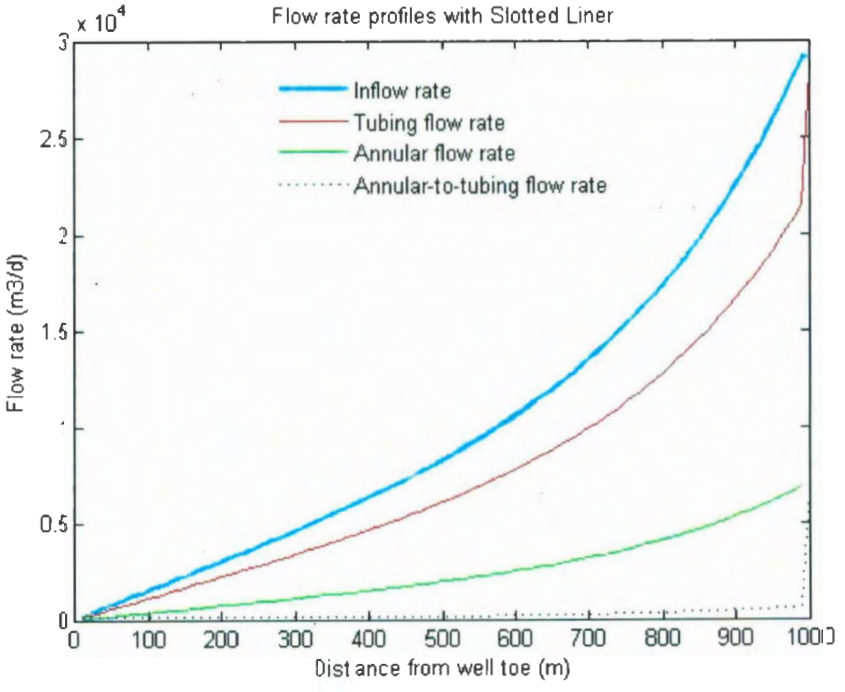

Figure 5.2.3 Flow Rates profile with Slotted Liner

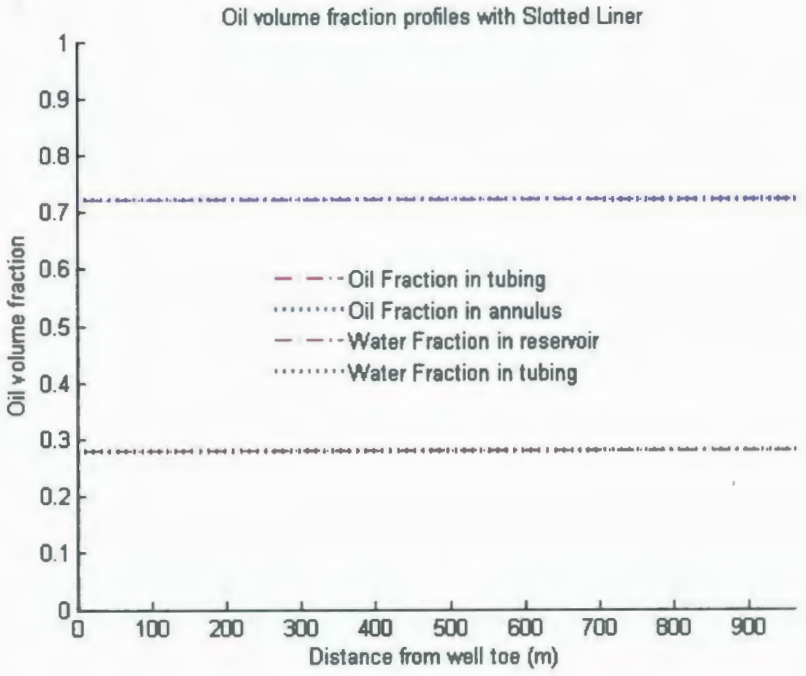

Figure 5.2.4 Oil and Water Fraction profile with Slotted Liner

5.3 Case 2: Restricted Flow in the Annulus

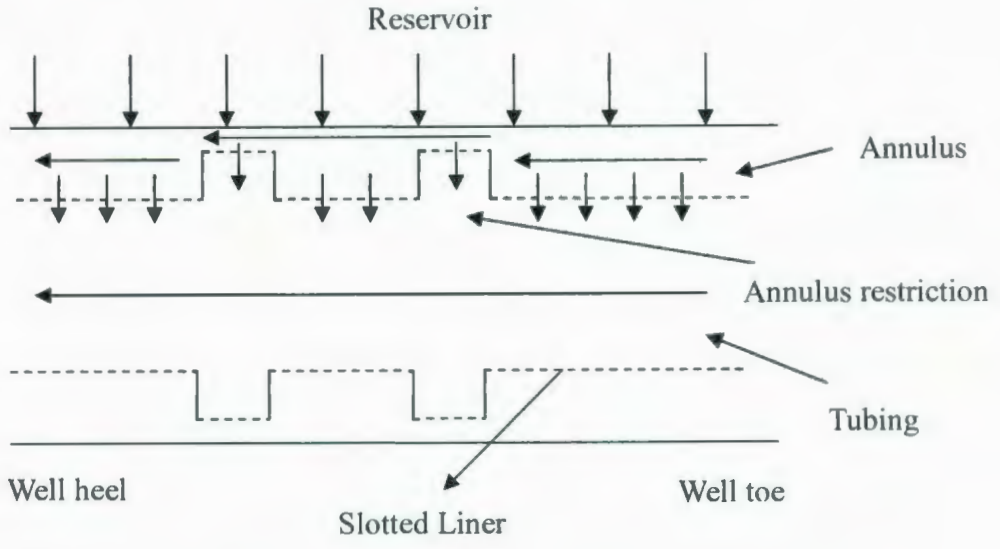

Figure 5.3.1 Sketch of Restricted flow in the annulus

Properties	Value
Well Length (m)	2000
Segment length (m)	10
Reservoir pressure (bara)	370
Pressure at heel (bara)	357.5
Reservoir temperature	100
Permeability (Darcy)	1
Near-wellbore skin factor	1
Oil saturation	.65
Water saturation	.35
Tubing diameter (m)	0.127
Well outside diameter (m)	0.167
Discharge coefficient for slot flow ($Pa \cdot (kg/m^3)^{-1} \cdot (m/s)^{-2}$)	10

Table 5.3.1 Properties and initial values for Restricted Flow in the Annulus

In oil and gas production, various down-hole facilities including casing inspection tools, down-hole tractors or inflow control devices are frequently installed in the wellbore. Consequently, the cross sections of annulus and tubing are altered during the installations. As demonstrated in Figure 4.3.1 and Table 4.2.1, the horizontal well with length of 2000 meter is divided into 200 segments. In the segment 140-142 and segment 170-172, the annulus channel is restricted, at the same time the tubing channel is enlarged, these lead to the corresponding flow rates changes in two channels.

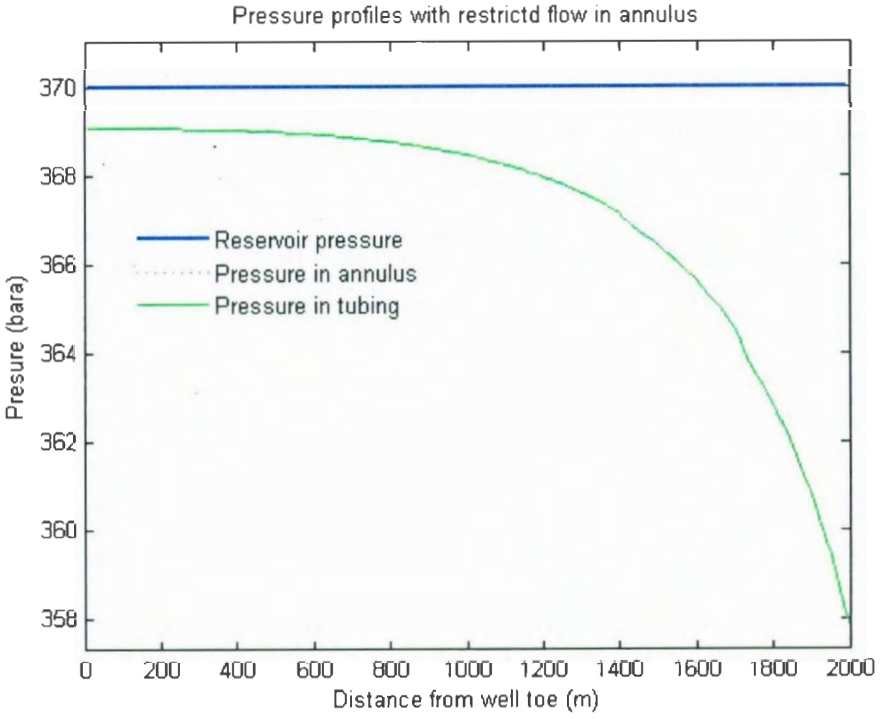

Figure 5.3.1 Pressure profile with restricted flow in the annulus

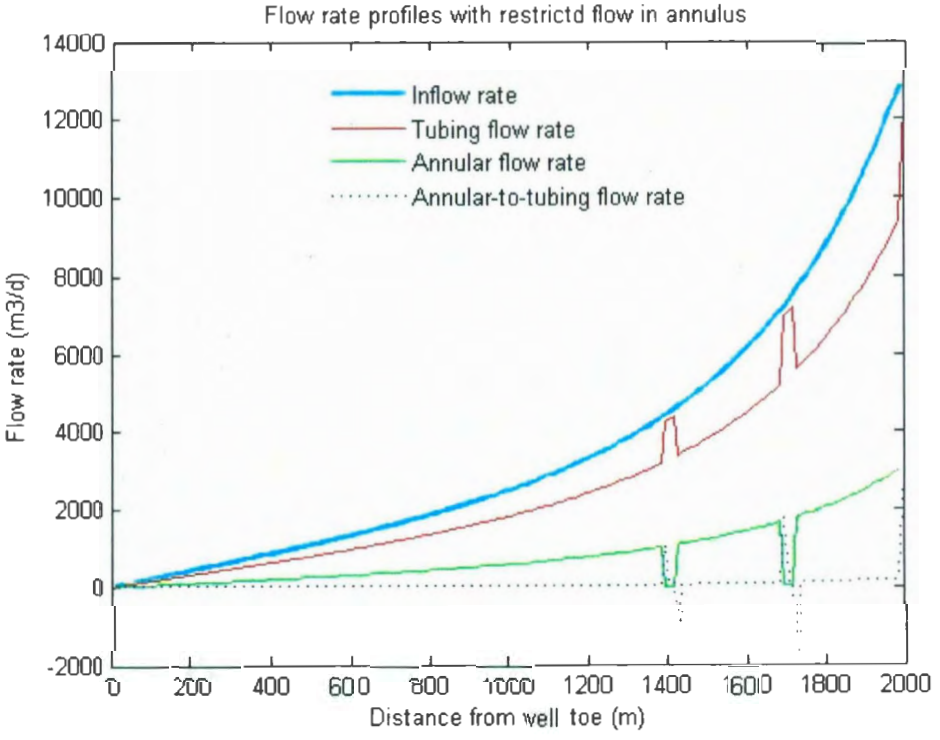

Figure 5.3.2 Flow rate profile with restricted flow in the annulus

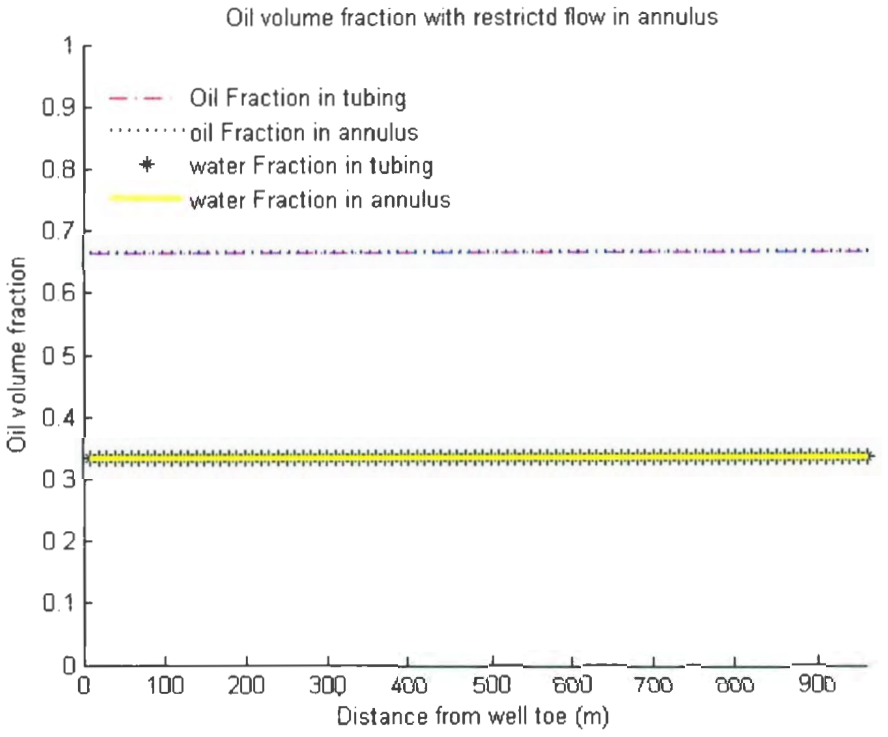

Figure 5.3.3 Phase fractions with restricted flow in the annulus

Unequal pressure drawdown problem for horizontal well

Pressure drawdown is the differential pressure that drives fluids from the reservoir into the wellbore. As discussed in Chapter 3, the wellbore pressure drop is described as $\frac{dp}{dz} = \frac{f\rho v^2}{2D_h}$, and the pressure drawdown is linearly dependent on the product of length and the square of flow velocity. Simple tendency of the pressure drawdown in wellbore is demonstrated as below:

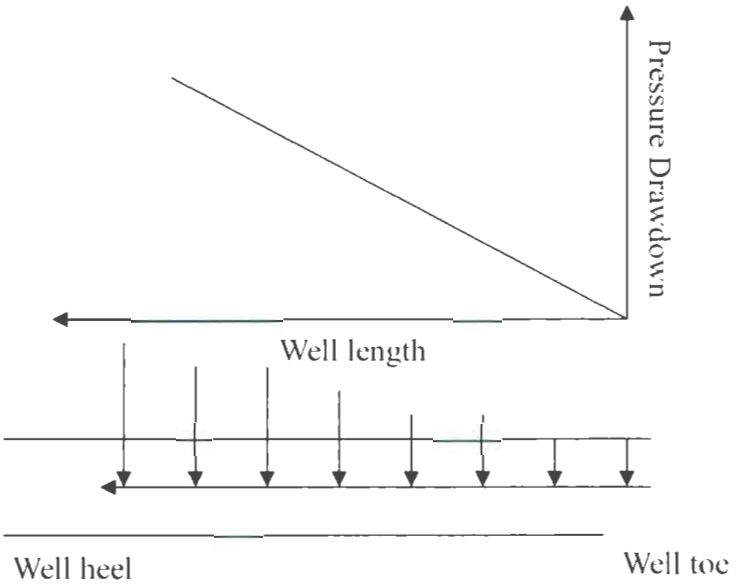

5.3.4 Pressure drawdown tendency

Fluids in wellbore flow from well toe the well heel, while the fluids are moving, the pressure drawdown increases heavily along the length of the wellbore, and near the bottom-hole (the end of the well/well heel), the significant unequal pressure drawdown disturbs the flow directions in both production formation and wellbore, causing problems like water and gas coning and inefficiency of well toe.

To equalize the pressure drop along the wellbore to achieve longer producing life due to delay of water/gas coning and improve production per unit length, and ensure of the well productivity and safety, some completions like multi inflow control device, packing off the end of the well, and inserting a stinger pipe are implemented in production.

5.4 Case 3: Multiple Inflow control devices (ICD)

Various inflow control devices (ICD) are designed to restrict the reservoir inflow to enter the wellbore within the specific positions, the purpose to equip ICD in the oil producer wells is

to equalize the pressure drop along the horizontal well, decrease flow rate of high mobility fluids and reach better sweep efficiency; ICD also could be beneficial in the injectors by avoiding breakthrough if injected fluid into producers, providing better placement of injection fluid into different formation layers, and evening out permeability differences and fractures. Basic components of ICD are the packers and the blank pipes, the packers could divide the annulus channel into several sections and the blank pipes could maintain a high pressure difference between annulus and tubing, therefore lead the inflow from reservoir to pass the section's annulus into the tubing through a channel with a very small diameter. By the effort of ICD, the annulus flow could be minimized; the reservoir fluids could be led to production tubing by the large pressure drop given by ICD. Basic structure of ICD is demonstrated in Figure 5.4.1.

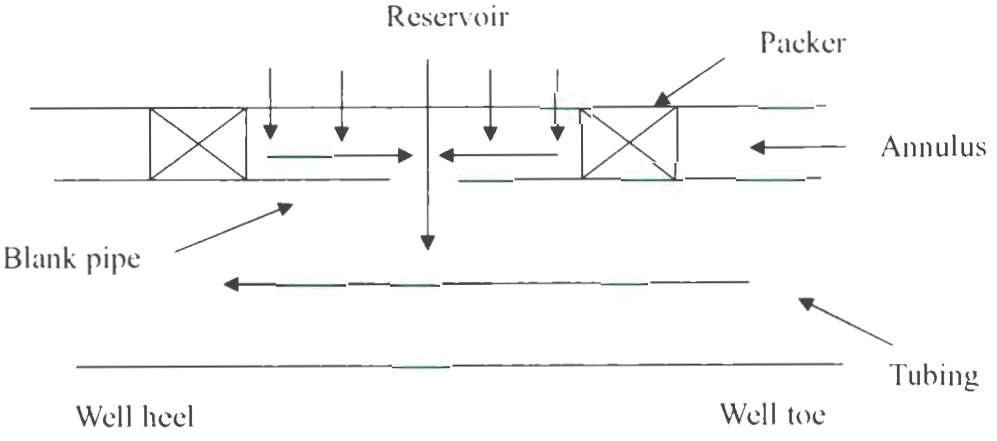

Figure 5.4.1 Sketch of basic inflow control valve

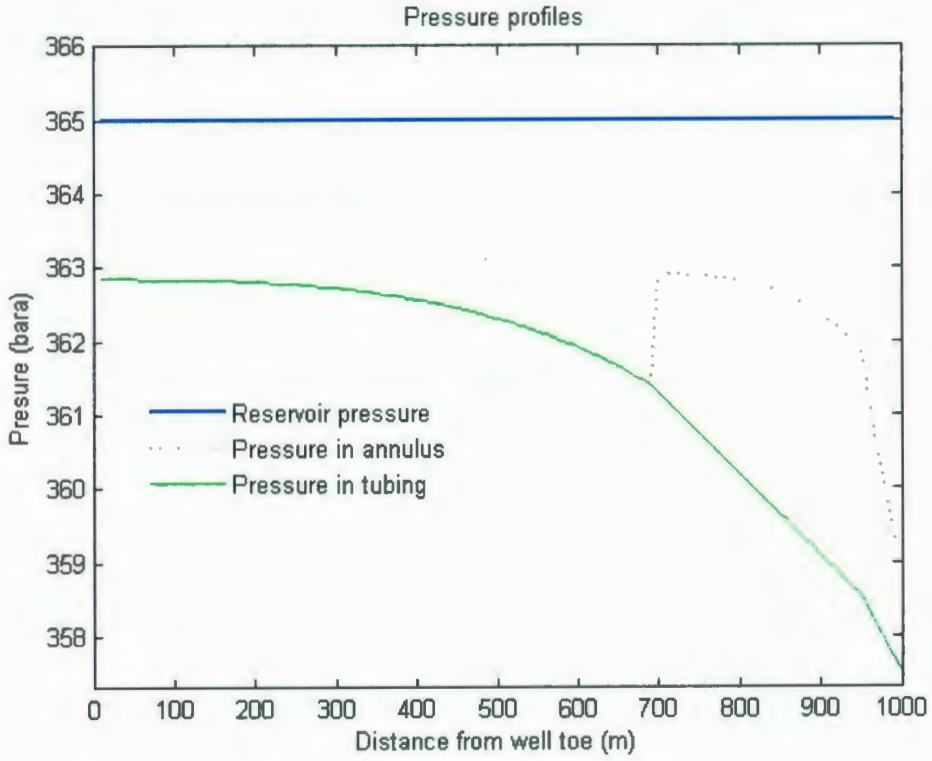

Figure 5.4.2 Pressure Profile of Multi Inflow control device

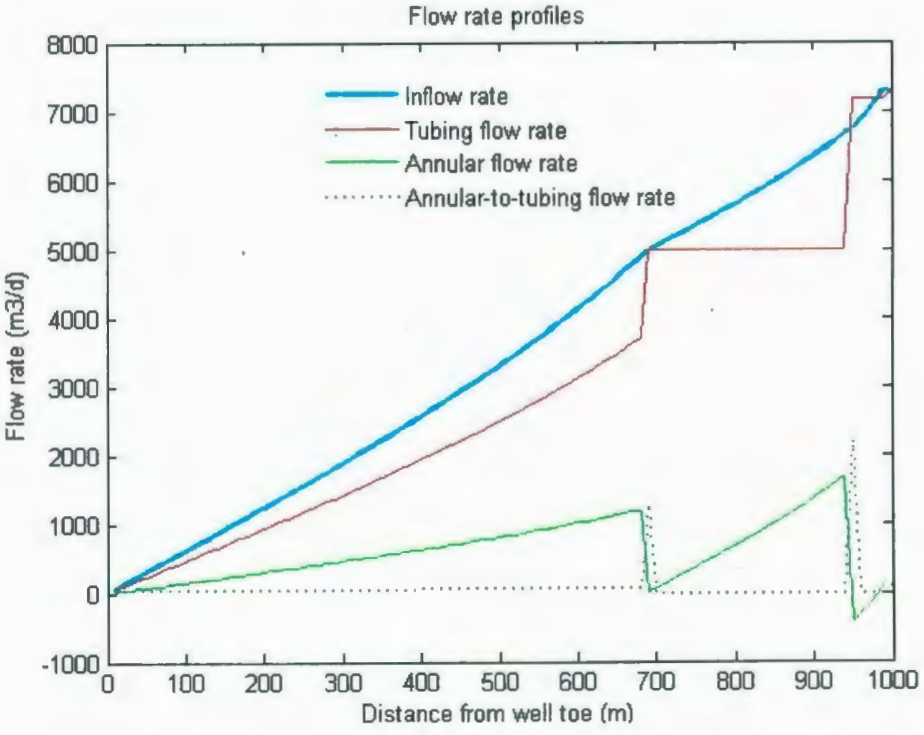

Figure 5.4.3 Flow rate Profile of Multi Inflow control device

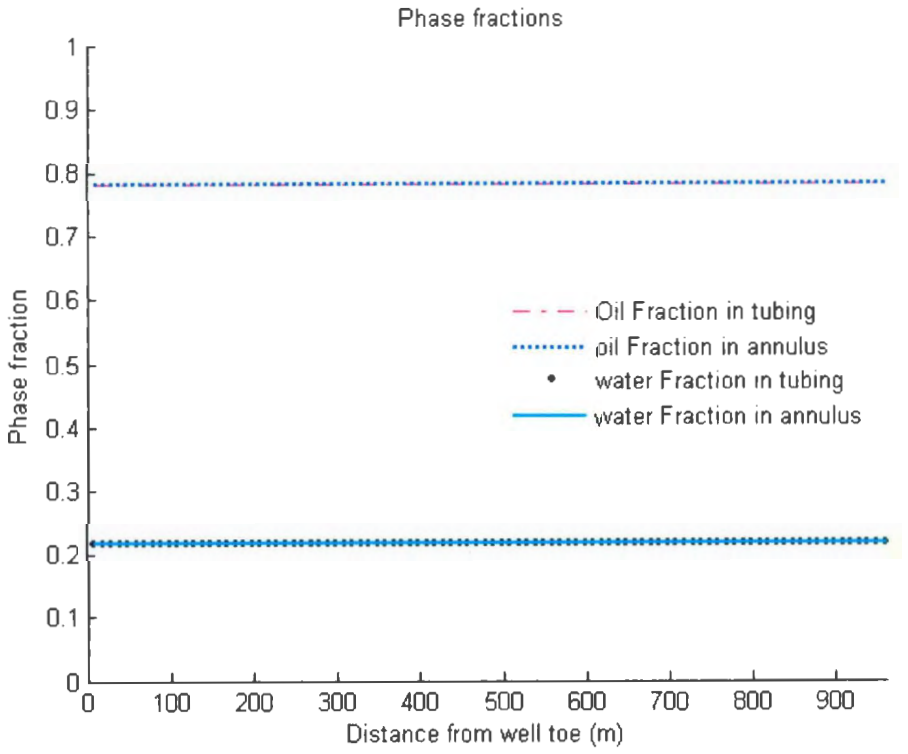

Figure 4.4.4 Phase fraction Profile of Multi Inflow control device

Properties	Value
Well Length (m)	1000
Segment length (m)	10
Reservoir pressure (bara)	365
Pressure at heel (bara)	357.5
Reservoir temperature	100
Permeability (Darcy)	1
Near-wellbore skin factor	1
Oil saturation	.75
Water saturation	.25
Tubing diameter (m)	0.127

Well outside diameter (m)	0.167
Discharge coefficient for slot flow ($Pa \cdot (kg/m^3)^{-1} \cdot (m/s)^{-2}$)	10

Table 5.4.1 Properties and initial values for Multi Inflow control device

5.5 Case 4: Completion with 500 meters packed off at the end of well

As demonstrated in Figure 5.5.1, in this completion, the total length of the horizontal well is 2000 meters, and the last 500 meters to the well heel are equipped with blank pipe, and the annulus to tubing flow of this part no longer exists, therefore the pressure drop of tubing in the completed part is only related to friction which is a linear function of pressure drop and pressure in annulus increases of this part of well because the out flow of annulus channel is restricted by the blank pipe, as shown in the Figure 5.5.2, in the 500 meter blank pipe section, tubing pressure decreases linearly with a constant pressure drawdown, and the annulus pressure surges due to the restriction of blank pipe, but pressure drop in annulus is more significantly than that in tubing, because the bottom-hole pressures for annulus and tubing are the same, so the pressure difference to be achieved in annulus is more than that in tubing.

As shown in Figure 5.5.1, the annulus is divided in two parts by a packer; the annulus flow from well toe is prevented and restricted into the tubing at this packer, and starts again from the blank pipe. The tubing flow remains constant along the blank pipe because there is no inflow to tubing due to the blank pipe.

The purpose for this completion is to reduce the unequal pressure drawdown problem, from the simulation results, the pressure drawdown in the end of tubing stays constant, but the pressure drawdown in the end of annulus is very high which could be judged from the slop of tangent on pressure curve, as the annulus flow is going to merge with tubing flow at the last segment of the well, so the bottom-hole point might need extra treatment to avoid the disorder.

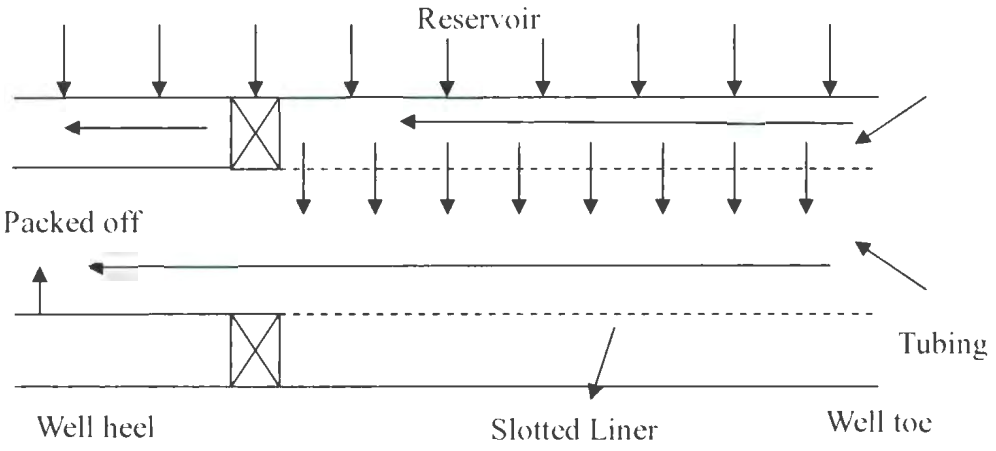

Figure 5.5.1 Case 5 Completion with 500 meters packed off at the end of well

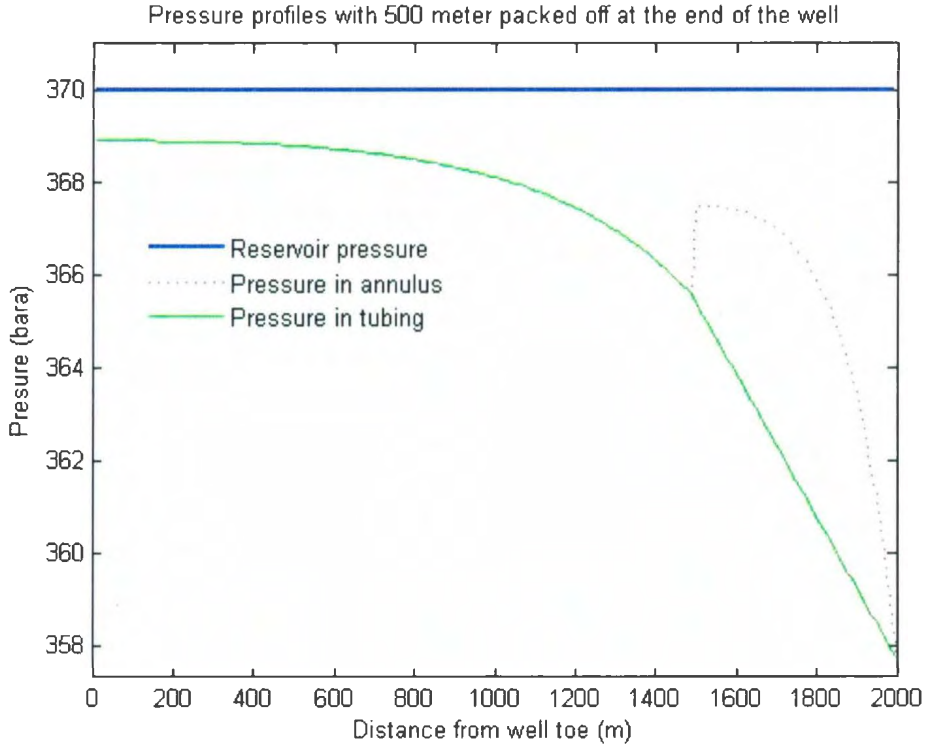

Figure 5.5.2 Pressure profile with 500 meters packed off at the end of well

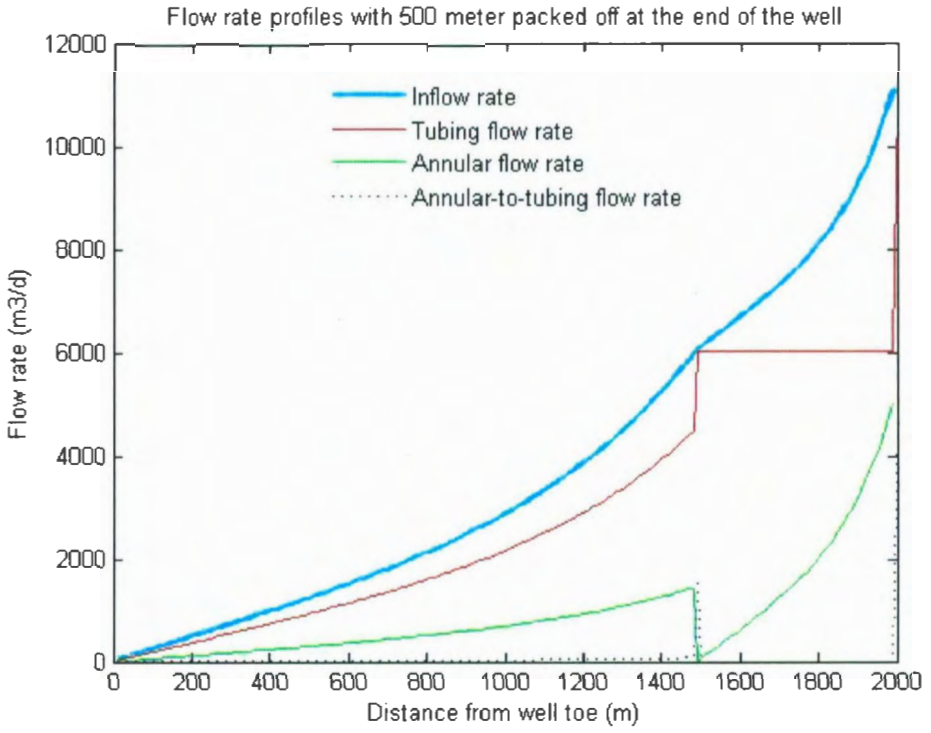

Figure 5.5.3 Flow rate profile with 500 meters packed off at the end of well

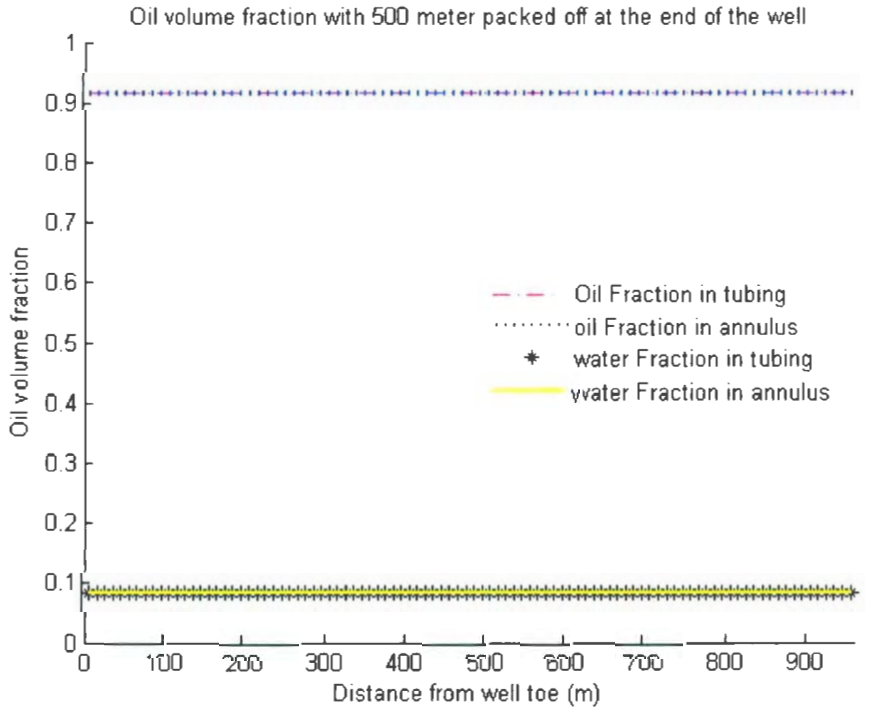

Figure 5.5.4 Phase Fraction profile with 500 meters packed off at the end of well

Properties	Value
Well Length (m)	2000
Segment length (m)	10
Reservoir pressure (bara)	370
Pressure at heel (bara)	357.5
Reservoir temperature	100
Permeability (Darcy)	1
Near-wellbore skin factor	1
Oil saturation	.65
Water saturation	.35
Tubing diameter (m)	0.127
Well outside diameter (m)	0.167
Discharge coefficient for slot flow ($Pa \cdot (kg/m^3)^{-1} \cdot (m/s)^{-2}$)	10

Table 5.5.1 Properties and initial values for Restricted Flow in the Annulus

5.6 Case 5: Stinger Completion

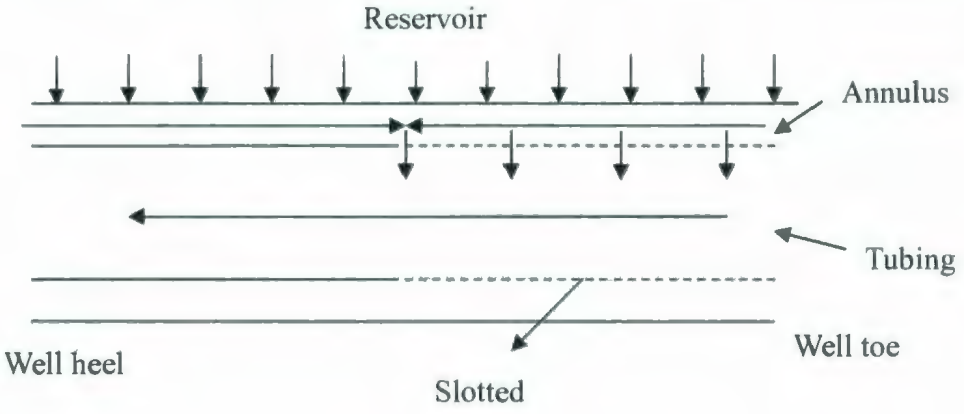

Figure 5.6.1 Sketch for stinger completion

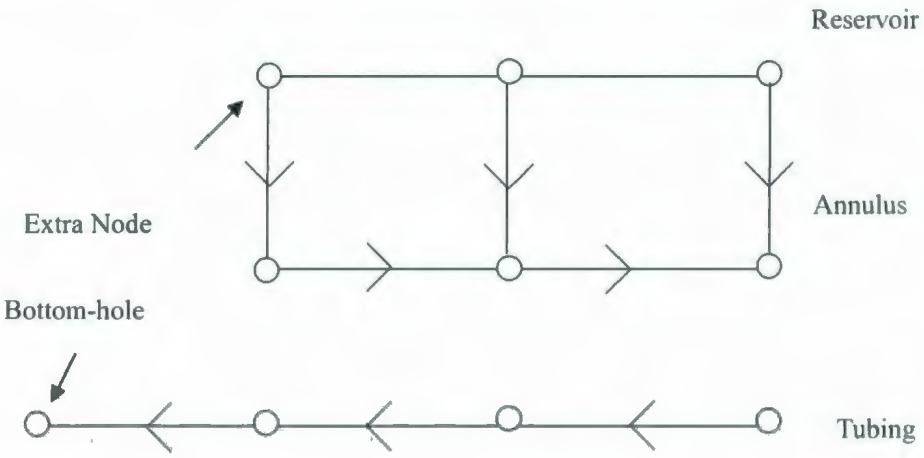

Figure 5.6.2 Network model modification for Stinger

The horizontal well has longer length and more contact with the reservoir than vertical well, but the resistance of the fluid in the horizontal well is also higher than the vertical well. The pressure drop over horizontal wells has been considered as a potential problem during the production, these problems include the unequal pressure drawdown along the well, this drawback could lead to the ineffectiveness for the toe of the well and higher chance for water and gas coning at the heel. In order to produce sustainablely and economically from the horizontal well, the stinger completion has been introduced to balance the unequal pressure

drawdown along the well from the toe to the heel. The structure and fluid physical movement is shown in Figure 5.6.1.

The entire well with stinger is divided into two sections; one is completed with stinger (blank pipe), the one is completed with slotted liner. And the heel of annulus is cemented and there is absolutely no annulus to tubing flow on stinger side into neither the bottom-hole nor the tubing. So that the annulus flow as shown in Figure 5.6.1 has two directions, one is from the toe to the heel, and the other one is from the heel to the toe. Two of these strings flow towards each other, and finally meet at the junction of two completions. As shown in the Figure 5.6.2, the pressure and flow distributions are completely changed in annulus channel; further more annulus flow are heel no longer flow into bottom-hole, but start to flow from annulus heel towards the well toe. Due to this change, an extra reservoir node would be added at the end of annulus, and bring in the inflow from reservoir to the annulus heel.

In this research, a horizontal well with the length of 520 meters is considered, and the stinger is completed with the length of 270 meters at the end of the well. And the pressure in annulus decreases gradually from two ends of the well (toe and heel), two pressure curves achieve a common value at the junction of the stinger section and slotted liner section, as shown Figure 5.6.2 the pressure drawdown in both annulus and tubing has been well controlled. As the pressure drop in these two sections of annulus, the flow rate grows up from the two ends of the well till the junction segment; Similar to Case 4, the tubing pressure at stinger section decreases linearly due to friction effect and no inflow existing.

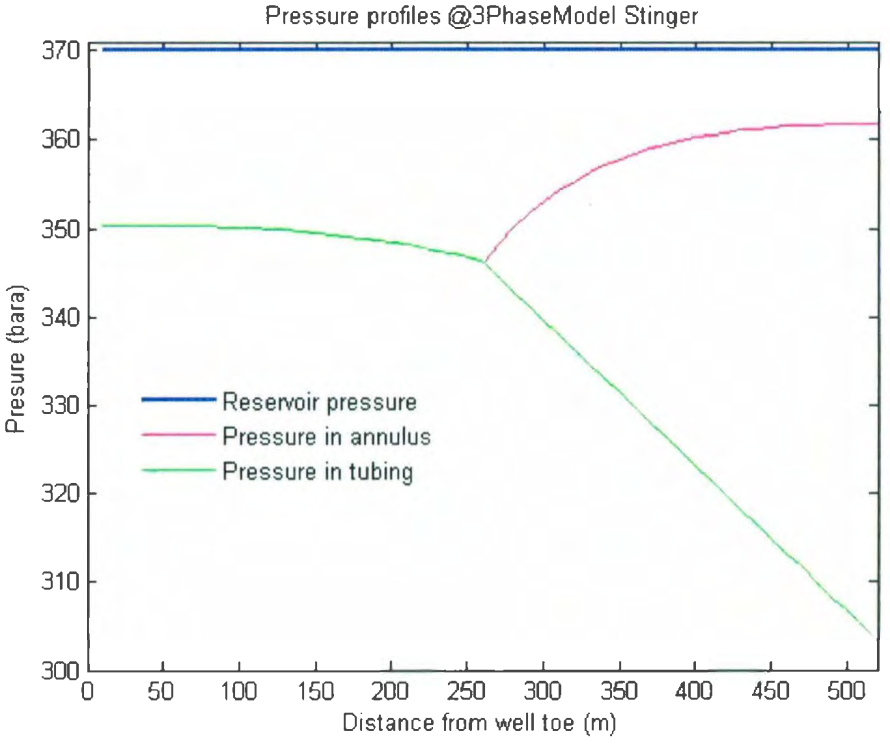

Figure 5.6.2 Pressure profile of Stinger completion

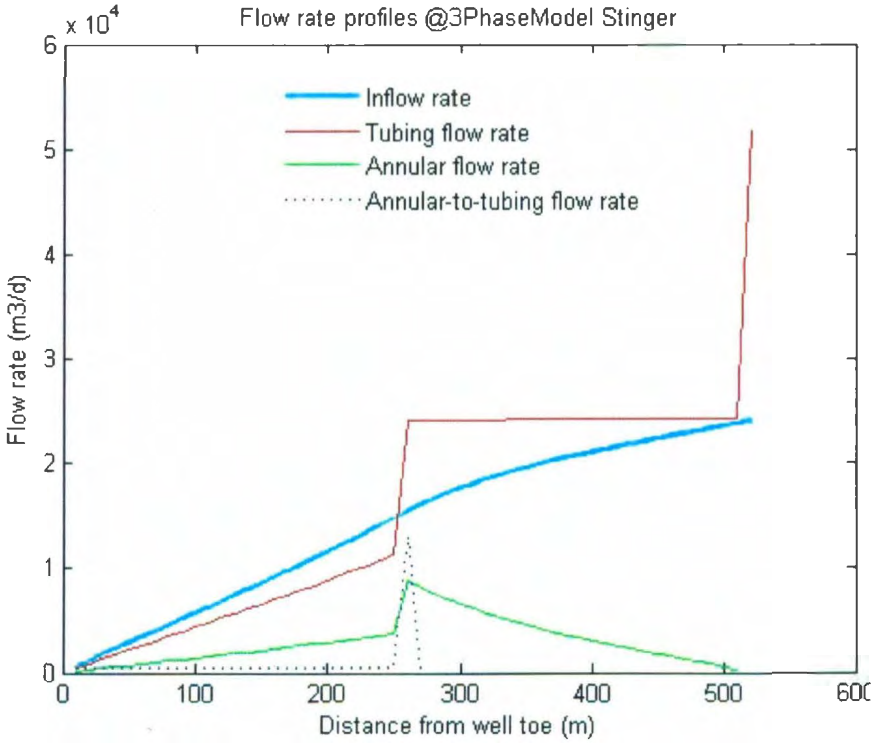

Figure 5.6.3 Flow rate profile of Stinger completion

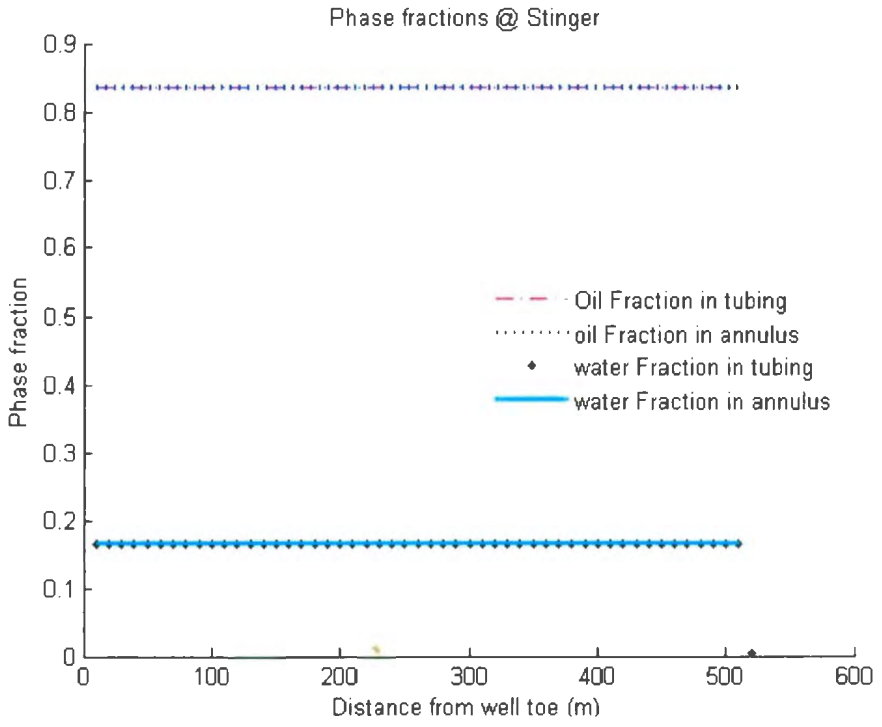

Figure 5.6.4 Phase Fraction of Stinger completion

From the simulation results for stinger completion, the wellbore performance at slotted liner section is the same as the Case 1, and the annulus fluid flow of the stinger section moves towards the well toe with no annulus to tubing flow because of the blank pipe restriction, consequently the tubing fluid flow rate at stinger section stays constant. At the junction segment, as two incoming fluids from the annulus merge together, therefore the tubing flow rate surges at this segment and two annulus flow rates reach the same value at the merging point which is also the maximal flow rate point at annulus.

Properties	Value
Well Length (m)	2000
Segment length (m)	10
Reservoir pressure (bara)	370
Pressure at heel (bara)	357.5
Reservoir temperature	100
Permeability (Darcy)	1
Near-wellbore skin factor	1
Oil saturation	.80
Water saturation	.20
Tubing diameter (m)	0.127
Well outside diameter (m)	0.167
Discharge coefficient for slot flow ($Pa \cdot (kg/m^3)^{-1} \cdot (m/s)^{-2}$)	10

Table 5.6.1 Properties and initial values for Stinger completion

5.7 Initial guess techniques

The Newton Raphson iterative method (N-R method) is the approach to solve the network model, and the iteration procedure starts from the 'initial guess'. This is where initial values of unknown variables are selected. As the base network solver is modified for different completions, the network structure could be complicated. Due to the complexity of the network structure and the nature of this numerical method, a suitable initial guess is crucial for the execution and time efficiency of the network solver.

The principal of the initial guess problem is to precisely construct the network model with different completion components, describe the initial flow parameters physically for each segment, and portray production tendency of whole system logically.

One good way to estimate the initial guess for starting N-R method is to linearize the problem with boundary conditions. In this research, all the cases studied could be summarized to two kind initial guess methods, which are practically distinguished by the annulus pressure and flow distributions. One common type is annulus pressure monotone decreasing along with tubing pressure from well toe to well heel, and the annulus fluid flow is parallel to the tubing flow; for the other type (Stinger completion), the annulus pressure decreases from two ends (well toe and well heel) of the horizontal well, and two direction fluid flows exist in the annulus channel, and flow towards each other respectively from well toe and well heel, eventually merge and flow into the tubing channel.

For both configurations, reservoir pressure and bottom-hole pressure are given as boundary conditions, the purpose of initial guess is to assign the initial pressure values at each wellbore nodes, calculate the initial fluid flow rates and phase fractions for each flow bridge.

For the first configuration, to initiate the network solver, the well toe pressure is assumed

equal to the reservoir pressure. And the pressures in annulus and tubing are considered as being equal and decreasing linearly with a constant difference within the segments. Then pressure difference between two ends of the well and the pressure interval for each segment could be calculated by the reservoir pressure, bottom-hole pressure and the number of segments; therefore the wellbore (including annulus and tubing) pressures at each node could be assigned gradually. Since the reservoir pressure and annulus pressure are known at this step, the inflow rate could be calculated using the productivity equation in Chapter 3. Annulus flow rate and tubing flow rate could be assigned as certain proportion of inflow rate, this proportion is decided by the cross-section areas of annulus and tubing; the annulus to tubing flow rate is assumed to be equal to tubing flow rate. Initial phase fractions in flow bridges are assigned equal to the respective phase fractions in the reservoir.

For the second configuration (Stinger completion), the only difference from the first one is the annulus pressure and flow distributions due to the blank pipe of the stinger. The critical step to initiate the singer completion is to specify the position of the blank pipe and merging point for two direction flows in annulus, and then all the flow parameters are assigned according to this condition. Similar to the first configuration, reservoir pressure and bottom-hole pressure are known, and the well toe pressure at tubing and two ends of annulus are assigned equal to the reservoir pressure. Then the initial values of flow parameters in tubing and slots are similar to the first case, and annulus initiation is a special case for stinger completion. After the merging point is spotted, and pressure drop from the annulus toe and the annulus heel simultaneously towards the merging point, As shown in Figure 4.7.1.

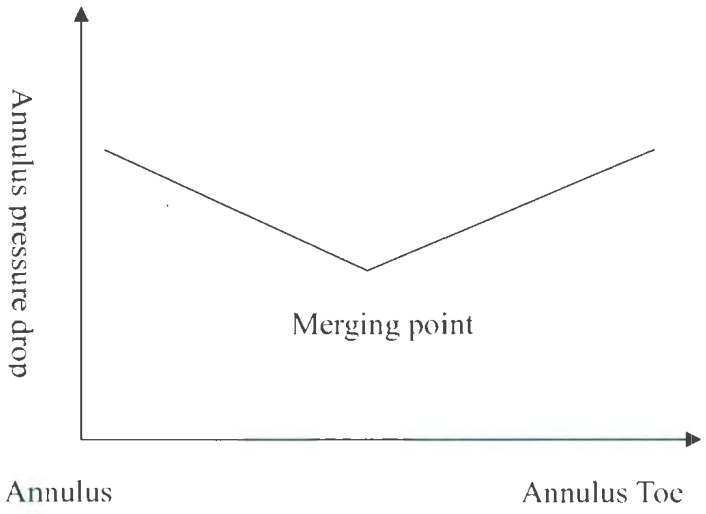

Figure 4.7.1: Sketch of pressure drop in annulus for stinger completion

Consequently the tubing pressure at merging point could be estimated by the total pressure difference and position of the merging point. Physically, the annulus pressure at merging point is assigned equal to that at tubing. So the initial pressure values at each annulus node could be calculated, from here, the inlet flow rate could be calculated from productivity equation by using reservoir pressure and annulus pressure. Phase fractions at annulus are initially equal to reservoir phase fractions. One important point to mention here, because there are two flow directions in annulus channel; the two different signs with positive (+1) and negative (-1) are associated to flow rate. Within the network system, flow directions are defined that the flow from well toe to well heel is positive flow, and the flow from well heel to well toe is negative.

Chapter 6 Conclusion and Recommendation

6.1 Conclusion and summary

A comprehensive network model is proposed to model the three phase fluid behavior in an isothermal environment. This network model has been modified to simulate different completions, such as slotted liner, inflow control device, pack-off, and stinger. The flow parameters including pressure distribution, flow rate, and three phase fractions are predicted along the whole horizontal wellbore.

In this research, several cases have been tested to ensure the robustness and stability of the model. These cases are oil-gas system and water-gas system above the bubble point pressure, open hole without annulus flow and completion, pressure under bubble point for the entire well, and encountering pressure under bubble point during the production.

Different completion components are demonstrated, and the fluids flow behavior has been simulated while crossing the complex completions. Pressure, flow rate, and three phase fraction were predicted along the well with advanced completions. Five cases were simulated in this research; they are Slotted liner, Restricted flow in the annulus, multiple inflow control devices, completion with 500 meter pack-off at the end of well, and stinger completion.

6.2 Recommendation

1. The present three phase model is for the isothermal environment, and the reservoir condition and properties are assumed constant along the wellbore. Based the proposed model, the reservoir temperature and properties such as permeability, skin factor, and phase saturations could be modified to precisely portray the real reservoir productions, which are

more complicated.

2. Split equations were used in the proposed model to meet the number of the governing equation to solve the flow parameters. The network structure could be refined by inserting more nodes on inflow bridges and annulus-to-tubing bridges for each segment, and the phase fraction change at split nodes could be investigated accurately.

3. The proposed three phase model assumes homogenized flow between the three phases, oil, water and gas, but phase slippage happens frequently in the fluid flow, which means phase velocities are different. Based on the proposed model, phase slippage could be investigated by coupling the drift flux model.

4. Multi-lateral wells could be investigated by a tree structure using nested iterations based on the proposed network model.

5. Deviation in the proposed model is 90 degrees, which means the well is exactly horizontal. By modifying the network structure, a complicated deviation condition could be investigated.

Appendix A: Example on assembling the Jacobian Matrix.

Take First segment for example:

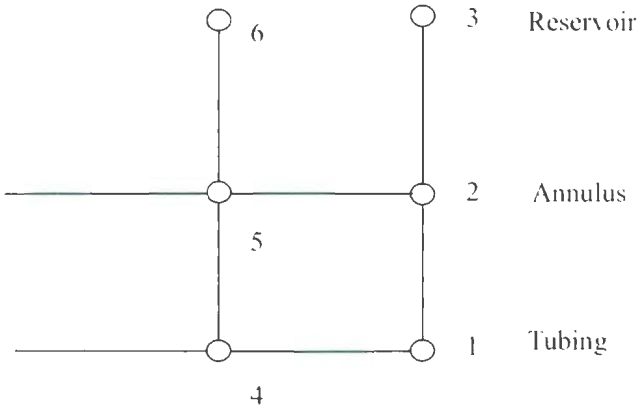

The first segment is constituted by 6 nodes, which are standing for the wellbore and near wellbore reservoir respectively as shown in the above figure. And a simple example about how to compute Jacobian matrix for Newton-Raphson method is given in the following part.

Parameters:

p : *pressure* q : *flowrate* α : *oil fraction* β : *water_fraction*

B_o : *oil_formation volume_factor* B_w : *water_formation volume factor*

B_g : *gas_formation_volume_factor* R_s : *gas_solubility* I : *productivity_index*

Beta : *pre-calculated_coefficience*

Subscripts:

digits : *nodes_or bridge* *res* : *reservoir_condition*

o : *oil_phase* *w* : *water_phase* *g* : *gas_phase*

ref : *reference_data*

$$variable\_matrix\_for\ segment\_1:$$
$$= \left[p_1, p_2, q_{1,13}, q_{2,1}, q_{2,14}, q_{3,2}, \alpha_{1,13}, \alpha_{2,1}, \alpha_{2,14}, \beta_{1,13}, \beta_{2,1}, \beta_{2,14} \right]$$

Equation system for segment 1:

Oil material balance:

$$f(1) = q_{2,1}\alpha_{2,1}/B_o(2) - q_{1,13}\alpha_{1,13}/B_o(1)$$

$$f(2) = q_6\alpha_{res}/B_o(3) - q_{2,14}\alpha_{2,14}/B_o(2) - q_{2,1}\alpha_{2,1}/B_o(2)$$

Water material balance:

$$f(3) = q_{2,1}\beta_{2,1}/B_w(2) - q_{1,13}\beta_{1,13}/B_w(1)$$
$$f(2) = q_6\beta_{res}/B_w(3) - q_{2,14}\beta_{2,14}/B_w(2) - q_{2,1}\beta_{2,1}/B_w(2)$$

Gas material balance:

$$f(5) = (1-\alpha_{2,1}-\beta_{2,1})q_{2,1}/B_g(2) + \alpha_{2,1}R_s q_{2,1}/B_o(2)$$
$$-\left\{(1-\alpha_{1,13}-\beta_{1,13})q_{1,13}/B_g(1) + \alpha_{1,13}q_{1,13}R_s(1)\ B_o(1)\right\}$$
$$f(6) = (1-\alpha_{res}-\beta_{res})q_{3,2}/B_g(3) + \alpha_{res}R_s q_{3,2}/B_o(3)$$
$$-\left\{(1-\alpha_{2,1}-\beta_{2,1})q_{2,1}/B_g(2) + \alpha_{2,1}R_s q_{2,1}/B_o(2)\right\}$$
$$-\left\{(1-\alpha_{2,14}-\beta_{2,14})q_{2,14}/B_g(2) + \alpha_{2,14}R_s q_{2,14}/B_o(2)\right\}$$

Inflow equation:

$$f(7) = q_{3,2} - I(1)(p_{res}(1)/p_{ref} - p_2)\,p_{ref}/q_{ref}$$

Momentum balance for tubing bridge:

$$f(8) = p_1 - p_{13} - beta(1)q_{1,13}^{1.75}rho3P(1)^{0.75}mu3P(1)^{0.25}$$

Flow equation for annular-to-tubing bridge:

$$f(9) = p_2 - p_1 - B(1)q_{2,1}^{2}rho3P(2)$$

Momentum balance for annular bridge:

$$f(10) = p_2 - p_{14} - alpha(1)q_{2,14}^{1.75}rho3P(3)^{0.75}mu3P(3)^{0.25}$$

Split Equations:

$$f(11) = \alpha_{2,1} - \alpha_{2,14}$$
$$f(12) = \beta_{2,1} - \beta_{2,14}$$

Phase Parameter calculation:

$$rho3P(1) = rho_{oil}\alpha_{1,13} + rho_{water}\beta_{1,13} + rho_{gas}(1-\alpha_{1,13}-\beta_{1,13})$$
$$rho3P(2) = rho_{oil}\alpha_{2,1} + rho_{water}\beta_{2,1} + rho_{gas}(1-\alpha_{2,1}-\beta_{2,1})$$
$$rho3P(3) = rho_{oil}\alpha_{2,14} + rho_{water}\beta_{2,14} + rho_{gas}(1-\alpha_{2,14}-\beta_{2,14})$$
$$mu3P(1) = mu_{oil}\alpha_{1,13} + mu_{water}\beta_{1,13} + mu_{gas}(1-\alpha_{1,13}-\beta_{1,13})$$
$$mu3P(2) = mu_{oil}\alpha_{2,1} + mu_{water}\beta_{2,1} + mu_{gas}(1-\alpha_{2,1}-\beta_{2,1})$$
$$mu3P(3) = mu_{oil}\alpha_{2,14} + mu_{water}\beta_{2,14} + mu_{gas}(1-\alpha_{2,14}-\beta_{2,14})$$

Example of Jacobian Matrix calculation:

Matrix involving volumetric formation factors:

$$J(1,1) = \frac{\partial f(1)}{\partial q_1} = \alpha_{1,13}\left(\frac{\partial B_o(1)}{\partial q_1}\right)^2$$

$$J(3,1) = \beta_{1,13}\left(\frac{\partial B_w(1)}{\partial q_1}\right)^2$$

Matrix involving three phase density and viscosity:

$$J(8,7) = -beta(1)\{1.75 q_{1,13}{}^{1.75} mu3P(1)^{0.25} rho3P(1)^{-0.25}\left(rho_{oil} - rho_{gas}\right)$$

$$+0.25 q_{1,13}{}^{1.75} rho3P(1)^{0.75} mu3P(1)^{0.75}\left(mu_{oil} - mu_{gas}\right)\}$$

Appendix B: Source Code for Network Solver

Main Solver:

```
% Network Solver
% This code is developed based on the two phase (oil/gas) model by
% Worakanok Thanyamanta and Chris Johansen.
% The code related to the water phase is originally done by Jiyi Liu

%----------DATA LOADING BEGIN----------
input_data;                 % Input data file

input_p;                    % Input reservoir pressures
input_L;                    % Input segment lengths
input_c;                    % Input slot/valve discharge coefficients
input_K;                    % Input absolute permeabilities
input_kro;                  % Calculate oil relative permeabilities
input_krg;                  % Calculate gas relative permeabilities
input_krw;
input_s;                    % Input skin factors


%----------GENERATING RESERVOIR FLUID PROPERTIES BEGIN--------
% Calculate fluid properties at inlet (reservoir) nodes.
[Bo_res Bw_res Bg_res Rs_res] = generateResprop(N,pres,pb);          % Calculate pressure-
dependent black-oil properties at reservoir conditions
mu_res = generatemures(Tres,pres,pb,N,Rs_res);              % Calculate pressure/temperature
dependent oil viscosities
input_alpha;                                % Calculate liquid holdups in the reservoir
[rho3P_res rho_res] = generateRhores(pres,pb,N,alpha_res);     % Calculate pressure-
dependent densities for each phase and two-phase (TP) fluid
mu3P_res = generatemu3P(mu_res,N,alpha_res,pres,pb);          % Calculate two-phase (TP)
fluid viscosities

%----------GENERATING RESERVOIR FLUID PROPERTIES END--------

%----------DATA LOADING END----------

clc;

%----------PRE-CALCULATIONS BEGIN----------

precalculations;            % Precalculate some coefficient values to help inerase the
calculation rate
```

```
guess;                  % Initial guessed values of unknown parameters


%----------GENERATING WELLBORE FLUID PROPERTIES BEGIN--------
% Calculate fluid properties at all nodes in the well network based on the guessed unknown
parameters.
Rs = generateRs(X1,pres,Rs_res,pref,pb,N,num_var,Nodes);    % Calculate pressure-
dependent gas solubilities
Bo = generateBo(X1,pres,Bo_res,pref,pb,N,num_var,Nodes);    % Calculate pressure-
dependent oil formation volume factors
Bw = generateBw(X1,pres,Bw_res,pref,pb,N,num_var,Nodes);
Bg = generateBg(X1,pres,Bg_res,pref,pb,N,num_var,Nodes);    % Calculate pressure-
dependent gas formation volume factors
[mu3P mu] =
generatemu(T_temp,X1,Tres,pref,pb,N,num_var,num_varT,Nodes,bridges,Rs,mu3P_res,mu_r
es);        % Calculate pressure/temperature dependent viscosities for each phase and two-
phase (TP) fluid
[rho3P rho] = generaterho(X1,pres,rho3P_res,rho_res,pref,pb,N,num_var,Nodes,bridges);
% Calculate pressure-dependent densities for each phase and two-phase (TP) fluid

%----------GENERATING WELLBORE FLUID PROPERTIES END--------

%----------PRE-CALCULATIONS END----------

%----------ITERATIVE PROCESS BEGIN----------

% SentinelCount counts how many iterations that has been done, so that the
% program stops when the desired number of iterations are reached.
sentinelCount = 0;
% Flag determines whether the iteration should stop (solutions converged)
flag = true;
generateBindex;             % Generate indexes for directions of flow through each bridge

iteration                   % Iterate function calculations to solve for unknowns using Newton-
Raphson method

%----------ITERATIVE PROCESS END----------

% Isothermal network model end
```

Iteration Function for Newton-Raphson Method:

```
% Iterate function calculations to solve for unknowns using Newton-Raphson
% method
% This code is developed based on the two phase (oil/gas) model by
% Worakanok Thanyamanta and Chris Johansen.
% The code related to the water phase is originally done by Jiyi Liu

f1 = zeros(1,12);              % Function matrix for Segment 1
f2 = zeros(1,num_var-(12+8));  % Function matrix for Segment 2 to N-1
f3 = zeros(1,8);               % Function matrix for Segment N

j1 = zeros(12,num_var);              % Jacobian matrix for Segment 1
j2 = zeros(num_var-(12+8),num_var);  % Jacobian matrix for Segment 2 to N-1
j3 = zeros(8,num_var);               % Jacobian matrix for Segment N

converge = 0;                  % Convergence value to be compared with the tolerance value

% guess;

while(flag)

   % Generating function matrices
   f1 = f1Generator(X1,I,pres,beta,alpha,B,Bo,Bw,Bg,Rs,mu3P,rho3P,alpha_res,f1,pref,qref);
   f2 =
f2Generator(X1,beta,alpha,B,I,pres,Bo,Bw,Bg,Rs,mu3P,rho3P,alpha_res,f2,pref,qref,N,bindex
);
   f3 =
f3Generator(X1,beta,B,Bo,Bw,Bg,Rs,mu3P,rho3P,f3,pref,pbh,N,num_var,Nodes,bridges,bind
ex);

   f = [f1 f2 f3];         % Combine the matrices

   % Generating jacobian matrices
   j1 = j1Generator(X1,I,beta,alpha,B,j1,Bo,Bw,Bg,Rs,rho3P,mu3P,alpha_res,pref,qref);
   j2 =
j2Generator(X1,beta,alpha,I,B,j2,Bo,Bw,Bg,Rs,rho3P,mu3P,alpha_res,pref,qref,N,bindex);
   j3 =
j3Generator(X1,beta,B,j3,Bo,Bw,Bg,Rs,rho3P,mu3P,pref,N,num_var,Nodes,bridges,bindex);

   jac = [j1;j2;j3];       % Combine the matrices

   % LU factorization -- Inversion of the jacobian matrix

   [L1 U1] = lu(jac);
```

```
L1_INV = inv(L1);
U1_INV = inv(U1);

temp1 = L1_INV*transpose(f);
temp2 = U1_INV*temp1;

temp3 = transpose(temp2);

X2 = X1 - temp3;

% Checking for convergence.  If checkConvergence finds that the method
% converges it will set flag to false and the program will stop.

[flag, test] = checkConvergence(X1,X2,num_var,threshold);
converge(sentinelCount+1) = test          % Convergence value of each iteration

%Setting Xn = Xn+1 for the next iteration

X1 = X2;

%----------RECALCULATE WELLBORE FLUID PROPERTIES BEGIN--------
Rs = generateRs(X1,pres,Rs_res,pref,pb,N,num_var,Nodes);          % Calculate pressure-
dependent gas solubilities
Bo = generateBo(X1,pres,Bo_res,pref,pb,N,num_var,Nodes);          % Calculate pressure-
dependent oil formation volume factors
Bw = generateBw(X1,pres,Bw_res,pref,pb,N,num_var,Nodes);
Bg = generateBg(X1,pres,Bg_res,pref,pb,N,num_var,Nodes);          % Calculate pressure-
dependent gas formation volume factors
[mu3P mu] =
generatemu(T_temp,X1,Tres,pref,pb,N,num_var,num_varT,Nodes,bridges,Rs,mu3P_res,mu_r
es); % Calculate pressure/temperature dependent viscosities for each phase and two-phase
(TP) fluid
[rho3P rho] = generaterho(X1,pres,rho3P_res,rho_res,pref,pb,N,num_var,Nodes,bridges);
% Calculate pressure-dependent densities for each phase and two-phase (TP) fluid

%----------RECALCULATE WELLBORE FLUID PROPERTIES END--------

% This if statement makes sure that the iteration stops if
% the method does not converge whithin a number of iteration input by the
% user in input_data.m

if(sentinelCount == stop)

   disp(' ');
   disp('Did not converge whithin the limitations given!');
   break;
```

```
    end

    % Update iteration index (sentinelCount)
    sentinelCount = sentinelCount + 1;

end
    % Check for imaginary numbers
for i=1:num_var
    if imag(X1)<1e-12   % If the imaginary part of the solution is less than a value it is
negligible
        X1=real(X1);
    else                % If the imaginary part is large display "imag"
        disp('imag');
    end
end

% Conversions of the converged variables back to their appropriate units and
% result display
displayoutput;
```

Matlab Code for Equation system:

```
% Generate function matrix for Segment 1
% This code is developed based on the two phase (oil/gas) model by
% Worakanok Thanyamanta and Chris Johansen.
% The code related to the water phase is originally done by Jiyi Liu
%Input:
%
%X1        :  Unknown parameters at each iteration
%I         :  Pre-calculated coefficient for inflow equations
%pres      :  Reservoir pressures
%beta      :  Pre-calculated coefficient for tubing flow calculations
%alpha     :  Pre-calculated coefficient for annular flowcalculations
%B         :  Pre-calculated coefficient for slot/valve flow calculations
%Bo,Bw,Bg,Rs  :  Black-oil properties
%mu3P      :  Three-phase viscosities
%rho3P     :  Three-phase densities
%alpha_res :  Liquid holdups in reservoir
%f1        :  Generated zero function matrix
%pref      :  Reference pressure
%qref      :  Reference flow rate
%
%Return:
%Function matrix for Segment 1
```

```
function func =
f1Generator(X1,I,pres,beta,alpha,B,Bo,Bw,Bg,Rs,mu3P,rho3P,alpha_res,f1,pref,qref)


% oil-phase material balance
f1(1) = X1(4)*X1(8)/Bo(2) - X1(3)*X1(7)/Bo(1); % At node 1
f1(2) = X1(6)*alpha_res(1,1)/Bo(3) - X1(4)*X1(8)/Bo(2) - X1(5)*X1(9)/Bo(2);          %
At node 2
% water-phase material balance
f1(3) = X1(4)*X1(11)/Bw(2) - X1(3)*X1(10)/Bw(1); % At node 1
f1(4) = X1(6)*alpha_res(2,1)/Bw(3) - X1(4)*X1(11)/Bw(2) - X1(5)*X1(12)/Bw(2);
% At node 2
% Inflow equation
f1(5) = X1(6) - I(1)*(pres(1)/pref - X1(2))*pref/qref;
% Momentum balance for tubing bridge
f1(6) = X1(1) - X1(13) - beta(1)*(X1(3)^1.75)*rho3P(1)^0.75*mu3P(1)^0.25;
% Flow equation for annular-to-tubing bridge
f1(7) = X1(2) - X1(1) - B(1)*(X1(4)^2)*rho3P(2);
% Momentum balance for annular bridge
f1(8) = X1(2) - X1(14) - alpha(1)*(X1(5)^1.75)*rho3P(3)^0.75*mu3P(3)^0.25;
% Gas-phase material balance
f1(9) = ((1-X1(8)-X1(11))*X1(4)/Bg(2) + X1(8)*Rs(2)*X1(4)/Bo(2)) - ((1-X1(7)-
X1(10))*X1(3)/Bg(1) + X1(7)*Rs(1)*X1(3)/Bo(1));   % At node 1
f1(10) = (alpha_res(3,1)*X1(6)/Bg(3) + alpha_res(1,1)*Rs(3)*X1(6)/Bo(3)) - ((1-X1(8)-
X1(11))*X1(4)/Bg(2) + X1(8)*Rs(2)*X1(4)/Bo(2)) - ((1-X1(9)-X1(12))*X1(5) Bg(2) +
X1(9)*Rs(2)*X1(5)/Bo(2));   % At node 2
% Split equation
f1(11) = X1(9) - X1(8);
f1(12) = X1(12) - X1(11);

func = f1;


% Generate function matrix for Segment 2 to N-1
% This code is developed based on the two phase (oil/gas) model by
% Worakanok Thanyamanta and Chris Johansen.
% The code related to the water phase is originally done by Jiyi Liu
%Input:
%
%X1       :  Unknown parameters at each iteration
%beta     :  Pre-calculated coefficient for tubing flow calculations
%alpha    :  Pre-calculated coefficient for annular flowcalculations
%B        :  Pre-calculated coefficient for slot/valve flow calculations
%I        :  Pre-calculated coefficient for inflow equations
%pres     :  Reservoir pressures
```

```
%Bo,Bw,Bg,Rs   :  Black-oil properties
%mu3P      :  Three-phase viscosities
%rho3P     :  Three-phase densities
%alpha_res :  Liquid holdups in reservoir
%f2        :  Generated zero function matrix
%pref      :  Reference pressure
%qref      :  Reference flow rate
%N         :  Number of segments
%b         :  Bridge indexes
%
%Return:
%Function matrix for Segment 2 to N-1

function func =
f2Generator(X1,beta,alpha,B,I,pres,Bo,Bw,Bg,Rs,mu3P,rho3P,alpha_res,f2,pref,qref,N,b)

for i=0:N-3

   var = i*12;

   % oil-phase material balance
   f2(1+var) = X1(16+var)*X1(20+var)/Bo(3*i+5)*b(4*i+6) +
X1(3+var)*X1(7+var)/Bo(3*i+1)*b(4*i+1) - X1(15+var)*X1(19+var)/Bo(3*i+4)*b(4*i+5);
% At tubing node
   f2(2+var) = X1(5+var)*X1(9+var)/Bo(3*i+2)*b(4*i+3) +
X1(18+var)*alpha_res(1,i+2)/Bo(3*i+6)*b(4*i+8) -
X1(17+var)*X1(21+var)/Bo(3*i+5)*b(4*i+7) - X1(16+var)*X1(20+var)/Bo(3*i+5)*b(4*i+6);
% At annular node

   % water-phase material balance
   f2(3+var) = X1(16+var)*X1(23+var)/Bw(3*i+5)*b(4*i+6) +
X1(3+var)*X1(10+var)/Bw(3*i+1)*b(4*i+1) - X1(15+var)*X1(22+var)/Bw(3*i+4)*b(4*i+5);
% At tubing node
   f2(4+var) = X1(5+var)*X1(12+var)/Bw(3*i+2)*b(4*i+3) +
X1(18+var)*alpha_res(2,i+2)/Bw(3*i+6)*b(4*i+8) -
X1(17+var)*X1(24+var)/Bw(3*i+5)*b(4*i+7) -
X1(16+var)*X1(23+var)/Bw(3*i+5)*b(4*i+6);       % At annular node

   % Inflow equation
   if b(4*i+8) ~= 0       % Inlet flow exists
      f2(5+var) = X1(18+var) - (I(i+2)*(pres(i+2)/pref - X1(14+var)))*pref/qref;
   else                   % No inlet flow
      f2(5+var) = 0;
   end
   % Momentum balance for tubing bridge
```

```
    f2(6+var) = X1(13+var) - X1(25+var) -
beta(i+2)*(X1(15+var)^1.75)*rho3P(4*i+5)^0.75*mu3P(4*i+5)^0.25;
    % Flow equation for annular-to-tubing bridge
    if b(4*i+6) ~= 0        % Annular-to-tubing flow exists
      f2(7+var) = X1(14+var) - X1(13+var) - B(i+2)*(X1(16+var)^2)*rho3P(4*i+6);
    else                    % No annular-to-tubing flow
      f2(7+var) = 0;
      f2(11+var) = 0;
      f2(12+var) = 0;       % No split equation
    end
    % Momentum balance for annular bridge
    if b(4*i+7) ~= 0        % Annular flow exists
      f2(8+var) = X1(14+var) - X1(26+var) -
alpha(i+2)*(X1(17+var)^1.75)*rho3P(4*i+7)^0.75*mu3P(4*i+7)^0.25*b(4*i+7);
      if b(4*i+7) == 1
        if b(4*i+6) ~= 0    % If there is both annular and annular-to-tubing flows
          f2(11+var) = X1(20+var) - X1(21+var);
          f2(12+var) = X1(23+var) - X1(24+var);    % Split equation
        end
      elseif b(4*i+7) == -1   % If flow in annulus is toward toe of well
        f2(11+var) = 0;
        f2(12+var) = 0;                    % No split equation
      end
    else                    % No annular flow
      f2(8+var) = 0;
      f2(11+var) = 0;
      f2(12+var) = 0;
    end
    % Gas-phase material balance
    f2(9+var) = ((1-X1(20+var)-X1(23+var))*X1(16+var)/Bg(3*i+5) +
X1(20+var)*Rs(3*i+5)*X1(16+var)/Bo(3*i+5))*b(4*i+6) + ((1-X1(7+var)-
X1(10+var))*X1(3+var)/Bg(3*i+1) + X1(7+var)*Rs(3*i+1)*X1(3+var)/Bo(3*i+1))*b(4*i+1)
- ((1-X1(19+var)-X1(22+var))*X1(15+var)/Bg(3*i+4) +
X1(19+var)*Rs(3*i+4)*X1(15+var)/Bo(3*i+4))*b(4*i+5);        % At tubing node

    f2(10+var) = ((1-X1(9+var)-X1(12+var))*X1(5+var)/Bg(3*i+2) +
X1(9+var)*Rs(3*i+2)*X1(5+var)/Bo(3*i+2))*b(4*i+3) +
(alpha_res(3,i+2)*X1(18+var)/Bg(3*i+6) +
alpha_res(1,i+2)*Rs(3*i+6)*X1(18+var)/Bo(3*i+6))*b(4*i+8) - ((1-X1(21+var)-
X1(24+var))*X1(17+var)/Bg(3*i+5) +
X1(21+var)*Rs(3*i+5)*X1(17+var)/Bo(3*i+5))*b(4*i+7) - ((1-X1(20+var)-
X1(23+var))*X1(16+var)/Bg(3*i+5) +
X1(20+var)*Rs(3*i+5)*X1(16+var)/Bo(3*i+5))*b(4*i+6);        % At annular node

end
```

```
func = f2;



% Generate function matrix for Segment N
% This code is developed based on the two phase (oil/gas) model by
% Worakanok Thanyamanta and Chris Johansen.
% The code related to the water phase is originally done by Jiyi Liu
%Input:
%
%X1        :  Unknown parameters at each iteration
%beta      :  Pre-calculated coefficient for tubing flow calculations
%B         :  Pre-calculated coefficient for slot/valve flow calculations
%Bo,Bw,Bg,Rs  :  Black-oil properties
%mu3P      :  Three-phase viscosities
%rho3P     :  Three-phase densities
%f3        :  Generated zero function matrix
%pref      :  Reference pressure
%pbh       :  Bottomhole pressure
%N         :  Number of segments
%num_var   :  Number of unknowns
%Nodes     :  Number of nodes
%bridges   :  Number of bridges
%b         :  Bridge indexes
%
%Return:
%Function matrix for Segment N

function func =
f3Generator(X1,beta,B,Bo,Bw,Bg,Rs,mu3P,rho3P,f3,pref,pbh,N,num_var,Nodes,bridges,b)

% oil-phase material balance
f3(1) = X1(num_var-17)*X1(num_var-13)/Bo(Nodes-4)*b(bridges-5) + X1(num_var-
4)*X1(num_var-2)/Bo(Nodes)*b(bridges) - X1(num_var-5)*X1(num_var-3)/Bo(Nodes-
1)*b(bridges-1);       % At tubing node
f3(2) = X1(num_var-15)*X1(num_var-11)/Bo(Nodes-3)*b(bridges-3) - X1(num_var-
4)*X1(num_var-2)/Bo(Nodes)*b(bridges);          % At annular node
% water-phase material balance
f3(3) = X1(num_var-17)*X1(num_var-10)/Bw(Nodes-4)*b(bridges-5) + X1(num_var-
4)*X1(num_var)/Bw(Nodes)*b(bridges) - X1(num_var-5)*X1(num_var-1)/Bw(Nodes-
1)*b(bridges-1);       % At tubing node
f3(4) = X1(num_var-15)*X1(num_var-8)/Bw(Nodes-3)*b(bridges-3) - X1(num_var-
4)*X1(num_var)/Bw(Nodes)*b(bridges);          % At annular node
```

```
% Momentum balance for tubing bridge
f3(5) = X1(num_var-7) - pbh/pref - beta(N)*(X1(num_var-5)^1.75)*rho3P(bridges-
1)^0.75*mu3P(bridges-1)^0.25;
% Flow equation for annular-to-tubing bridge
if b(bridges) ~= 0        % Annular-to-tubing flow exists
   f3(6) = X1(num_var-6) - X1(num_var-7) - B(N)*(X1(num_var-4)^2)*rho3P(bridges);
else                      % No annular-to-tubing flow
   f3(6) = 0;
end
% Gas-phase material balance
f3(7) = ((1-X1(num_var-13)-X1(num_var-10))*X1(num_var-17)/Bg(Nodes-4) +
X1(num_var-13)*Rs(Nodes-4)*X1(num_var-17)/Bo(Nodes-4))*b(bridges-5) + ((1-
X1(num_var-2)-X1(num_var))*X1(num_var-4)/Bg(Nodes) + X1(num_var-
2)*Rs(Nodes)*X1(num_var-4)/Bo(Nodes))*b(bridges) - ((1-X1(num_var-3)-X1(num_var-
1))*X1(num_var-5)/Bg(Nodes-1) + X1(num_var-3)*Rs(Nodes-1)*X1(num_var-5)/Bo(Nodes-
1))*b(bridges-1);       % At tubing node
f3(8) = ((1-X1(num_var-8)-X1(num_var-11))*X1(num_var-15)/Bg(Nodes-3) + X1(num_var-
11)*Rs(Nodes-3)*X1(num_var-15)/Bo(Nodes-3))*b(bridges-3) - ((1-X1(num_var-2)-
X1(num_var))*X1(num_var-4)/Bg(Nodes) + X1(num_var-2)*Rs(Nodes)*X1(num_var-
4)/Bo(Nodes))*b(bridges);                % At annular node

func = f3;


% Generate jacobian matrix for Segment 1
% This code is developed based on the two phase (oil/gas) model by
% Worakanok Thanyamanta and Chris Johansen.
% The code related to the water phase is originally done by Jiyi Liu
%Input:
%
%I          :  Pre-calculated coefficient for inflow equations
%X1         :  Unknown parameters at each iteration
%beta       :  Pre-calculated coefficient for tubing flow calculations
%alpha      :  Pre-calculated coefficient for annular flowcalculations
%B          :  Pre-calculated coefficient for slot/valve flow calculations
%j1         :  Generated zero jacobian matrix
%Bo,Bw,Bg,Rs  :  Black-oil properties
%mu3P       :  Three-phase viscosities
%rho3P      :  Three-phase densities
%alpha_res  :  Liquid holdups in reservoir
%pref       :  Reference pressure
%qref       :  Reference flow rate
%
%Return:
%Jacobian matrix for Segment 1
```

```
function func =
j1Generator(X1,I,beta,alpha,B,j1,Bo,Bw,Bg,Rs,rho3P,mu3P,alpha_res,pref,qref)

j1(1,3) = -X1(7)/Bo(1);
j1(1,4) = X1(8)/Bo(2);
j1(1,7) = -X1(3)/Bo(1);
j1(1,8) = X1(4)/Bo(2);

j1(2,4) = -X1(8)/Bo(2);
j1(2,5) = -X1(9)/Bo(2);
j1(2,6) = alpha_res(1,1)/Bo(3);
j1(2,8) = -X1(4)/Bo(2);
j1(2,9) = -X1(5)/Bo(2);

%

j1(3,3) = -X1(10)/Bw(1);
j1(3,4) = X1(11)/Bw(2);
j1(3,10) = -X1(3)/Bw(1);
j1(3,11) = X1(4)/Bw(2);

j1(4,4) = -X1(11)/Bw(2);
j1(4,5) = -X1(12)/Bw(2);
j1(4,6) = alpha_res(2,1)/Bw(3);
j1(4,11) = -X1(4)/Bw(2);
j1(4,12) = -X1(5)/Bw(2);

j1(5,2) = I(1)*pref/qref;
j1(5,6) = 1;

j1(6,1) = 1;
j1(6,3) = -1.75*beta(1)*(X1(3)^0.75)*rho3P(1)^0.75*mu3P(1)^0.25;
j1(6,13) = -1;

j1(7,1) = -1;
j1(7,2) = 1;
j1(7,4) = -2*B(1)*X1(4)*rho3P(2);

j1(8,2) = 1;
j1(8,5) = -1.75*alpha(1)*(X1(5)^0.75)*rho3P(3)^0.75*mu3P(3)^0.25;
j1(8,14) = -1;

j1(9,3) = -((1-X1(7)-X1(10))/Bg(1) + X1(7)*Rs(1)/Bo(1));
j1(9,4) = ((1-X1(8)-X1(11))/Bg(2) + X1(8)*Rs(2)/Bo(2));
j1(9,7) = -(-X1(3)/Bg(1) + Rs(1)*X1(3)/Bo(1));
j1(9,8) = (-X1(4)/Bg(2) + Rs(2)*X1(4)/Bo(2));
```

```
j1(9,10) = X1(3)/Bg(1);
j1(9,11) = -X1(4)/Bg(2);

j1(10,4) = -((1-X1(8)-X1(11))/Bg(2) + X1(8)*Rs(2)/Bo(2));
j1(10,5) = -((1-X1(9)-X1(12))/Bg(2) + X1(9)*Rs(2)/Bo(2));
j1(10,6) = alpha_res(3,1)/Bg(3) + alpha_res(1,1)*Rs(3)/Bo(3);
j1(10,8) = -(-X1(4)/Bg(2) + Rs(2)*X1(4)/Bo(2));
j1(10,9) = -(-X1(5)/Bg(2) + Rs(2)*X1(5)/Bo(2));
j1(10,11) = X1(4)/Bg(2);
j1(10,12) = X1(5)/Bg(2);

j1(11,8) = -1;
j1(11,9) = 1;
j1(12,11) = -1;
j1(12,12) = 1;

func = j1;



% Generate jacobian matrix for Segment 2 to N-1
% This code is developed based on the two phase (oil/gas) model by
% Worakanok Thanyamanta and Chris Johansen.
% The code related to the water phase is originally done by Jiyi Liu
%Input:
%
%X1        :  Unknown parameters at each iteration
%beta      :  Pre-calculated coefficient for tubing flow calculations
%alpha     :  Pre-calculated coefficient for annular flowcalculations
%I         :  Pre-calculated coefficient for inflow equations
%B         :  Pre-calculated coefficient for slot/valve flow calculations
%j2        :  Generated zero jacobian matrix
%Bo,Bw,Bg,Rs   :  Black-oil properties
%mu3P      :  Three-phase viscosities
%rho3P     :  Three-phase densities
%alpha_res :  Liquid holdups in reservoir
%pref      :  Reference pressure
%qref      :  Reference flow rate
%N         :  Number of segments
%b         :  Bridge indexes
%
%Return:
%Jacobian matrix for Segment 2 to N-1

function func =
j2Generator(X1,beta,alpha,I,B,j2,Bo,Bw,Bg,Rs,rho3P,mu3P,alpha_res,pref,qref,N,b)
```

```
for i=0:N-3

   var = 12*i;

   j2(1+var,3+var) = X1(7+var)/Bo(3*i+1)*b(4*i+1);
   j2(1+var,7+var) = X1(3+var)/Bo(3*i+1)*b(4*i+1);
   j2(1+var,15+var) = -X1(19+var)/Bo(3*i+4)*b(4*i+5);
   j2(1+var,16+var) = X1(20+var)/Bo(3*i+5)*b(4*i+6);
   j2(1+var,19+var) = -X1(15+var)/Bo(3*i+4)*b(4*i+5);
   j2(1+var,20+var) = X1(16+var)/Bo(3*i+5)*b(4*i+6);

   j2(2+var,5+var) = X1(9+var)/Bo(3*i+2)*b(4*i+3);
   j2(2+var,9+var) = X1(5+var)/Bo(3*i+2)*b(4*i+3);
   j2(2+var,16+var) = -X1(20+var)/Bo(3*i+5)*b(4*i+6);
   j2(2+var,17+var) = -X1(21+var)/Bo(3*i+5)*b(4*i+7);
   j2(2+var,18+var) = alpha_res(1,i+2)/Bo(3*i+6)*b(4*i+8);
   j2(2+var,20+var) = -X1(16+var)/Bo(3*i+5)*b(4*i+6);
   j2(2+var,21+var) = -X1(17+var)/Bo(3*i+5)*b(4*i+7);

   %

   j2(3+var,3+var) = X1(10+var)/Bw(3*i+1)*b(4*i+1);
   j2(3+var,10+var) = X1(3+var)/Bw(3*i+1)*b(4*i+1);
   j2(3+var,15+var) = -X1(22+var)/Bw(3*i+4)*b(4*i+5);
   j2(3+var,16+var) = X1(23+var)/Bw(3*i+5)*b(4*i+6);
   j2(3+var,22+var) = -X1(15+var)/Bw(3*i+4)*b(4*i+5);
   j2(3+var,23+var) = X1(16+var)/Bw(3*i+5)*b(4*i+6);

   j2(4+var,5+var) = X1(12+var)/Bw(3*i+2)*b(4*i+3);
   j2(4+var,12+var) = X1(5+var)/Bw(3*i+2)*b(4*i+3);
   j2(4+var,16+var) = -X1(23+var)/Bw(3*i+5)*b(4*i+6);
   j2(4+var,17+var) = -X1(24+var)/Bw(3*i+5)*b(4*i+7);
   j2(4+var,18+var) = alpha_res(2,i+2)/Bw(3*i+6)*b(4*i+8);
   j2(4+var,23+var) = -X1(16+var)/Bw(3*i+5)*b(4*i+6);
   j2(4+var,24+var) = -X1(17+var)/Bw(3*i+5)*b(4*i+7);

   %
   j2(9+var,3+var) = ((1-X1(7+var)-X1(10+var))/Bg(3*i+1) +
X1(7+var)*Rs(3*i+1)/Bo(3*i+1))*b(4*i+1);
   j2(9+var,7+var) = (-X1(3+var)/Bg(3*i+1) + Rs(3*i+1)*X1(3+var)/Bo(3*i+1))*b(4*i+1);
   j2(9+var,10+var) = (-X1(3+var)/Bg(3*i+1))*b(4*i+1);

   j2(9+var,15+var) = - ((1-X1(19+var)-X1(22+var))/Bg(3*i+4) +
X1(19+var)*Rs(3*i+4)/Bo(3*i+4))*b(4*i+5);
```

```
   j2(9+var,16+var) = ((1-X1(20+var)-X1(23+var))/Bg(3*i+5) +
X1(20+var)*Rs(3*i+5)/Bo(3*i+5))*b(4*i+6);

   j2(9+var,19+var) = - (-X1(15+var)/Bg(3*i+4) +
Rs(3*i+4)*X1(15+var)/Bo(3*i+4))*b(4*i+5);
   j2(9+var,20+var) = (-X1(16+var)/Bg(3*i+5) + Rs(3*i+5)*X1(16+var)/Bo(3*i+5))*b(4*i+6);

   j2(9+var,22+var) = (X1(15+var)/Bg(3*i+4))*b(4*i+5);
   j2(9+var,23+var) = (-X1(16+var)/Bg(3*i+5))*b(4*i+6);

   j2(10+var,5+var) = ((1-X1(9+var)-X1(12+var))/Bg(3*i+2) +
X1(9+var)*Rs(3*i+2)/Bo(3*i+2))*b(4*i+3);
   j2(10+var,9+var) = (-X1(5+var)/Bg(3*i+2) + Rs(3*i+2)*X1(5+var)/Bo(3*i+2))*b(4*i+3);
   j2(10+var,12+var) = (-X1(5+var)/Bg(3*i+2))*b(4*i+3);

   j2(10+var,16+var) = - ((1-X1(20+var)-X1(23+var))/Bg(3*i+5) +
X1(20+var)*Rs(3*i+5)/Bo(3*i+5))*b(4*i+6);
   j2(10+var,17+var) = - ((1-X1(21+var)-X1(24+var))/Bg(3*i+5) +
X1(21+var)*Rs(3*i+5)/Bo(3*i+5))*b(4*i+7);
   j2(10+var,18+var) = (alpha_res(3,i+2)/Bg(3*i+6) +
alpha_res(1,i+2)*Rs(3*i+6)/Bo(3*i+6))*b(4*i+8);

   j2(10+var,20+var) = - (-X1(16+var)/Bg(3*i+5) +
Rs(3*i+5)*X1(16+var)/Bo(3*i+5))*b(4*i+6);
   j2(10+var,21+var) = - (-X1(17+var)/Bg(3*i+5) +
Rs(3*i+5)*X1(17+var)/Bo(3*i+5))*b(4*i+7);
   j2(10+var,23+var) = (X1(16+var)/Bg(3*i+5))*b(4*i+6);
   j2(10+var,24+var) = (X1(17+var)/Bg(3*i+5))*b(4*i+7);


   if b(4*i+8) ~= 0    % There is inflow equation
      j2(5+var,14+var) = I(i+2)*pref/qref;
      j2(5+var,18+var) = 1;
   else                % There is no inflow equation
      j2(5+var,18+var) = 0;
   end

   j2(6+var,13+var) = 1;
   j2(6+var,15+var) = -
1.75*beta(i+2)*(X1(15+var)^(0.75))*rho3P(4*i+5)^0.75*mu3P(4*i+5)^0.25;
   j2(6+var,25+var) = -1;

   if b(4*i+6) ~= 0    % There is annular-to-tubing flow equation
      j2(7+var,14+var) = 1;
      j2(7+var,13+var) = -1;
      j2(7+var,16+var) = -2*B(i+2)*X1(16+var)*rho3P(4*i+6);
```

```
    else                % There is no annular-to-tubing flow equation
        j2(7+var,16+var) = 1;
        j2(11+var,20+var) = 1;
        j2(11+var,21+var) = 1;
        j2(12+var,23+var) = 1;
        j2(12+var,24+var) = 1;
    end

    if b(4*i+7) ~= 0        % There is annular flow equation
        j2(8+var,14+var) = 1;
        j2(8+var,17+var) = -
1.75*alpha(i+2)*(X1(17+var)^0.75)*rho3P(4*i+7)^0.75*mu3P(4*i+7)^0.25;
        j2(8+var,26+var) = -1;
        if b(4*i+6) ~= 0    % There is tubing flow equation -- there is split equation
            j2(11+var,20+var) = 1;
            j2(11+var,21+var) = -1;
            j2(12+var,23+var) = 1;
            j2(12+var,24+var) = -1;
        end
        if b(4*i+7) == -1   % If flow in annulus is toward toe of well
            j2(8+var,14+var) = -1;
            j2(8+var,26+var) = 1;
        end
    elseif b(4*i+7) == 0    % There is no annular flow equation
        j2(8+var,17+var) = 1;          % The value "1" does not affect the results
        j2(11+var,20+var) = 1;
        j2(11+var,21+var) = 1;
        j2(12+var,23+var) = 1;
        j2(12+var,24+var) = 1;
        if b(4*i+6) == 0
            j2(8+var,20+var) = 1e-20;   % To avoid singularity
            j2(8+var,23+var) = 1e-20;
            j2(2+var,17+var) = 1e-20;
            j2(2+var,20+var) = 1e-20;
            j2(2+var,23+var) = 1e-20;
            j2(4+var,17+var) = 1e-20;
            j2(4+var,20+var) = 1e-20;
            j2(4+var,23+var) = 1e-20;
            j2(10+var,17+var) = 1e-20;
            j2(10+var,20+var) = 1e-20;
            j2(10+var,23+var) = 1e-20;
        end
    end

end
```

```
func = j2;


% Generate jacobian matrix for Segment N
% This code is developed based on the two phase (oil/gas) model by
% Worakanok Thanyamanta and Chris Johansen.
% The code related to the water phase is originally done by Jiyi Liu
%Input:
%
%X1        :  Unknown parameters at each iteration
%beta      :  Pre-calculated coefficient for tubing flow calculations
%B         :  Pre-calculated coefficient for slot/valve flow calculations
%j3        :  Generated zero jacobian matrix
%Bo,Bw,Bg,Rs  :  Black-oil properties
%mu3P      :  Three-phase viscosities
%rho3P     :  Three-phase densities
%pref      :  Reference pressure
%N         :  Number of segments
%num_var   :  Number of unknowns
%Nodes     :  Number of nodes
%bridges   :  Number of bridges
%b         :  Bridge indexes
%
%Return:
%Jacobian matrix for Segment N

function func =
j3Generator(X1,beta,B,j3,Bo,Bw,Bg,Rs,rho3P,mu3P,pref,N,num_var,Nodes,bridges,b)

j3(1,num_var-17) = X1(num_var-13)/Bo(Nodes-4)*b(bridges-5);
j3(1,num_var-13) = X1(num_var-17)/Bo(Nodes-4)*b(bridges-5);
j3(1,num_var-5) = -X1(num_var-3)/Bo(Nodes-1)*b(bridges-1);
j3(1,num_var-4) = X1(num_var-2)/Bo(Nodes)*b(bridges);
j3(1,num_var-3) = -X1(num_var-5)/Bo(Nodes-1)*b(bridges-1);
j3(1,num_var-2) = X1(num_var-4)/Bo(Nodes)*b(bridges);

j3(2,num_var-15) = X1(num_var-11)/Bo(Nodes-3)*b(bridges-3);
j3(2,num_var-11) = X1(num_var-15)/Bo(Nodes-3)*b(bridges-3);
j3(2,num_var-4) = -X1(num_var-2)/Bo(Nodes)*b(bridges);
j3(2,num_var-2) = -X1(num_var-4)/Bo(Nodes)*b(bridges);

j3(3,num_var-17) = X1(num_var-10)/Bw(Nodes-4)*b(bridges-5);
j3(3,num_var-10) = X1(num_var-17)/Bw(Nodes-4)*b(bridges-5);
j3(3,num_var-5) = -X1(num_var-1)/Bw(Nodes-1)*b(bridges-1);
j3(3,num_var-4) = X1(num_var)/Bw(Nodes)*b(bridges);
j3(3,num_var-1) = -X1(num_var-5)/Bw(Nodes-1)*b(bridges-1);
```

```
j3(3,num_var) = X1(num_var-4)/Bw(Nodes)*b(bridges);

j3(4,num_var-15) = X1(num_var-8)/Bw(Nodes-3)*b(bridges-3);
j3(4,num_var-8) = X1(num_var-15)/Bw(Nodes-3)*b(bridges-3);
j3(4,num_var-4) = -X1(num_var)/Bw(Nodes)*b(bridges);
j3(4,num_var)   = -X1(num_var-4)/Bw(Nodes)*b(bridges);

j3(7,num_var-17) = ((1-X1(num_var-13)-X1(num_var-10))/Bg(Nodes-4) + X1(num_var-
13)*Rs(Nodes-4)/Bo(Nodes-4))*b(bridges-5);
j3(7,num_var-13) = (-X1(num_var-17)/Bg(Nodes-4) + Rs(Nodes-4)*X1(num_var-
17)/Bo(Nodes-4))*b(bridges-5);
j3(7,num_var-10) = (-X1(num_var-17)/Bg(Nodes-4))*b(bridges-5);
j3(7,num_var-5) = - ((1-X1(num_var-3)-X1(num_var-1))/Bg(Nodes-1) + X1(num_var-
3)*Rs(Nodes-1)/Bo(Nodes-1))*b(bridges-1);
j3(7,num_var-4) = ((1-X1(num_var-2)-X1(num_var))/Bg(Nodes) + X1(num_var-
2)*Rs(Nodes)/Bo(Nodes))*b(bridges);
j3(7,num_var-3) = - (-X1(num_var-5)/Bg(Nodes-1) + Rs(Nodes-1)*X1(num_var-
5)/Bo(Nodes-1))*b(bridges-1);
j3(7,num_var-2) = (-X1(num_var-4)/Bg(Nodes) + Rs(Nodes)*X1(num_var-
4)/Bo(Nodes))*b(bridges);
j3(7,num_var-1) = (X1(num_var-5)/Bg(Nodes-1))*b(bridges-1);
j3(7,num_var) = -(X1(num_var-4)/Bg(Nodes))*b(bridges);

j3(8,num_var-15) = ((1-X1(num_var-8)-X1(num_var-11))/Bg(Nodes-3) + X1(num_var-
11)*Rs(Nodes-3)/Bo(Nodes-3))*b(bridges-3);
j3(8,num_var-11) = (-X1(num_var-15)/Bg(Nodes-3) + Rs(Nodes-3)*X1(num_var-
15)/Bo(Nodes-3))*b(bridges-3);
j3(8,num_var-8) = -X1(num_var-15)/Bg(Nodes-3)*b(bridges-3);
j3(8,num_var-4) = -((1-X1(num_var-2)-X1(num_var))/Bg(Nodes) + X1(num_var-
2)*Rs(Nodes)/Bo(Nodes))*b(bridges);
j3(8,num_var-2) = -(-X1(num_var-4)/Bg(Nodes) + Rs(Nodes)*X1(num_var-
4)/Bo(Nodes))*b(bridges);
j3(8,num_var) = -(-X1(num_var-4)/Bg(Nodes))*b(bridges);

j3(5,num_var-7) = 1;
j3(5,num_var-5) = -1.75*beta(N)*(X1(num_var-5)^0.75)*rho3P(bridges-
1)^0.75*mu3P(bridges-1)^0.25;

if b(bridges) ~= 0          % There is annular-to-tubing flow equation
   j3(6,num_var-7) = -1;
   j3(6,num_var-6) = 1;
   j3(6,num_var-4) = -2*B(N)*X1(num_var-4)*rho3P(bridges);
else                        % There is no annular-to-tubing flow equation
   j3(6,num_var-7) = 1;    % The value "1" does not affect the results
   j3(6,num_var-6) = 1;
   j3(6,num_var-4) = 1;
```

```
end

func = j3;
```

Equation System and Jacobian System for Stinger Completions:

```
% Generate function matrix for Segment 1
% This code is developed based on the two phase (oil/gas) model by
% Worakanok Thanyamanta and Chris Johansen.
% The code related to the water phase is originally done by Jiyi Liu

%Input:
%
%X1        :  Unknown parameters at each iteration
%I         :  Pre-calculated coefficient for inflow equations
%pres      :  Reservoir pressures
%beta      :  Pre-calculated coefficient for tubing flow calculations
%alpha     :  Pre-calculated coefficient for annular flowcalculations
%B         :  Pre-calculated coefficient for slot/valve flow calculations
%Bo,Bw,Bg,Rs  :  Black-oil properties
%mu3P      :  Three-phase viscosities
%rho3P     :  Three-phase densities
%alpha_res :  Liquid holdups in reservoir
%f1        :  Generated zero function matrix
%pref      :  Reference pressure
%qref      :  Reference flow rate
%
%Return:
%Function matrix for Segment 1

function func =
f1Generator(X1,I,pres,beta,alpha,B,Bo,Bw,Bg,Rs,mu3P,rho3P,alpha_res,f1,pref,qref)


% oil-phase material balance
f1(1) = X1(4)*X1(8)/Bo(2) - X1(3)*X1(7)/Bo(1); % At node 1
f1(2) = X1(6)*alpha_res(1,1)/Bo(3) - X1(4)*X1(8)/Bo(2) - X1(5)*X1(9)/Bo(2);          %
At node 2
% water-phase material balance
f1(3) = X1(4)*X1(11)/Bw(2) - X1(3)*X1(10)/Bw(1); % At node 1
f1(4) = X1(6)*alpha_res(2,1)/Bw(3) - X1(4)*X1(11)/Bw(2) - X1(5)*X1(12)/Bw(2);
% At node 2
% Inflow equation
f1(5) = X1(6) - I(1)*(pres(1)/pref - X1(2))*pref/qref;
% Momentum balance for tubing bridge
```

```
f1(6) = X1(1) - X1(13) - beta(1)*(X1(3)^1.75)*rho3P(1)^0.75*mu3P(1)^0.25;
% Flow equation for annular-to-tubing bridge
f1(7) = X1(2) - X1(1) - B(1)*(X1(4)^2)*rho3P(2);
% Momentum balance for annular bridge
f1(8) = X1(2) - X1(14) - alpha(1)*(X1(5)^1.75)*rho3P(3)^0.75*mu3P(3)^0.25;
% Gas-phase material balance
f1(9) = ((1-X1(8)-X1(11))*X1(4)/Bg(2) + X1(8)*Rs(2)*X1(4)/Bo(2)) - ((1-X1(7)-
X1(10))*X1(3)/Bg(1) + X1(7)*Rs(1)*X1(3)/Bo(1));   % At node 1
f1(10) = (alpha_res(3,1)*X1(6)/Bg(3) + alpha_res(1,1)*Rs(3)*X1(6)/Bo(3)) - ((1-X1(8)-
X1(11))*X1(4)/Bg(2) + X1(8)*Rs(2)*X1(4)/Bo(2)) - ((1-X1(9)-X1(12))*X1(5)/Bg(2) +
X1(9)*Rs(2)*X1(5)/Bo(2));   % At node 2
% Split equation
f1(11) = X1(9) - X1(8);
f1(12) = X1(12) - X1(11);

func = f1;


% Generate function matrix for Segment 2 to N-1
% This code is developed based on the two phase (oil/gas) model by
% Worakanok Thanyamanta and Chris Johansen.
% The code related to the water phase is originally done by Jiyi Liu
%Input:
%
%X1       :  Unknown parameters at each iteration
%beta     :  Pre-calculated coefficient for tubing flow calculations
%alpha    :  Pre-calculated coefficient for annular flowcalculations
%B        :  Pre-calculated coefficient for slot/valve flow calculations
%I        :  Pre-calculated coefficient for inflow equations
%pres     :  Reservoir pressures
%Bo,Bw,Bg,Rs  :  Black-oil properties
%mu3P     :  Three-phase viscosities
%rho3P    :  Three-phase densities
%alpha_res :  Liquid holdups in reservoir
%f2       :  Generated zero function matrix
%pref     :  Reference pressure
%qref     :  Reference flow rate
%N        :  Number of segments
%b        :  Bridge indexes
%
%Return:
%Function matrix for Segment 2 to N-1

function func =
f2Generator(X1,beta,alpha,B,I,pres,Bo,Bw,Bg,Rs,mu3P,rho3P,alpha_res,f2,pref,qref,N,b)
```

```
for i=0:23   %for i=0:N-3 (12-3)

   var = i*12;

   % oil-phase material balance
   f2(1+var) = X1(16+var)*X1(20+var)/Bo(3*i+5)*b(4*i+6)...
      + X1(3+var)*X1(7+var)/Bo(3*i+1)*b(4*i+1)...
      - X1(15+var)*X1(19+var)/Bo(3*i+4)*b(4*i+5);       % At tubing node
   f2(2+var) = X1(5+var)*X1(9+var)/Bo(3*i+2)*b(4*i+3)...
      + X1(18+var)*alpha_res(1,i+2)/Bo(3*i+6)*b(4*i+8)...
      - X1(17+var)*X1(21+var)/Bo(3*i+5)*b(4*i+7)...
      - X1(16+var)*X1(20+var)/Bo(3*i+5)*b(4*i+6);       % At annular node

   % water-phase material balance
   f2(3+var) = X1(16+var)*X1(23+var)/Bw(3*i+5)*b(4*i+6)...
      + X1(3+var)*X1(10+var)/Bw(3*i+1)*b(4*i+1)...
      - X1(15+var)*X1(22+var)/Bw(3*i+4)*b(4*i+5);       % At tubing node
   f2(4+var) = X1(5+var)*X1(12+var)/Bw(3*i+2)*b(4*i+3)...
      + X1(18+var)*alpha_res(2,i+2)/Bw(3*i+6)*b(4*i+8)...
      - X1(17+var)*X1(24+var)/Bw(3*i+5)*b(4*i+7)...
      - X1(16+var)*X1(23+var)/Bw(3*i+5)*b(4*i+6);       % At annular node

   % Inflow equation
   if b(4*i+8) ~= 0       % Inlet flow exists
      f2(5+var) = X1(18+var) - (I(i+2)*(pres(i+2)/pref - X1(14+var)))*pref/qref;
   else                   % No inlet flow
      f2(5+var) = 0;
   end
   % Momentum balance for tubing bridge
   f2(6+var) = X1(13+var) - X1(25+var) -
beta(i+2)*(X1(15+var)^1.75)*rho3P(4*i+5)^0.75*mu3P(4*i+5)^0.25;
   % Flow equation for annular-to-tubing bridge
   if b(4*i+6) ~= 0       % Annular-to-tubing flow exists
      f2(7+var) = X1(14+var) - X1(13+var) - B(i+2)*(X1(16+var)^2)*rho3P(4*i+6);
   else                   % No annular-to-tubing flow
      f2(7+var) = 0;
      f2(11+var) = 0;
      f2(12+var) = 0;     % No split equation
   end
   % Momentum balance for annular bridge
   if b(4*i+7) ~= 0       % Annular flow exists
      f2(8+var) = X1(14+var) - X1(26+var) -
alpha(i+2)*(X1(17+var)^1.75)*rho3P(4*i+7)^0.75*mu3P(4*i+7)^0.25*b(4*i+7);
      if b(4*i+7) == 1
         if b(4*i+6) ~= 0    % If there is both annular and annular-to-tubing flows
            f2(11+var) = X1(20+var) - X1(21+var);
```

```
            f2(12+var) = X1(23+var) - X1(24+var);    % Split equation
        end
    elseif b(4*i+7) == -1   % If flow in annulus is toward toe of well
        f2(11+var) = 0;
        f2(12+var) = 0;                    % No split equation
    end
else                % No annular flow
    f2(8+var) = 0;
    f2(11+var) = 0;
    f2(12+var) = 0;
end
% Gas-phase material balance
f2(9+var) = ((1-X1(20+var)-X1(23+var))*X1(16+var)/Bg(3*i+5)...
    + X1(20+var)*Rs(3*i+5)*X1(16+var)/Bo(3*i+5))*b(4*i+6)...
    + ((1-X1(7+var)-X1(10+var))*X1(3+var)/Bg(3*i+1)...
    + X1(7+var)*Rs(3*i+1)*X1(3+var)/Bo(3*i+1))*b(4*i+1)...
    - ((1-X1(19+var)-X1(22+var))*X1(15+var)/Bg(3*i+4)...
    + X1(19+var)*Rs(3*i+4)*X1(15+var)/Bo(3*i+4))*b(4*i+5);        % At tubing node

f2(10+var) = ((1-X1(9+var)-X1(12+var))*X1(5+var)/Bg(3*i+2)...
    + X1(9+var)*Rs(3*i+2)*X1(5+var)/Bo(3*i+2))*b(4*i+3)...
    + (alpha_res(3,i+2)*X1(18+var)/Bg(3*i+6)...
    + alpha_res(1,i+2)*Rs(3*i+6)*X1(18+var)/Bo(3*i+6))*b(4*i+8)...
    - ((1-X1(21+var)-X1(24+var))*X1(17+var)/Bg(3*i+5)...
    + X1(21+var)*Rs(3*i+5)*X1(17+var)/Bo(3*i+5))*b(4*i+7)...
    - ((1-X1(20+var)-X1(23+var))*X1(16+var)/Bg(3*i+5)...
    + X1(20+var)*Rs(3*i+5)*X1(16+var)/Bo(3*i+5))*b(4*i+6);        % At annular node

end

for i=24   %for i=0:N-3 (13-3) (N=14)

    var = i*12;

    % oil-phase material balance
    f2(1+var) = X1(16+var)*X1(20+var)/Bo(3*i+5)*b(4*i+6)...
        + X1(3+var)*X1(7+var)/Bo(3*i+1)*b(4*i+1)...
        - X1(15+var)*X1(19+var)/Bo(3*i+4)*b(4*i+5);        % At tubing node
    f2(2+var) = X1(5+var)*X1(9+var)/Bo(3*i+2)*b(4*i+3)...
        + X1(18+var)*alpha_res(1,i+2)/Bo(3*i+6)*b(4*i+8)...
        + X1(17+var)*X1(21+var)/Bo(3*i+5)*b(4*i+7)...
        - X1(16+var)*X1(20+var)/Bo(3*i+5)*b(4*i+6);        % At annular node

    % water-phase material balance
    f2(3+var) = X1(16+var)*X1(23+var)/Bw(3*i+5)*b(4*i+6)...
        + X1(3+var)*X1(10+var)/Bw(3*i+1)*b(4*i+1)...
```

```
    - X1(15+var)*X1(22+var)/Bw(3*i+4)*b(4*i+5);        % At tubing node
  f2(4+var) = X1(5+var)*X1(12+var)/Bw(3*i+2)*b(4*i+3)...
    + X1(18+var)*alpha_res(2,i+2)/Bw(3*i+6)*b(4*i+8)...
    + X1(17+var)*X1(24+var)/Bw(3*i+5)*b(4*i+7)...
    - X1(16+var)*X1(23+var)/Bw(3*i+5)*b(4*i+6);        % At annular node

  % Inflow equation
  f2(5+var) = X1(18+var) - (I(i+2)*(pres(i+2)/pref - X1(14+var)))*pref/qref;

  % Momentum balance for tubing bridge
  f2(6+var) = X1(13+var) - X1(25+var) -
beta(i+2)*(X1(15+var)^1.75)*rho3P(4*i+5)^0.75*mu3P(4*i+5)^0.25;
  % Flow equation for annular-to-tubing bridge

  f2(7+var) = X1(14+var) - X1(13+var) - B(i+2)*(X1(16+var)^2)*rho3P(4*i+6);

  % Momentum balance for annular bridge

  f2(8+var) = - X1(14+var) + X1(26+var) -
alpha(i+2)*(X1(17+var)^1.75)*rho3P(4*i+7)^0.75*mu3P(4*i+7)^0.25*b(4*i+7);

  % Gas-phase material balance
  f2(9+var) = ((1-X1(20+var)-X1(23+var))*X1(16+var)/Bg(3*i+5)...
    + X1(20+var)*Rs(3*i+5)*X1(16+var)/Bo(3*i+5))*b(4*i+6)...
    + ((1-X1(7+var)-X1(10+var))*X1(3+var)/Bg(3*i+1)...
    + X1(7+var)*Rs(3*i+1)*X1(3+var)/Bo(3*i+1))*b(4*i+1)...
    - ((1-X1(19+var)-X1(22+var))*X1(15+var)/Bg(3*i+4)...
    + X1(19+var)*Rs(3*i+4)*X1(15+var)/Bo(3*i+4))*b(4*i+5);        % At tubing node

  f2(10+var) = ((1-X1(9+var)-X1(12+var))*X1(5+var)/Bg(3*i+2)...
    + X1(9+var)*Rs(3*i+2)*X1(5+var)/Bo(3*i+2))*b(4*i+3)...
    + (alpha_res(3,i+2)*X1(18+var)/Bg(3*i+6)...
    + alpha_res(1,i+2)*Rs(3*i+6)*X1(18+var)/Bo(3*i+6))*b(4*i+8)...
    + ((1-X1(21+var)-X1(24+var))*X1(17+var)/Bg(3*i+5)...
    + X1(21+var)*Rs(3*i+5)*X1(17+var)/Bo(3*i+5))*b(4*i+7)...
    - ((1-X1(20+var)-X1(23+var))*X1(16+var)/Bg(3*i+5)...
    + X1(20+var)*Rs(3*i+5)*X1(16+var)/Bo(3*i+5))*b(4*i+6);        % At annular node

end

func = f2;


% Generate function matrix for Segment N
% This code is developed based on the two phase (oil/gas) model by
% Worakanok Thanyamanta and Chris Johansen.
```

```
% The code related to the water phase is originally done by Jiyi Liu
%Input:
%
%X1        :  Unknown parameters at each iteration
%beta      :  Pre-calculated coefficient for tubing flow calculations
%B         :  Pre-calculated coefficient for slot/valve flow calculations
%Bo,Bw,Bg,Rs  :  Black-oil properties
%mu3P      :  Three-phase viscosities
%rho3P     :  Three-phase densities
%f3        :  Generated zero function matrix
%pref      :  Reference pressure
%pbh       :  Bottomhole pressure
%N         :  Number of segments
%num_var   :  Number of unknowns
%Nodes     :  Number of nodes
%bridges   :  Number of bridges
%b         :  Bridge indexes
%
%Return:
%Function matrix for Segment N

function func =
f3Generator(X1,I,beta,B,Bo,Bw,Bg,Rs,mu3P,rho3P,alpha_res,f3,pres,pref,qref,pbh,N,num_va
r,Nodes,bridges,b)

% oil-phase material balance
   f3(1) = X1(num_var-12)*X1(num_var-9)/Bo(Nodes-5)*b(bridges-6) - X1(num_var-
3)*X1(num_var-1)/Bo(Nodes-2)*b(bridges-2);       % At tubing node
   f3(2) = X1(num_var-2)*alpha_res(1,N)/Bo(Nodes)*b(bridges) - X1(num_var-
11)*X1(num_var-8)/Bo(Nodes-4)*b(bridges-4);            % At annular node

% water-phase material balance
f3(3) = X1(num_var-12)*X1(num_var-7)/Bw(Nodes-5)*b(bridges-6) - X1(num_var-
3)*X1(num_var)/Bw(Nodes-2)*b(bridges-2);       % At tubing node
f3(4) = X1(num_var-2)*alpha_res(2,N)/Bw(Nodes)*b(bridges) - X1(num_var-
11)*X1(num_var-6)/Bw(Nodes-4)*b(bridges-4);            % At annular node

% Inflow equation

   f3(5) = X1(num_var-2) - I(N)*(pres(N)/pref - X1(num_var-4))*pref/qref;

% Momentum balance for tubing bridge
   f3(6) = X1(num_var-5) - pbh/pref - beta(N)*(X1(num_var-3)^1.75)*rho3P(bridges-
2)^0.75*mu3P(bridges-2)^0.25;

% Gas-phase material balance
```

```
   f3(7) = ((1-X1(num_var-9)-X1(num_var-7))*X1(num_var-12)/Bg(Nodes-5) +
X1(num_var-9)*Rs(Nodes-5)*X1(num_var-12)/Bo(Nodes-5))*b(bridges-6)
      - ((1-X1(num_var-1)-X1(num_var))*X1(num_var-3)/Bg(Nodes-2) + X1(num_var-
1)*Rs(Nodes-2)*X1(num_var-3)/Bo(Nodes-2))*b(bridges-2);      % At tubing node
   f3(8) = (alpha_res(3,N)*X1(num_var-2)/Bg(Nodes) +
alpha_res(1,N)*Rs(Nodes)*X1(num_var-2)/Bo(Nodes))*b(bridges)...
      - ((1-X1(num_var-8)-X1(num_var-6))*X1(num_var-11)/Bg(Nodes-4) + X1(num_var-
8)*Rs(Nodes-4)*X1(num_var-11)/Bo(Nodes-4))*b(bridges-4);              % At annular node

func = f3;


% Generate function matrix for Segment 2 to N-1
% This code is developed based on the two phase (oil/gas) model by
% Worakanok Thanyamanta and Chris Johansen.
% The code related to the water phase is originally done by Jiyi Liu
%Input:
%
%X1       :  Unknown parameters at each iteration
%beta     :  Pre-calculated coefficient for tubing flow calculations
%alpha    :  Pre-calculated coefficient for annular flowcalculations
%B        :  Pre-calculated coefficient for slot/valve flow calculations
%I        :  Pre-calculated coefficient for inflow equations
%pres     :  Reservoir pressures
%Bo,Bw,Bg,Rs  :  Black-oil properties
%mu3P     :  Three-phase viscosities
%rho3P    :  Three-phase densities
%alpha_res :  Liquid holdups in reservoir
%f2       :  Generated zero function matrix
%pref     :  Reference pressure
%qref     :  Reference flow rate
%N        :  Number of segments
%b        :  Bridge indexes
%
%Return:
%Function matrix for Segment 2 to N-1

function func =
f4Generator(X1,beta,alpha,B,I,pres,Bo,Bw,Bg,Rs,mu3P,rho3P,alpha_res,f4,pref,qref,N,b)

for i=25   %for i=0:N-3 (12-3)

   var = (i-25)*9;

% oil-phase material balance
   f4(1+var) = X1(15+12*24)*X1(19+12*24)/Bo(3*i+1)*b(4*i+1)...
```

```
    - X1(3+var+26*12)*X1(6+var+26*12)/Bo(3*i+4)*b(4*i+5);      % At tubing node
  f4(2+var) = -X1(17+12*24)*X1(21+12*24)/Bo(3*i+2)*b(4*i+3)...
    + X1(5+var+26*12)*alpha_res(1,i+2)/Bo(3*i+6)*b(4*i+8)...
    + X1(4+var+26*12)*X1(7+var+26*12)/Bo(3*i+5)*b(4*i+7);      % At annular node

% water-phase material balance
  f4(3+var) =  X1(15+12*24)*X1(22+12*24)/Bw(3*i+1)*b(4*i+1)...
    - X1(3+var+26*12)*X1(8+var+26*12)/Bw(3*i+4)*b(4*i+5);      % At tubing node
  f4(4+var) = -X1(17+12*24)*X1(24+12*24)/Bw(3*i+2)*b(4*i+3)...
    + X1(5+var+26*12)*alpha_res(2,i+2)/Bw(3*i+6)*b(4*i+8)...
    + X1(4+var+26*12)*X1(9+var+26*12)/Bw(3*i+5)*b(4*i+7);      % At annular node

% Inflow equation

    f4(5+var)    X1(5+var+26*12) ...
      - (l(i+2)*(pres(i+2)/pref - X1(2+var+26*12)))*pref/qref;

% Momentum balance for tubing bridge
  f4(6+var) = X1(1+var+26*12) - X1(10+var+26*12)...
    - beta(i+2)*X1(3+var+26*12)^1.75*rho3P(4*i+5)^0.75*mu3P(4*i+5)^0.25;

% Momentum balance for annular bridge

    f4(7+var) = X1(11+var+26*12) - X1(2+var+26*12)...
      - alpha(i+2)*X1(4+var+26*12)^1.75*rho3P(4*i+7)^0.75*mu3P(4*i+7)^0.25*b(4*i+7);

% Gas-phase material balance
  f4(8+var) = ((1-X1(19+12*24)-X1(22+12*24))*X1(15+12*24)/Bg(3*i+1)...
    + X1(19+12*24)*Rs(3*i+1)*X1(15+12*24)/Bo(3*i+1))*b(4*i+1)...
    - ((1-X1(6+var+26*12)-X1(8+var+26*12))*X1(3+var+26*12)/Bg(3*i+4)...
    + X1(6+var+26*12)*Rs(3*i+4)*X1(3+var+26*12)/Bo(3*i+4))*b(4*i+5);      % At
tubing node

  f4(9+var) = -((1-X1(21+12*24)-X1(24+12*24))*X1(17+12*24)/Bg(3*i+2)...
    + X1(21+12*24)*Rs(3*i+2)*X1(17+12*24)/Bo(3*i+2))*b(4*i+3)...
    + (alpha_res(3,i+2)*X1(5+var+26*12)/Bg(3*i+6)...
    + alpha_res(1,i+2)*Rs(3*i+6)*X1(5+var+26*12)/Bo(3*i+6))*b(4*i+8)...
    + ((1-X1(7+var+26*12)-X1(9+var+26*12))*X1(4+var+26*12)/Bg(3*i+5)...
    + X1(7+var+26*12)*Rs(3*i+5)*X1(4+var+26*12)/Bo(3*i+5))*b(4*i+7);      % At
annular node

end

for i=26:N-3   %for i=0:N-3 (13-3) (N=14)

  var = (i-26)*9;
```

```
% oil-phase material balance
   f4(1+var+9) = X1(3+var+26*12)*X1(6+var+26*12)/Bo(3*i+1)*b(4*i+1)...
      - X1(12+var+26*12)*X1(15+var+26*12)/Bo(3*i+4)*b(4*i+5);      % At tubing node
   f4(2+var+9) = -X1(4+var+26*12)*X1(7+var+26*12)/Bo(3*i+2)*b(4*i+3)...
      + X1(14+var+26*12)*alpha_res(1,i+2)/Bo(3*i+6)*b(4*i+8)...
      + X1(13+var+26*12)*X1(16+var+26*12)/Bo(3*i+5)*b(4*i+7);      % At annular node

% water-phase material balance
   f4(3+var+9)    X1(3+var+26*12)*X1(8+var+26*12)/Bw(3*i+1)*b(4*i+1)...
      - X1(12+var+26*12)*X1(17+var+26*12)/Bw(3*i+4)*b(4*i+5);      % At tubing node
   f4(4+var+9) = -X1(4+var+26*12)*X1(9+var+26*12)/Bw(3*i+2)*b(4*i+3)...
      + X1(14+var+26*12)*alpha_res(2,i+2)/Bw(3*i+6)*b(4*i+8)...
      + X1(13+var+26*12)*X1(18+var+26*12)/Bw(3*i+5)*b(4*i+7);      % At annular node

% Inflow equation

      f2(5+var+9) = X1(14+var+26*12) ...
         - (I(i+2)*(pres(i+2)/pref - X1(11+var+26*12)))*pref/qref;

% Momentum balance for tubing bridge
   f4(6+var+9) = X1(10+var+26*12) - X1(19+var+26*12)...
      - beta(i+2)*X1(12+var+26*12)^1.75*rho3P(4*i+5)^0.75*mu3P(4*i+5)^0.25;

% Momentum balance for annular bridge

      f4(7+var+9) = X1(20+var+26*12) - X1(11+var+26*12)...
         -
alpha(i+2)*X1(13+var+26*12)^1.75*rho3P(4*i+7)^0.75*mu3P(4*i+7)^0.25*b(4*i+7);

% Gas-phase material balance
   f4(8+var+9) = ((1-X1(6+var+26*12)-X1(8+var+26*12))*X1(3+var+26*12)/Bg(3*i+1)...
      + X1(6+var+26*12)*Rs(3*i+4)*X1(3+var+26*12)/Bo(3*i+1))*b(4*i+1)...
      - ((1-X1(15+var+26*12)-X1(17+var+26*12))*X1(12+var+26*12)/Bg(3*i+4)...
      + X1(15+var+26*12)*Rs(3*i+4)*X1(12+var+26*12)/Bo(3*i+4))*b(4*i+5);      % At
tubing node

   f4(9+var+9) = -((1-X1(7+var+26*12)-X1(9+var+26*12))*X1(4+var+26*12)/Bg(3*i+2)...
      + X1(7+var+26*12)*Rs(3*i+5)*X1(4+var+26*12)/Bo(3*i+2))*b(4*i+3)...
      + (alpha_res(3,i+2)*X1(14+var+26*12)/Bg(3*i+6)...
      + alpha_res(1,i+2)*Rs(3*i+6)*X1(14+var+26*12)/Bo(3*i+6))*b(4*i+8)...
      + ((1-X1(16+var+26*12)-X1(18+var+26*12))*X1(13+var+26*12)/Bg(3*i+5)...
      + X1(16+var+26*12)*Rs(3*i+5)*X1(13+var+26*12)/Bo(3*i+5))*b(4*i+7);      % At
annular node

end
```

```
func = f4;


% Generate jacobian matrix for Segment 1
% This code is developed based on the two phase (oil/gas) model by
% Worakanok Thanyamanta and Chris Johansen.
% The code related to the water phase is originally done by Jiyi Liu
%Input:
%
%I        :  Pre-calculated coefficient for inflow equations
%X1       :  Unknown parameters at each iteration
%beta     :  Pre-calculated coefficient for tubing flow calculations
%alpha    :  Pre-calculated coefficient for annular flowcalculations
%B        :  Pre-calculated coefficient for slot/valve flow calculations
%j1       :  Generated zero jacobian matrix
%Bo,Bw,Bg,Rs  :  Black-oil properties
%mu3P     :  Three-phase viscosities
%rho3P    :  Three-phase densities
%alpha_res :  Liquid holdups in reservoir
%pref     :  Reference pressure
%qref     :  Reference flow rate
%
%Return:
%Jacobian matrix for Segment 1

function func =
j1Generator(X1,I,beta,alpha,B,j1,Bo,Bw,Bg,Rs,rho3P,mu3P,alpha_res,pref,qref)

j1(1,3) = -X1(7)/Bo(1);
j1(1,4) = X1(8)/Bo(2);
j1(1,7) = -X1(3)/Bo(1);
j1(1,8) = X1(4)/Bo(2);

j1(2,4) = -X1(8)/Bo(2);
j1(2,5) = -X1(9)/Bo(2);
j1(2,6) = alpha_res(1,1)/Bo(3);
j1(2,8) = -X1(4)/Bo(2);
j1(2,9) = -X1(5)/Bo(2);

%

j1(3,3) = -X1(10)/Bw(1);
j1(3,4) = X1(11)/Bw(2);
j1(3,10) = -X1(3)/Bw(1);
j1(3,11) = X1(4)/Bw(2);
```

```
j1(4,4) = -X1(11)/Bw(2);
j1(4,5) = -X1(12)/Bw(2);
j1(4,6) = alpha_res(2,1)/Bw(3);
j1(4,11) = -X1(4)/Bw(2);
j1(4,12) = -X1(5)/Bw(2);

j1(5,2) = l(1)*pref/qref;
j1(5,6) = 1;

j1(6,1) = 1;
j1(6,3) = -1.75*beta(1)*(X1(3)^0.75)*rho3P(1)^0.75*mu3P(1)^0.25;
j1(6,13) = -1;

j1(7,1) = -1;
j1(7,2) = 1;
j1(7,4) = -2*B(1)*X1(4)*rho3P(2);

j1(8,2) = 1;
j1(8,5) = -1.75*alpha(1)*(X1(5)^0.75)*rho3P(3)^0.75*mu3P(3)^0.25;
j1(8,14) = -1;

j1(9,3) = -((1-X1(7)-X1(10))/Bg(1) + X1(7)*Rs(1)/Bo(1));
j1(9,4) = ((1-X1(8)-X1(11))/Bg(2) + X1(8)*Rs(2)/Bo(2));
j1(9,7) = -(-X1(3)/Bg(1) + Rs(1)*X1(3)/Bo(1));
j1(9,8) = (-X1(4)/Bg(2) + Rs(2)*X1(4)/Bo(2));
j1(9,10) = X1(3)/Bg(1);
j1(9,11) = -X1(4)/Bg(2);

j1(10,4) = -((1-X1(8)-X1(11))/Bg(2) + X1(8)*Rs(2)/Bo(2));
j1(10,5) = -((1-X1(9)-X1(12))/Bg(2) + X1(9)*Rs(2)/Bo(2));
j1(10,6) = alpha_res(3,1)/Bg(3) + alpha_res(1,1)*Rs(3)/Bo(3);
j1(10,8) = -(-X1(4)/Bg(2) + Rs(2)*X1(4)/Bo(2));
j1(10,9) = -(-X1(5)/Bg(2) + Rs(2)*X1(5)/Bo(2));
j1(10,11) = X1(4)/Bg(2);
j1(10,12) = X1(5)/Bg(2);

j1(11,8) = -1;
j1(11,9) = 1;
j1(12,11) = -1;
j1(12,12) = 1;

func = j1;



% Generate Jacobian matrix for Segment 2 to N-1
```

```
% This code is developed based on the two phase (oil/gas) model by
% Worakanok Thanyamanta and Chris Johansen.
% The code related to the water phase is originally done by Jiyi Liu
%Input:
%
%X1        :  Unknown parameters at each iteration
%beta      :  Pre-calculated coefficient for tubing flow calculations
%alpha     :  Pre-calculated coefficient for annular flowcalculations
%l         :  Pre-calculated coefficient for inflow equations
%B         :  Pre-calculated coefficient for slot/valve flow calculations
%j2        :  Generated zero jacobian matrix
%Bo,Bw,Bg,Rs  :  Black-oil properties
%mu3P      :  Three-phase viscosities
%rho3P     :  Three-phase densities
%alpha_res :  Liquid holdups in reservoir
%pref      :  Reference pressure
%qref      :  Reference flow rate
%N         :  Number of segments
%b         :  Bridge indexes
%
%Return:
%Jacobian matrix for Segment 2 to N-1

function func =
j2Generator(X1,beta,alpha,l,B,j2,Bo,Bw,Bg,Rs,rho3P,mu3P,alpha_res,pref,qref,N,b)

for i=0:23

   var = 12*i;

   j2(1+var,3+var) = X1(7+var)/Bo(3*i+1)*b(4*i+1);
   j2(1+var,7+var) = X1(3+var)/Bo(3*i+1)*b(4*i+1);
   j2(1+var,15+var) = -X1(19+var)/Bo(3*i+4)*b(4*i+5);
   j2(1+var,16+var) = X1(20+var)/Bo(3*i+5)*b(4*i+6);
   j2(1+var,19+var) = -X1(15+var)/Bo(3*i+4)*b(4*i+5);
   j2(1+var,20+var) = X1(16+var)/Bo(3*i+5)*b(4*i+6);

   j2(2+var,5+var) = X1(9+var)/Bo(3*i+2)*b(4*i+3);
   j2(2+var,9+var) = X1(5+var)/Bo(3*i+2)*b(4*i+3);
   j2(2+var,16+var) = -X1(20+var)/Bo(3*i+5)*b(4*i+6);
   j2(2+var,17+var) = -X1(21+var)/Bo(3*i+5)*b(4*i+7);
   j2(2+var,18+var)   alpha_res(1,i+2)/Bo(3*i+6)*b(4*i+8);
   j2(2+var,20+var) = -X1(16+var)/Bo(3*i+5)*b(4*i+6);
   j2(2+var,21+var) = -X1(17+var)/Bo(3*i+5)*b(4*i+7);

   %
```

```
    j2(3+var,3+var) = X1(10+var)/Bw(3*i+1)*b(4*i+1);
    j2(3+var,10+var) = X1(3+var)/Bw(3*i+1)*b(4*i+1);
    j2(3+var,15+var) = -X1(22+var)/Bw(3*i+4)*b(4*i+5);
    j2(3+var,16+var) = X1(23+var)/Bw(3*i+5)*b(4*i+6);
    j2(3+var,22+var) = -X1(15+var)/Bw(3*i+4)*b(4*i+5);
    j2(3+var,23+var) = X1(16+var)/Bw(3*i+5)*b(4*i+6);

    j2(4+var,5+var) = X1(12+var)/Bw(3*i+2)*b(4*i+3);
    j2(4+var,12+var) = X1(5+var)/Bw(3*i+2)*b(4*i+3);
    j2(4+var,16+var) = -X1(23+var)/Bw(3*i+5)*b(4*i+6);
    j2(4+var,17+var) = -X1(24+var)/Bw(3*i+5)*b(4*i+7);
    j2(4+var,18+var) = alpha_res(2,i+2)/Bw(3*i+6)*b(4*i+8);
    j2(4+var,23+var) = -X1(16+var)/Bw(3*i+5)*b(4*i+6);
    j2(4+var,24+var) = -X1(17+var)/Bw(3*i+5)*b(4*i+7);

    %
    j2(9+var,3+var) = ((1-X1(7+var)-X1(10+var))/Bg(3*i+1) +
X1(7+var)*Rs(3*i+1)/Bo(3*i+1))*b(4*i+1);
    j2(9+var,7+var) = (-X1(3+var)/Bg(3*i+1) + Rs(3*i+1)*X1(3+var)/Bo(3*i+1))*b(4*i+1);
    j2(9+var,10+var) = (-X1(3+var)/Bg(3*i+1))*b(4*i+1);

    j2(9+var,15+var) = - ((1-X1(19+var)-X1(22+var))/Bg(3*i+4) +
X1(19+var)*Rs(3*i+4)/Bo(3*i+4))*b(4*i+5);
    j2(9+var,16+var) = ((1-X1(20+var)-X1(23+var))/Bg(3*i+5) +
X1(20+var)*Rs(3*i+5)/Bo(3*i+5))*b(4*i+6);

    j2(9+var,19+var) = - (-X1(15+var)/Bg(3*i+4) +
Rs(3*i+4)*X1(15+var)/Bo(3*i+4))*b(4*i+5);
    j2(9+var,20+var) = (-X1(16+var)/Bg(3*i+5) + Rs(3*i+5)*X1(16+var)/Bo(3*i+5))*b(4*i+6);

    j2(9+var,22+var) = (X1(15+var)/Bg(3*i+4))*b(4*i+5);
    j2(9+var,23+var) = (-X1(16+var)/Bg(3*i+5))*b(4*i+6);

    j2(10+var,5+var) = ((1-X1(9+var)-X1(12+var))/Bg(3*i+2) +
X1(9+var)*Rs(3*i+2)/Bo(3*i+2))*b(4*i+3);
    j2(10+var,9+var) = (-X1(5+var)/Bg(3*i+2) + Rs(3*i+2)*X1(5+var)/Bo(3*i+2))*b(4*i+3);
    j2(10+var,12+var) = (-X1(5+var)/Bg(3*i+2))*b(4*i+3);

    j2(10+var,16+var) = - ((1-X1(20+var)-X1(23+var))/Bg(3*i+5) +
X1(20+var)*Rs(3*i+5)/Bo(3*i+5))*b(4*i+6);
    j2(10+var,17+var) = - ((1-X1(21+var)-X1(24+var))/Bg(3*i+5) +
X1(21+var)*Rs(3*i+5)/Bo(3*i+5))*b(4*i+7);
    j2(10+var,18+var) = (alpha_res(3,i+2)/Bg(3*i+6) +
alpha_res(1,i+2)*Rs(3*i+6)/Bo(3*i+6))*b(4*i+8);
```

```
   j2(10+var,20+var) = - (-X1(16+var)/Bg(3*i+5) +
Rs(3*i+5)*X1(16+var)/Bo(3*i+5))*b(4*i+6);
   j2(10+var,21+var) = - (-X1(17+var)/Bg(3*i+5) +
Rs(3*i+5)*X1(17+var)/Bo(3*i+5))*b(4*i+7);
   j2(10+var,23+var) = (X1(16+var)/Bg(3*i+5))*b(4*i+6);
   j2(10+var,24+var) = (X1(17+var)/Bg(3*i+5))*b(4*i+7);


   j2(5+var,14+var) = l(i+2)*pref/qref;
   j2(5+var,18+var) = 1;

   j2(6+var,13+var) = 1;
   j2(6+var,15+var)    -
1.75*beta(i+2)*X1(15+var)^0.75*rho3P(4*i+5)^0.75*mu3P(4*i+5)^0.25;
   j2(6+var,25+var) = -1;


   j2(7+var,14+var) = 1;
   j2(7+var,13+var) = -1;
   j2(7+var,16+var) = -2*B(i+2)*X1(16+var)*rho3P(4*i+6);


   j2(8+var,14+var) = 1;
   j2(8+var,17+var) = -
1.75*alpha(i+2)*X1(17+var)^0.75*rho3P(4*i+7)^0.75*mu3P(4*i+7)^0.25;
   j2(8+var,26+var) = -1;

   j2(11+var,20+var) = 1;
   j2(11+var,21+var) = -1;
   j2(12+var,23+var) = 1;
   j2(12+var,24+var) = -1;


end

for i=24

   var = 12*i;

   j2(1+var,3+var) = X1(7+var)/Bo(3*i+1)*b(4*i+1);
   j2(1+var,7+var) = X1(3+var)/Bo(3*i+1)*b(4*i+1);
   j2(1+var,15+var) = -X1(19+var)/Bo(3*i+4)*b(4*i+5);
   j2(1+var,16+var) = X1(20+var)/Bo(3*i+5)*b(4*i+6);
   j2(1+var,19+var) = -X1(15+var)/Bo(3*i+4)*b(4*i+5);
   j2(1+var,20+var) = X1(16+var)/Bo(3*i+5)*b(4*i+6);
```

```
j2(2+var,5+var) = X1(9+var)/Bo(3*i+2)*b(4*i+3);
j2(2+var,9+var) = X1(5+var)/Bo(3*i+2)*b(4*i+3);
j2(2+var,16+var) = -X1(20+var)/Bo(3*i+5)*b(4*i+6);
j2(2+var,17+var) = X1(21+var)/Bo(3*i+5)*b(4*i+7);
j2(2+var,18+var) = alpha_res(1,i+2)/Bo(3*i+6)*b(4*i+8);
j2(2+var,20+var) = -X1(16+var)/Bo(3*i+5)*b(4*i+6);
j2(2+var,21+var) = X1(17+var)/Bo(3*i+5)*b(4*i+7);

%

j2(3+var,3+var) = X1(10+var)/Bw(3*i+1)*b(4*i+1);
j2(3+var,10+var) = X1(3+var)/Bw(3*i+1)*b(4*i+1);
j2(3+var,15+var) = -X1(22+var)/Bw(3*i+4)*b(4*i+5);
j2(3+var,16+var) = X1(23+var)/Bw(3*i+5)*b(4*i+6);
j2(3+var,22+var) = -X1(15+var)/Bw(3*i+4)*b(4*i+5);
j2(3+var,23+var) = X1(16+var)/Bw(3*i+5)*b(4*i+6);

j2(4+var,5+var) = X1(12+var)/Bw(3*i+2)*b(4*i+3);
j2(4+var,12+var) = X1(5+var)/Bw(3*i+2)*b(4*i+3);
j2(4+var,16+var) = -X1(23+var)/Bw(3*i+5)*b(4*i+6);
j2(4+var,17+var) = X1(24+var)/Bw(3*i+5)*b(4*i+7);
j2(4+var,18+var) = alpha_res(2,i+2)/Bw(3*i+6)*b(4*i+8);
j2(4+var,23+var) = -X1(16+var)/Bw(3*i+5)*b(4*i+6);
j2(4+var,24+var) = X1(17+var)/Bw(3*i+5)*b(4*i+7);

%
j2(9+var,3+var) = ((1-X1(7+var)-X1(10+var))/Bg(3*i+1) +
X1(7+var)*Rs(3*i+1)/Bo(3*i+1))*b(4*i+1);
j2(9+var,7+var) = (-X1(3+var)/Bg(3*i+1) + Rs(3*i+1)*X1(3+var)/Bo(3*i+1))*b(4*i+1);
j2(9+var,10+var) = (-X1(3+var)/Bg(3*i+1))*b(4*i+1);

j2(9+var,15+var) = - ((1-X1(19+var)-X1(22+var))/Bg(3*i+4) +
X1(19+var)*Rs(3*i+4)/Bo(3*i+4))*b(4*i+5);
j2(9+var,16+var) = ((1-X1(20+var)-X1(23+var))/Bg(3*i+5) +
X1(20+var)*Rs(3*i+5)/Bo(3*i+5))*b(4*i+6);

j2(9+var,19+var) = - (-X1(15+var)/Bg(3*i+4) +
Rs(3*i+4)*X1(15+var)/Bo(3*i+4))*b(4*i+5);
j2(9+var,20+var) = (-X1(16+var)/Bg(3*i+5) + Rs(3*i+5)*X1(16+var)/Bo(3*i+5))*b(4*i+6);

j2(9+var,22+var) = (X1(15+var)/Bg(3*i+4))*b(4*i+5);
j2(9+var,23+var) = (-X1(16+var)/Bg(3*i+5))*b(4*i+6);

j2(10+var,5+var) = ((1-X1(9+var)-X1(12+var))/Bg(3*i+2) +
X1(9+var)*Rs(3*i+2)/Bo(3*i+2))*b(4*i+3);
j2(10+var,9+var) = (-X1(5+var)/Bg(3*i+2) + Rs(3*i+2)*X1(5+var)/Bo(3*i+2))*b(4*i+3);
```

```
    j2(10+var,12+var) = (-X1(5+var)/Bg(3*i+2))*b(4*i+3);

    j2(10+var,16+var) = - ((1-X1(20+var)-X1(23+var))/Bg(3*i+5) +
X1(20+var)*Rs(3*i+5)/Bo(3*i+5))*b(4*i+6);
    j2(10+var,17+var) =  ((1-X1(21+var)-X1(24+var))/Bg(3*i+5) +
X1(21+var)*Rs(3*i+5)/Bo(3*i+5))*b(4*i+7);
    j2(10+var,18+var) = (alpha_res(3,i+2)/Bg(3*i+6) +
alpha_res(1,i+2)*Rs(3*i+6)/Bo(3*i+6))*b(4*i+8);

    j2(10+var,20+var) = - (-X1(16+var)/Bg(3*i+5) +
Rs(3*i+5)*X1(16+var)/Bo(3*i+5))*b(4*i+6);
    j2(10+var,21+var) =  (-X1(17+var)/Bg(3*i+5) +
Rs(3*i+5)*X1(17+var)/Bo(3*i+5))*b(4*i+7);
    j2(10+var,23+var) = (X1(16+var)/Bg(3*i+5))*b(4*i+6);
    j2(10+var,24+var) = -(X1(17+var)/Bg(3*i+5))*b(4*i+7);

    j2(5+var,14+var) = l(i+2)*pref/qref;
    j2(5+var,18+var) = 1;

    j2(6+var,13+var) = 1;
    j2(6+var,15+var) = -
1.75*beta(i+2)*X1(15+var)^0.75*rho3P(4*i+5)^0.75*mu3P(4*i+5)^0.25;
    j2(6+var,25+var) = -1;


    j2(7+var,14+var) = 1;
    j2(7+var,13+var) = -1;
    j2(7+var,16+var)  = -2*B(i+2)*X1(16+var)*rho3P(4*i+6);


    j2(8+var,17+var) = -
1.75*alpha(i+2)*X1(17+var)^0.75*rho3P(4*i+7)^0.75*mu3P(4*i+7)^0.25;
    j2(8+var,14+var) = -1;
    j2(8+var,26+var) = 1;


end

func = j2;


% Generate Jacobian matrix for Segment N
% This code is developed based on the two phase (oil/gas) model by
% Worakanok Thanyamanta and Chris Johansen.
% The code related to the water phase is originally done by Jiyi Liu
%Input:
```

```
%
%X1        :  Unknown parameters at each iteration
%beta      :  Pre-calculated coefficient for tubing flow calculations
%B         :  Pre-calculated coefficient for slot/valve flow calculations
%j3        :  Generated zero jacobian matrix
%Bo,Bw,Bg,Rs  :  Black-oil properties
%mu3P      :  Three-phase viscosities
%rho3P     :  Three-phase densities
%pref      :  Reference pressure
%N         :  Number of segments
%num_var   :  Number of unknowns
%Nodes     :  Number of nodes
%bridges   :  Number of bridges
%b         :  Bridge indexes
%
%Return:
%Jacobian matrix for Segment N

function func =
j3Generator(X1,I,beta,B,j3,Bo,Bw,Bg,Rs,rho3P,mu3P,alpha_res,pres,pref,qref,N,num_var,No
des,bridges,b)


j3(1,num_var-12) = X1(num_var-9)/Bo(Nodes-5)*b(bridges-6);
j3(1,num_var-9) = X1(num_var-12)/Bo(Nodes-5)*b(bridges-6);
j3(1,num_var-3) = -X1(num_var-1)/Bo(Nodes-2)*b(bridges-2);
j3(1,num_var-1) = -X1(num_var-3)/Bo(Nodes-2)*b(bridges-2);

j3(2,num_var-11) = -X1(num_var-8)/Bo(Nodes-4)*b(bridges-4);
j3(2,num_var-8) = -X1(num_var-11)/Bo(Nodes-4)*b(bridges-4);
j3(2,num_var-2) = alpha_res(1,N)/Bo(Nodes)*b(bridges);


j3(3,num_var-12) = X1(num_var-7)/Bw(Nodes-5)*b(bridges-6);
j3(3,num_var-7) = X1(num_var-12)/Bw(Nodes-5)*b(bridges-6);
j3(3,num_var-3) = -X1(num_var)/Bw(Nodes-2)*b(bridges-2);
j3(3,num_var) = -X1(num_var-3)/Bw(Nodes-2)*b(bridges-2);

j3(4,num_var-11) = -X1(num_var-6)/Bw(Nodes-4)*b(bridges-4);
j3(4,num_var-6) = -X1(num_var-11)/Bw(Nodes-4)*b(bridges-4);
j3(4,num_var-2) = alpha_res(2,N)/Bo(Nodes)*b(bridges);

j3(5,num_var-4) = I(N)*pref/qref;
j3(5,num_var-2) = 1;

j3(6,num_var-5) = 1;
```

```
j3(6,num_var-3) = -1.75*beta(N)*(X1(num_var-3)^0.75)*rho3P(bridges-
2)^0.75*mu3P(bridges-2)^0.25;


j3(7,num_var-12) = ((1-X1(num_var-9)-X1(num_var-7))/Bg(Nodes-5) + X1(num_var-
9)*Rs(Nodes-5)/Bo(Nodes-5))*b(bridges-6);
j3(7,num_var-9) = (-X1(num_var-12)/Bg(Nodes-5) + Rs(Nodes-5)*X1(num_var-
12)/Bo(Nodes-5))*b(bridges-6);
j3(7,num_var-7) = (-X1(num_var-12)/Bg(Nodes-5))*b(bridges-6);
j3(7,num_var-3) = - ((1-X1(num_var-1)-X1(num_var))/Bg(Nodes-2) + X1(num_var-
1)*Rs(Nodes-2)/Bo(Nodes-2))*b(bridges-2);
j3(7,num_var-1) = - (-X1(num_var-3)/Bg(Nodes-2) + Rs(Nodes-2)*X1(num_var-
3)/Bo(Nodes-2))*b(bridges-2);
j3(7,num_var) = (X1(num_var-3)/Bg(Nodes-2))*b(bridges-2);

%
j3(8,num_var-11) = -((1-X1(num_var-6)-X1(num_var-8))/Bg(Nodes-4) + X1(num_var-
8)*Rs(Nodes-4)/Bo(Nodes-4))*b(bridges-4);
j3(8,num_var-8) = -(-X1(num_var-11)/Bg(Nodes-4) + Rs(Nodes-4)*X1(num_var-
11)/Bo(Nodes-4))*b(bridges-4);
j3(8,num_var-6) = X1(num_var-11)/Bg(Nodes-4)*b(bridges-4);
j3(8,num_var-2) = (alpha_res(3,N)/Bg(Nodes) +
alpha_res(1,N)*Rs(Nodes)/Bo(Nodes))*b(bridges);

%
func = j3;


% Generate function matrix for Segment 2 to N-1
% This code is developed based on the two phase (oil/gas) model by
% Worakanok Thanyamanta and Chris Johansen.
% The code related to the water phase is originally done by Jiyi Liu
%Input:
%
%X1      : Unknown parameters at each iteration
%beta    : Pre-calculated coefficient for tubing flow calculations
%alpha   : Pre-calculated coefficient for annular flowcalculations
%B       : Pre-calculated coefficient for slot/valve flow calculations
%I       : Pre-calculated coefficient for inflow equations
%pres    : Reservoir pressures
%Bo,Bw,Bg,Rs : Black-oil properties
%mu3P    : Three-phase viscosities
%rho3P   : Three-phase densities
%alpha_res : Liquid holdups in reservoir
%f2      : Generated zero function matrix
%pref    : Reference pressure
```

```
%qref      :  Reference flow rate
%N         :  Number of segments
%b         :  Bridge indexes
%
%Return:
%Function matrix for Segment 2 to N-1

function func =
j4Generator(X1,beta,alpha,I,B,j4,Bo,Bw,Bg,Rs,rho3P,mu3P,alpha_res,pref,qref,N,bindex);

for i=25   %for i=0:N-3 (12-3)

   var = (i-25)*9;

   % oil-phase material balance
% At tubing node

   j4(1+var,15+12*24) = X1(19+12*24)/Bo(3*i+1);
   j4(1+var,19+12*24) =  X1(15+12*24)/Bo(3*i+1);
   j4(1+var, 3+var+26*12)=-X1(6+var+26*12)/Bo(3*i+1);
   j4(1+var, 6+var+26*12)=- X1(3+var+26*12)/Bo(3*i+4);

% At annular node

   j4(2+var, 17+12*24)=-X1(21+12*24)/Bo(3*i+2);
   j4(2+var, 21+12*24)=-X1(17+12*24)/Bo(3*i+2);
   j4(2+var,5+var+26*12)=alpha_res(1,i+2)/Bo(3*i+6);
   j4(2+var,4+var+26*12)=X1(7+var+26*12)/Bo(3*i+5);
   j4(2+var,7+var+26*12)=X1(4+var+26*12)/Bo(3*i+5);
   % water-phase material balance
% At tubing node

   j4(3+var,15+12*24)=X1(22+12*24)/Bw(3*i+1);
   j4(3+var,22+12*24)=X1(15+12*24)/Bw(3*i+1);
   j4(3+var, 3+var+26*12)=-X1(8+var+26*12)/Bw(3*i+4);
   j4(3+var,8+var+26*12)=-X1(3+var+26*12)/Bw(3*i+4);
% At annular node

   j4(4+var, 17+12*24)=-X1(24+12*24)/Bw(3*i+2);
   j4(4+var,24+12*24)=-X1(17+12*24)/Bw(3*i+2);
   j4(4+var,5+var+26*12)=alpha_res(2,i+2)/Bw(3*i+6);
   j4(4+var,4+var+26*12)=X1(9+var+26*12)/Bw(3*i+5);
   j4(4+var,9+var+26*12)=X1(4+var+26*12)/Bw(3*i+5);

   % Inflow equation
```

```
   j4(5+var,5+var+26*12)=1;
   j4(5+var,2+var+26*12)=I(i+2)*pref/qref;

   % Momentum balance for tubing bridge

   j4(6+var, 1+var+26*12)=1;
   j4(6+var,10+var+26*12)=-1;
   j4(6+var, 3+var+26*12)=-
beta(i+2)*(1.75*X1(3+var+26*12)^0.75)*rho3P(4*i+5)^0.75*mu3P(4*i+5)^0.25;

   % Momentum balance for annular bridge

   j4(7+var, 11+var+26*12)=1;
   j4(7+var, 2+var+26*12)=-1;
   j4(7+var,4+var+26*12)=-
alpha(i+2)*(1.75*X1(4+var+26*12)^0.75)*rho3P(4*i+7)^0.75*mu3P(4*i+7)^0.25;

   % Gas-phase material balance
% At tubing node

   j4(8+var, 19+12*24)=(-X1(15+12*24)/Bg(3*i+1)+Rs(3*i+1)*X1(15+12*24)/Bo(3*i+1));
   j4(8+var, 22+12*24)=-X1(15+12*24)/Bg(3*i+1);
   j4(8+var, 15+12*24)=((1-X1(19+12*24)-
X1(22+12*24))/Bg(3*i+1)+Rs(3*i+1)*X1(19+12*24)/Bo(3*i+1));
   j4(8+var, 6+var+12*26)=X1(3+var+12*26)/Bg(3*i+4)-
Rs(3*i+4)*X1(3+var+12*26)/Bo(3*i+4);
   j4(8+var, 8+var+12*26)=X1(3+var+12*26)/Bg(3*i+4);
   j4(8+var, 3+var+12*26)=-(1-X1(6+var+12*26)-X1(8+var+12*26))/Bg(3*i+4)-
Rs(3*i+4)*X1(6+var+12*26)/Bo(3*i+4);

% At annular node

   j4(9+var, 21+12*24)=(X1(17+12*24)/Bg(3*i+2)-Rs(3*i+2)*X1(17+12*24)/Bo(3*i+2));
   j4(9+var, 24+12*24)  X1(17+12*24)/Bg(3*i+2);
   j4(9+var, 17+12*24)= (-(1-X1(21+12*24)-X1(24+12*24))/Bg(3*i+2)-
Rs(3*i+2)*X1(21+12*24)/Bo(3*i+2));
   j4(9+var, 5+var+12*26)=(alpha_res(3,i+2)/Bg(3*i+6)+
alpha_res(1,i+2)*Rs(3*i+6)/Bo(3*i+6));
   j4(9+var, 7+var+12*26)=(-
X1(4+var+12*26)/Bg(3*i+5)+Rs(3*i+5)*X1(4+var+12*26)/Bo(3*i+5));
   j4(9+var,9+var+12*26)=-X1(4+var+12*26)/Bg(3*i+5);
   j4(9+var,4+var+12*26)=((1-X1(7+var+12*26)-X1(9+var+12*26))/Bg(3*i+5)+
X1(7+var+12*26)*Rs(3*i+5)/Bo(3*i+5));


end
```

```
for i=26:N-3   %for i=0:N-3 (13-3) (N=14)

   var = (i-26)*9;
   % oil-phase material balance
% At tubing node
   j4(1+var+9, 3+var+12*26)=X1(6+var+12*26)/Bo(3*i+1);
   j4(1+var+9,6+var+12*26)=X1(3+var+12*26)/Bo(3*i+1);
   j4(1+var+9,12+var+12*26)=-X1(15+var+12*26)/Bo(3*i+4);
   j4(1+var+9,15+var+12*26)=-X1(12+var+12*26)/Bo(3*i+4);

% At annular node
   j4(2+var+9, 4+var+12*26)=-X1(7+var+12*26)/Bo(3*i+2);
   j4(2+var+9,7+var+12*26)=-X1(4+var+12*26)/Bo(3*i+2);
   j4(2+var+9,14+var+12*26)=alpha_res(1,i+2)/Bo(3*i+6);
   j4(2+var+9, 13+var+12*26)=X1(16+var+12*26)/Bo(3*i+5);
   j4(2+var+9,16+var+12*26)=X1(13+var+12*26)/Bo(3*i+5);

   % water-phase material balance
   % At tubing node
   j4(3+var+9,3+var+12*26)=X1(8+var+12*26)/Bw(3*i+1);
   j4(3+var+9,8+var+12*26)=X1(3+var+12*26)/Bw(3*i+1);
   j4(3+var+9,12+var+12*26)=-X1(17+var+12*26)/Bw(3*i+4);
   j4(3+var+9,17+var+12*26)=-X1(12+var+12*26)/Bw(3*i+4);

% At annular node
   j4(4+var+9,4+var+12*26)=-X1(9+var+12*26)/Bw(3*i+2);
   j4(4+var+9,9+var+12*26)=-X1(4+var+12*26)/Bw(3*i+2);
   j4(4+var+9, 14+var+12*26)=alpha_res(2,i+2)/Bw(3*i+6);
   j4(4+var+9, 13+var+12*26)=X1(18+var+12*26)/Bw(3*i+5);
   j4(4+var+9, 18+var+12*26)=X1(13+var+12*26)/Bw(3*i+5);

   % Inflow equation

   j4(5+var+9, 14+var+12*26)=1;
   j4(5+var+9, 11+var+12*26)=I(i+2)*pref/qref;

   % Momentum balance for tubing bridge
   j4(6+var+9, 10+var+12*26)=1;
   j4(6+var+9, 19+var+12*26)=-1;
   j4(6+var+9, 12+var+12*26)=-
beta(i+2)*(1.75*X1(12+var+12*26)^0.75)*rho3P(4*i+5)^0.75*mu3P(4*i+5)^0.25;

   % Momentum balance for annular bridge

   j4(7+var+9, 20+var+12*26)=1;
```

```
   j4(7+var+9, 11+var+12*26)=-1;
   j4(7+var+9, 13+var+12*26)=-
alpha(i+2)*1.75*X1(13+var+12*26)^0.75*rho3P(4*i+7)^0.75*mu3P(4*i+7)^0.25;
   % Gas-phase material balance
% At tubing node
   j4(8+var+9, 6+var+12*26)=(-X1(3+var+12*26)/Bg(3*i+1)+
Rs(3*i+4)*X1(3+var+12*26)/Bo(3*i+1));
   j4(8+var+9, 8+var+12*26)=-X1(3+var+12*26)/Bg(3*i+1);
   j4(8+var+9, 3+var+12*26)=((1-X1(6+var+12*26)-X1(8+var+12*26))/Bg(3*i+1)+
X1(6+var+12*26)*Rs(3*i+4)/Bo(3*i+1));
   j4(8+var+9, 15+var+12*26)=-(-X1(12+var+12*26)/Bg(3*i+4)+
Rs(3*i+4)*X1(12+var+12*26)/Bo(3*i+4));
   j4(8+var+9, 17+var+12*26)=X1(12+var+12*26)/Bg(3*i+4);
   j4(8+var+9, 12+var+12*26)= - ((1-X1(15+var+12*26)-X1(17+var+12*26))/Bg(3*i+4)+
X1(15+var+12*26)*Rs(3*i+4)/Bo(3*i+4));

% At annular node
   j4(9+var+9, 7+var+12*26)=-(-X1(4+var+12*26)/Bg(3*i+2)+
Rs(3*i+5)*X1(4+var+12*26)/Bo(3*i+2));
   j4(9+var+9, 9+var+12*26)=X1(4+var+12*26)/Bg(3*i+2);
   j4(9+var+9, 4+var+12*26)=-((1-X1(7+var+12*26)-X1(9+var+12*26))/Bg(3*i+2)+
X1(7+var+12*26)*Rs(3*i+5)/Bo(3*i+2));
   j4(9+var+9, 14+var+12*26)=(alpha_res(3,i+2)/Bg(3*i+6)+
alpha_res(1,i+2)*Rs(3*i+6)/Bo(3*i+6));
   j4(9+var+9, 16+var+12*26)=(-X1(13+var+12*26)/Bg(3*i+5)+
Rs(3*i+5)*X1(13+var+12*26)/Bo(3*i+5));
   j4(9+var+9, 18+var+12*26)=-X1(13+var+12*26)/Bg(3*i+5);
   j4(9+var+9, 13+var+12*26)= ((1-X1(16+var+12*26)-X1(18+var+12*26))/Bg(3*i+5)+
X1(16+var+12*26)*Rs(3*i+5)/Bo(3*i+5));


end

func = j4;
```

Reference

Ben J. Dikken."Pressure drop in horizontal wells and its effect on production performance", JPT, Nov, 1990.

Blasius, H. (1908), "Grenzschichten in Flüssigkeiten mit kleiner Reibung", Z. Math. U. Phys., Vol. 56 pp.1-37.

K. Brekke, L. Thompson, "Horizontal well productivity and risk assessment", SPE36579, 1996.

D. Collins, L. Nghiem, R. Sharma, "Field-scale simulation of horizontal wells", CMG

Collins D. A., Nghiem L. X., Sharma R., Agarwal R. K. and Jha K. N., "Field -Scale Simulation of Horizontal Wells with Hybrid Grids", paper SPE 21218, presented at the 1991 Reservoir Simulation Symposium, Anaheim, California, February 17-20, 1991.

S. Haaland, "Simple and explicit formulas for the friction factor in turbulent pipe flow", Journal of fluid engineering, Vol 105, 1983.

L-B Ouyang, S. Arbabi, K. Aziz, "General Wellbore flow model for horizontal, vertical and slanted well completions", Stanford, SPE 36608.

J. Holmes, T. Barkve, O. Lund, "Application of multisegment well model to simulate flow in advanced wells", SPE 50646

S. Joshi, "Augmentation of well productivity with slant and horizontal wells", JPT, June 1998, SPE 15375.

D. Babu, A. Odeh, "Productivity of a horizontal well", SPE 18298, 1989.

K. Brekke, T. Johansen, "A new modular approach to comprehensive simulation of horizontal wells", SPE 26518, 1993.

J. Holmes, "Modeling Advanced Wells in Reservoir Simulation", SPE, 72493, 2001.

K. Bendiksen, R. Moe, "The Dynamic Two-Fluid Model OLGA: Theory and application", SPE Production Engineering, May 1991.

W. Thanyamanta, "Well Modeling Incorporating Compositional and Non-Isothermal effects", Ph.D. Thesis, Memorial University of Newfoundland, 2006.

T. Johansen, V. Khoriakov, "Iterative techniques in modeling of multi-phase flow in advanced wells in the near well region", Journal of petroleum Science and Engineering, Volume 58, Issues 1-2, August 2007.

H. Asheim, J. Kolnes, and P. Oudeman. A flow resistance correlation for completed wellbore. Journal of Petroleum Science and Engineering, 8:97-104, 1992.

K. Baker. Understanding paraffin and asphaltene problems in oil and gas wells. South Midcontinent Region Workshop, Smackover, Arkansas, July 2003.

J. P. Brill and H. Mukherjee. Multiphase Flow in Wells, volume Monograph volume 17 of SPE Henry L. Doherty Series. Society of Petroleum Engineers Inc., Richardson, Texas, 1999.

A. Danesh. PVT and Phase Behaviour of Petroleum Reservoir Fluids. Elsevier, Amsterdam, The Netherlands, 1998.

S. E. Haaland. Simple and explicit formulas for the friction factor in turbulent pipe flow. Journal of Fluids Engineering, 105, Mar 1983.

A. C. Johansen. Work term report. Faculty of Engineering and Applied Science, Memorial University of Newfoundland, St.John's, NL, Canada, 2005.

T. E. Johansen. Principles of reservoir engineering. Advanced Reservoir Engineering course note (Draft), 2005. Faculty of Engineering and Applied Science, Memorial University of Newfoundland.

T. M. V. Kaiser, S. Wilson, and L. A. Venning. Inflow analysis and optimization of slotted

liners. SPE Drilling & Completion, pages 200-208, Dec 2002.

M. Konopczynski and A. Ajayi. Design of intelligent well downhole valves for adjustable flow control. 2004. SPE paper 90664.

D. Y. Peng and D. B. Robinson. A new two-constant equation of state. Ind. Eng. Chem. Fundam., 15(1):59-64, 1976.

T. K. Perkins. Critical and subcritical flow of multiphase mixtures through chokes. SPE Drilling, 8:271-276, Dec 1993.

C. F. Spencer and R.P. Danner. Prediction of bubble point pressure of mixtures. Journal of. Chem. Eng. Data, 18(2):230-234, 1973.

Z. Su and J. S. Gudmundsson. Friction factor of perforation roughness in pipes. 1993. SPE paper 26521.

M. Vazquez and H. D. Beggs. Correlations for fluid physical property prediction. Journal of Petroleum Technology, pages 968-70, Jun 1980.s